

# Quantum Algorithms using the Curvelet Transform

Yi-Kai Liu

Institute for Quantum Information  
California Institute of Technology  
yikailiu@caltech.edu

Oct. 27, 2008

## Abstract

The curvelet transform is a directional wavelet transform over  $\mathbb{R}^n$ , originally due to Candes and Donoho (2002). It is used to analyze functions that have singularities along smooth surfaces. I demonstrate how this can lead to new quantum algorithms. I give an efficient implementation of a quantum curvelet transform, together with two applications: a single-shot measurement procedure for approximately finding the center of a ball in  $\mathbb{R}^n$ , given quantum-samples over the ball; and, a quantum algorithm for finding the center of a radial function over  $\mathbb{R}^n$ , given oracle access to the function. I conjecture that these algorithms only require a constant number of quantum-samples or oracle queries, independent of the dimension  $n$  — this can be interpreted as a quantum speed-up. Finally, I prove some rigorous bounds on the distribution of probability mass for the continuous curvelet transform. This almost proves my conjecture, except for issues of discretization.

## 1 Introduction

One of the most remarkable demonstrations of the power of a quantum computer is Shor’s algorithm for factoring and discrete logarithms [19]. This has motivated many researchers to try to generalize its key components—the quantum Fourier transform over  $\mathbb{Z}_N$ , and the algorithm for period-finding—to solve other problems. In particular, this motivated the study of the quantum Fourier transform and the hidden subgroup problem (HSP) on non-Abelian groups, as a route to solving certain lattice problems and the graph isomorphism problem [17, 3, 18].

In this paper we take a different direction. We study the curvelet transform over  $\mathbb{R}^n$  [7]. This is a kind of “directional” wavelet transform, which can resolve features over the spatial and frequency domains simultaneously. A curvelet basis function resembles a wavepacket, with high-frequency oscillations in one direction (like a plane wave as in the Fourier transform), but which is also supported on a small region of space (unlike the plane wave). We show that this leads to fast quantum algorithms for some new classes of problems, outside the framework of the HSP. To the best of our knowledge, this is the first attempt to design quantum algorithms based on the curvelet transform.

We start by studying the continuous curvelet transform on  $\mathbb{R}^n$ . Intuitively, the curvelet transform is helpful in analyzing functions on  $\mathbb{R}^n$  that are discontinuous along  $(n - 1)$ -dimensional surfaces. If a function  $f$  is discontinuous along a surface  $S$ , then the curvelet transform  $\Gamma_f$  is “large” at those locations  $(\vec{b}, \vec{\theta})$ , where  $\vec{b}$  is a point on  $S$  and  $\vec{\theta}$  is the vector normal to  $S$  at  $\vec{b}$ . The set of all such pairs  $(\vec{b}, \vec{\theta})$  is called the “wavefront set” of  $f$ .

Our first goal is to make this intuition precise. We can interpret the curvelet transform  $\Gamma_f$  as a wavefunction, and we want to show that its probability mass  $|\Gamma_f|^2$  is concentrated near the wavefront set. This is a strong claim—in particular, it does not seem to follow from the

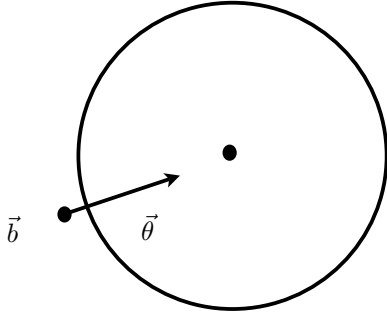


Figure 1: A point  $\vec{b}$  and vector  $\vec{\theta}$  that lie near the wavefront set of the ball / spherical shell.

results shown in [5]. It is similar in spirit to [7], though that paper only considers functions on  $\mathbb{R}^2$ , not  $\mathbb{R}^n$ .

We do not have a proof of this claim for general functions on  $\mathbb{R}^n$ . But we can prove it for two particular cases, where the input  $f$  is a quantum-sample state (i.e., a uniform superposition) over a ball or a spherical shell in  $\mathbb{R}^n$ . In these cases,  $(\vec{b}, \vec{\theta})$  is near the wavefront set with high probability. This implies that the line  $\{\vec{b} + \lambda\vec{\theta} \mid \lambda \in \mathbb{R}\}$  passes near the center of the ball or spherical shell (see Figure 1) — we will use this fact to design quantum algorithms.

Next, we study quantum algorithms based on discrete versions of the curvelet transform. We give an efficient implementation of a quantum curvelet transform, for a certain class of curvelets. This uses ideas from the classical setting [4], but the curvelets must be specially designed so that certain quantum superposition states can be prepared efficiently.

Then we propose polynomial-time quantum algorithms for two problems: (1) given a single quantum-sample over a ball in  $\mathbb{R}^n$ , find the center of the ball, with accuracy  $\pm\Delta$  where  $\Delta$  is a constant fraction of the radius of the ball; (2) given oracle access to a function  $f$  that is radial around some unknown point  $\vec{c} \in \mathbb{R}^n$ , find the point  $\vec{c}$  exactly (i.e., with accuracy  $\pm\Delta$  in time  $\text{poly}(\log \frac{1}{\Delta})$ , assuming that the function  $f$  fluctuates on sufficiently small scales).

For the first problem, we conjecture that our quantum procedure succeeds with constant probability, while the best classical procedure succeeds with probability that is exponentially small in  $n$ . For the second problem, we conjecture that our quantum algorithm uses only a constant number of queries, independent of the dimension  $n$ . These conjectures are supported by our (rigorous) results on the continuous curvelet transform; and we can argue (heuristically) that the effects caused by discretization should be small.

These examples demonstrate that one can use the curvelet transform to obtain a quantum speed-up. These examples are artificially simple, in order to allow a rigorous analysis. But the underlying idea—using the curvelet transform to find normal vectors to a surface—should work on more complicated geometric objects.

## 1.1 Technical Contributions

First, we briefly describe the continuous curvelet transform, following [6]. The complete definition is given in Section 2.

Given a function  $f(\vec{x})$ , the continuous curvelet transform returns a function  $\Gamma_f(a, \vec{b}, \vec{\theta})$ . Here,  $\vec{x} \in \mathbb{R}^n$  represents a “location,” while  $0 < a < 1$  is a “scale” (smaller values denote finer scales, larger values denote coarser scales),  $\vec{b} \in \mathbb{R}^n$  is a “location,” and  $\vec{\theta} \in S^{n-1}$  (the unit sphere in  $\mathbb{R}^n$ ) is a “direction.” All functions return values in  $\mathbb{C}$ .

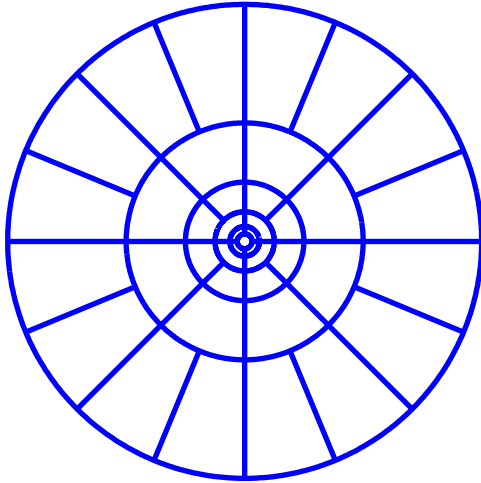


Figure 2: “Tiling” of the frequency domain into sectors with depth  $\approx 1/a$  and width  $\approx 1/\sqrt{a}$  (note that this corresponds to angular width  $\approx \sqrt{a}$ ), where  $a = 1, \frac{1}{2}, \frac{1}{4}, \frac{1}{8}, \dots$

The curvelet transform is given by:

$$\Gamma_f(a, \vec{b}, \vec{\theta}) := \int_{\mathbb{R}^n} \hat{f}(\vec{k}) \chi_{a, \vec{\theta}}(\vec{k}) e^{2\pi i \vec{k} \cdot \vec{b}} d\vec{k}. \quad (1)$$

Here,  $\hat{f}$  is the Fourier transform of  $f$ , and  $\chi_{a, \vec{\theta}}$  is a smooth window function, real, non-negative, supported on a sector of frequency space which depends on the scale  $a$  and direction  $\vec{\theta}$ . In particular,  $a$  scales like a power of 2, and  $\chi_{a, \vec{\theta}}$  is supported on a sector which is centered around direction  $\vec{\theta}$ , with depth  $\approx 1/a$  and width  $\approx 1/\sqrt{a}$  (note that this corresponds to angular width  $\approx \sqrt{a}$ ). These sectors form a “tiling” of the frequency domain. (See figure 2.)

Evidently, the curvelet transform consists of (1) taking the Fourier transform of  $f$ , (2) separating  $\hat{f}$  into pieces corresponding to different scales and directions, and (3) taking the inverse Fourier transform. The window functions  $\chi_{a, \vec{\theta}}$  can be constructed in various ways. When done properly, the curvelet transform has a natural inversion formula for recovering  $f$  from  $\Gamma_f$ , and it preserves the  $L^2$  norm.

In section 2 we give one such construction, for curvelets over  $\mathbb{R}^n$ . Our construction is somewhat more complicated than the construction in [6], which was over  $\mathbb{R}^2$ . This is because the volume of a sector of frequency space scales in a more complicated way over  $\mathbb{R}^n$ , compared to  $\mathbb{R}^2$ .

Next, we want to understand the distribution of probability mass  $|\Gamma_f|^2$  over different values of  $(a, \vec{b}, \vec{\theta})$ . This is technically quite difficult.  $\Gamma_f(a, \vec{b}, \vec{\theta})$  is defined by an oscillatory integral, and while there are various methods for bounding the asymptotic decay rates of such quantities [21, 5], we need non-asymptotic bounds. We cannot solve this problem in general, but we can handle some special cases.

In section 3 we specialize to the case where  $f$  is a radial function,  $f(\vec{x}) = f_0(|\vec{x}|)$ . This implies that  $\hat{f}$  is also radial,  $\hat{f}(\vec{k}) = F_0(|\vec{k}|)$ . We show that the probability of observing a fine-scale element  $a \leq \eta$  is essentially given by the amount of probability mass of  $\hat{f}$  at frequencies above  $1/\eta$ . Also, by symmetry, the direction  $\vec{\theta}$  is uniformly random, and the

location  $\vec{b}$  has expectation value  $\vec{0}$ . Finally, we bound the variance of  $\vec{b}$ . Our argument is somewhat indirect, since even for a radial function  $f$ , we do not have an exact closed-form expression for  $\Gamma_f$ . Instead, we use Plancherel’s theorem to convert the integral over  $\vec{b}$  into an integral over  $\vec{k}$ . This is helpful because  $\Gamma_f$  has a simpler description over frequency space, while multiplication by  $b_j$  turns into differentiation with respect to  $k_j$ . We can then bound this integral in a (relatively) straightforward way.

In section 4 we consider the case where  $f$  is the indicator function of a ball in  $\mathbb{R}^n$ , with radius  $\beta$ , centered at the origin. We expect that, after applying the curvelet transform,  $\vec{b}$  and  $\vec{\theta}$  will be concentrated near the wavefront set of  $f$ : that is,  $\vec{b}$  will be concentrated near the line  $\{\lambda\vec{\theta} \mid \lambda \in \mathbb{R}\}$ , at about distance  $\beta$  from the origin. Furthermore, we expect that  $\vec{b}$  will become more tightly concentrated, the smaller the value of  $a$ .

We show that this is essentially what happens. We show that the probability of observing  $a \leq \eta$  is at least  $\Omega(\eta)$ . This is due to the fact that  $\hat{f}$  has a “heavy tail,” which is caused by the discontinuity of  $f$  along the surface of the ball. (For comparison, one would not observe this behavior if  $f$  were, say, a Gaussian.) Next, we show that the variance of  $\vec{b}$ , conditioned on  $a \leq \eta$ , is at most  $O(\beta^2)$  in the  $\vec{\theta}$  direction, and at most  $O(\eta\beta^2)$  in the subspace orthogonal to  $\vec{\theta}$ . We interpret this as follows:  $\vec{b}$  and  $\vec{\theta}$  define a line that passes near the center of the ball; and, with constant probability, the error (i.e., the displacement away from the center) is at most a constant fraction of the radius of the ball.

As mentioned previously, it is remarkable that these bounds do not depend on the dimension  $n$ .

In section 5, we consider the case where  $f$  is supported on a thin spherical shell, having radius  $\beta$  and thickness  $\delta \ll \beta$ . Here, after applying the curvelet transform, we get a qualitatively similar behavior of  $a$ ,  $\vec{b}$  and  $\vec{\theta}$ . Quantitatively, however, we find that we can observe much smaller scales  $a$ , on the order of  $\delta/\beta$ ; and thus we can find the center of the shell with much greater precision. Essentially, by making the shell extremely thin, we can find its center with arbitrarily high precision.

We show the following. Let  $\varepsilon = \delta/\beta$ , and let  $\eta_c = \varepsilon(n-2)/e$ . Then we observe  $a \leq \eta_c$  with at least constant probability. Furthermore, conditioned on this event, the variance of  $\vec{b}$  is at most  $O(\beta^2)$  in the  $\vec{\theta}$  direction, and at most  $O(\varepsilon n\beta^2)$  in the subspace orthogonal to  $\vec{\theta}$ . Here,  $\varepsilon$  is the dominant factor. In the context of a quantum algorithm for finding the center of a radial function,  $\varepsilon$  can be extremely small: when the oracle computes the function to  $m$  bits of precision,  $\varepsilon$  can be of size  $2^{-\Omega(m)}$ .

Interestingly, these bounds, on the concentration of probability mass as a function of  $\vec{b}$ , hold even when the window function  $\chi_{a,\vec{\theta}}$  is not  $C^\infty$ -smooth—it only has to be  $C^1$ -smooth. By contrast, most bounds on the asymptotic rate of decay of  $\Gamma_f$  require the window function to be  $C^\infty$ -smooth.

Finally, we turn to the discrete curvelet transform, and quantum algorithms. In Section 6 we give an efficient implementation of a quantum curvelet transform. At a high level, this consists of a quantum Fourier transform, followed by an operation  $\mathcal{X}$  that prepares certain superpositions over  $a$  and  $\vec{\theta}$ , followed by an inverse quantum Fourier transform:

$$\begin{aligned}
\sum_{\vec{x}} f(\vec{x})|\vec{x}\rangle|0, \vec{0}\rangle &\mapsto \sum_{\vec{k}} \hat{f}(\vec{k})|\vec{k}\rangle|0, \vec{0}\rangle \\
&\mapsto \sum_{\vec{k}} \hat{f}(\vec{k})|\vec{k}\rangle \sum_{a, \vec{\theta}} \chi_{a, \vec{\theta}}(\vec{k})|a, \vec{\theta}\rangle \\
&\mapsto \sum_{\vec{b}, a, \vec{\theta}} \Gamma_f(a, \vec{b}, \vec{\theta})|\vec{b}\rangle|a, \vec{\theta}\rangle.
\end{aligned} \tag{2}$$

This is the same basic approach used to calculate the classical curvelet transform [4]. However, in the quantum case, the operation  $\mathcal{X}$  is tricky to implement, since the superposition can

involve  $2^{\Theta(n)}$  different terms, when we are working over  $\mathbb{R}^n$ . This depends on the precise form of the window functions  $\chi_{a,\vec{\theta}}$ . We show how to implement  $\mathcal{X}$  when the window functions are constructed in a particular way, using spherical coordinates in  $\mathbb{R}^n$ . (It is not clear how to do this for the window functions used in [4].) We argue that this quantum curvelet transform is a reasonable approximation to the continuous curvelet transform that we studied previously.

In Section 7, we finally reach our goal of giving quantum algorithms for the two problems mentioned earlier: estimating the center of a ball, given a single quantum-sample state; and finding the center of a radial function, given oracle access. For the first problem, we conjecture that our quantum procedure succeeds with constant probability, while the best classical procedure succeeds with probability that is exponentially small in  $n$ . For the second problem, we conjecture that our quantum algorithm uses only a constant number of queries, independent of the dimension  $n$ . These conjectures are supported by our (rigorous) results on the continuous curvelet transform; and we can argue (heuristically) that the effects caused by discretization should be small.

## 1.2 Related Work

Curvelets were first studied as a tool for image processing, and simulating wave propagation [7, 4]. There are a few rigorous results on the behavior of the curvelet transform, which are similar in spirit to our work. For instance, in [7] it is shown that, if  $f$  is a function on  $\mathbb{R}^2$ , and  $f$  is  $C^2$ -smooth away from a  $C^2$ -smooth edge, then the curvelet coefficients decay at a certain rate. From the proof, it is clear that the large curvelet coefficients are concentrated around the wavefront set. Also, in [5], it is shown that, for a function  $f$  on  $\mathbb{R}^2$ , the wavefront set of  $f$  consists of points  $(\vec{b}, \vec{\theta})$  where  $\Gamma_f(a, \vec{b}, \vec{\theta})$  does not decay rapidly as  $a \rightarrow 0$ . Compared to our work, these results apply to much broader classes of functions, but only over  $\mathbb{R}^2$ , not  $\mathbb{R}^n$ .

The curvelet transform is also related to older ideas from the study of Fourier integral operators; see, e.g., Smith [20], and the technique of second dyadic decomposition [21].

In connection with quantum algorithms, there has been some work on the quantum wavelet transform [13, 10, 14, 11]. Essentially, the quantum wavelet transform (using, say, Daubechies wavelets) can be computed efficiently, but few applications are known. We remark that the curvelet transform on  $\mathbb{R}^n$  is quite different from the “ordinary” wavelet transform on  $\mathbb{R}^n$ , which consists of a product of 1-D transforms. The ordinary wavelet transform on  $\mathbb{R}^n$  can detect the locations of discontinuities, but it cannot resolve directions.

The geometric problems studied in this paper are reminiscent of some recent work on finding hidden nonlinear structures, although the details are different. Shifted subset problems [8, 16] involve translational invariance, so the natural tool for solving them is the Fourier transform, rather than curvelets. Hidden polynomial problems [8, 9] resemble our problem of finding the center of a radial function. However, they are much more general (and thus much harder), and they are set over a finite field rather than  $\mathbb{R}^n$ .

Finally, we recently became aware of a quantum algorithm for estimating the gradient of a function  $f$  on  $\mathbb{R}^n$ , using only  $O(1)$  queries [15]. This is quite similar to our algorithm for finding the center of a radial function. The algorithm of [15] starts with a superposition over a small region of space, computes the value of  $f$  into the phases, then takes the Fourier transform. This is like applying the curvelet transform at a single location  $\vec{b}$ , and it yields similar results. Viewing this as a curvelet transform has a couple of advantages, though. First, the curvelet transform is a more general tool for doing this procedure at all locations  $\vec{b}$ , in superposition, on an arbitrary input state. Secondly, the curvelet transform allows a more rigorous analysis of the variance of the final result, by going over to the frequency domain.

### 1.3 Open Problems

This work suggests a number of open problems. One is to improve our analysis of the curvelet transform, in particular, to consider more complicated geometric objects in  $\mathbb{R}^n$  (without radial symmetry), and to handle discretization issues more rigorously.

Another open problem is to find new quantum algorithms based on the curvelet transform. For example, can one construct a curvelet transform over  $\mathbb{F}_q^n$ , that might be used to solve hidden polynomial problems? Are there quantum states that have “wavefront” structures, from which the curvelet transform could extract useful information? We will revisit these questions at the conclusion of the paper.

## 2 The Continuous Curvelet Transform

We begin by defining the continuous curvelet transform over  $\mathbb{R}^n$ . This generalizes the definition of [6] over  $\mathbb{R}^2$ .

Given a function  $f(\vec{x})$ , the continuous curvelet transform returns a function  $\Gamma_f(a, \vec{b}, \vec{\theta})$ . Here,  $\vec{x} \in \mathbb{R}^n$  represents a “location,” while  $0 < a < 1$  is a “scale” (smaller values denote finer scales, larger values denote coarser scales),  $\vec{b} \in \mathbb{R}^n$  is a “location,” and  $\vec{\theta} \in S^{n-1}$  (the unit sphere in  $\mathbb{R}^n$ ) is a “direction.” All functions return values in  $\mathbb{C}$ .

Intuitively, if  $f$  is discontinuous along a smooth surface  $S$  of dimension  $n - 1$ , then  $\Gamma_f$  will be “large” near points  $(a, \vec{b}, \vec{\theta})$  that satisfy the following conditions:  $\vec{b}$  lies on the surface  $S$ ,  $a$  has an appropriate value that matches the “sharpness” of the discontinuity at  $\vec{b}$ , and  $\vec{\theta}$  points in the direction normal to  $S$  at  $\vec{b}$ .

We will give two equivalent definitions of the curvelet transform. First,

$$\Gamma_f(a, \vec{b}, \vec{\theta}) := \int_{\mathbb{R}^n} \hat{f}(\vec{k}) \chi_{a, \vec{\theta}}(\vec{k}) e^{2\pi i \vec{k} \cdot \vec{b}} d\vec{k}. \quad (3)$$

Here,  $\hat{f}$  is the Fourier transform of  $f$ , and  $\chi_{a, \vec{\theta}}$  is a smooth window function, real, non-negative, supported on a sector of frequency space which depends on the scale  $a$  and direction  $\vec{\theta}$ . In particular,  $a$  scales like a power of 2, and  $\chi_{a, \vec{\theta}}$  is supported on a sector which is centered around direction  $\vec{\theta}$ , with depth  $1/a$  and width  $1/\sqrt{a}$  (note that this corresponds to angular width  $\sqrt{a}$ ). Evidently, the curvelet transform consists of (1) taking the Fourier transform of  $f$ , (2) separating  $\hat{f}$  into pieces corresponding to different scales and directions, and (3) taking the inverse Fourier transform. This point of view suggests how to compute the curvelet transform efficiently.

Equivalently, one can define

$$\Gamma_f(a, \vec{b}, \vec{\theta}) := \langle \gamma_{a, \vec{b}, \vec{\theta}}, f \rangle = \int_{\mathbb{R}^n} \gamma_{a, \vec{b}, \vec{\theta}}(\vec{x})^* f(\vec{x}) d\vec{x}, \quad (4)$$

where the  $\gamma_{a, \vec{b}, \vec{\theta}}$  are curvelet basis elements, and the  $*$  denotes complex conjugation. We define  $\gamma_{a, \vec{b}, \vec{\theta}}$  by translation from  $\gamma_{a, \vec{0}, \vec{\theta}}$ ,

$$\gamma_{a, \vec{b}, \vec{\theta}}(\vec{x}) := \gamma_{a, \vec{0}, \vec{\theta}}(\vec{x} - \vec{b}), \quad (5)$$

and we define  $\gamma_{a, \vec{0}, \vec{\theta}}$  in terms of its Fourier transform, which is simply the window function  $\chi_{a, \vec{\theta}}$  mentioned above,

$$\hat{\gamma}_{a, \vec{0}, \vec{\theta}}(\vec{k}) := \chi_{a, \vec{\theta}}(\vec{k}). \quad (6)$$

It is easy to check that this second definition is equivalent to the first one:

$$\Gamma_f(a, \vec{b}, \vec{\theta}) = \langle \hat{\gamma}_{a, \vec{b}, \vec{\theta}}, \hat{f} \rangle = \int_{\mathbb{R}^n} \left( \chi_{a, \vec{\theta}}(\vec{k}) e^{-2\pi i \vec{k} \cdot \vec{b}} \right)^* \hat{f}(\vec{k}) d\vec{k}.$$

This second definition gives us some insight into the curvelet basis elements:  $\gamma_{a,\vec{b},\vec{\theta}}$  is supported on a plate-like region, centered at location  $\vec{b}$ , orthogonal to direction  $\vec{\theta}$ , with thickness  $a$  and width  $\sqrt{a}$ , and high-frequency oscillations in the  $\vec{\theta}$  direction. Essentially,  $\gamma_{a,\vec{b},\vec{\theta}}$  resembles a plane-wave in direction  $\vec{\theta}$ , localized around the point  $\vec{b}$ .

Finally, we define the window function  $\chi_{a,\vec{\theta}}$  as follows. Write  $\vec{k}$  using spherical coordinates  $(r, \phi_1, \dots, \phi_{n-1})$ , centered around the direction  $\vec{\theta}$ , so that  $\phi_1$  is the angle between  $\vec{k}$  and  $\vec{\theta}$ . Then define

$$\chi_{a,\vec{\theta}}(\vec{k}) := W(\lambda r)V(\phi_1/\sqrt{a})\Lambda_a(\phi_1). \quad (7)$$

Here  $\lambda$  is a constant, which can be chosen freely; we will explain how to set it later.  $W$  is a radial window function, real, nonnegative, supported on the interval  $[1/e, 1]$ , and satisfying the admissibility condition

$$\int_0^\infty W(r)^2 \frac{dr}{r} = 1. \quad (8)$$

$V$  is an angular window function, real, nonnegative, supported on the interval  $[0, \pi/2]$ , and satisfying the admissibility condition

$$\int_{S^{n-1}} V(\phi_1)^2 d\sigma(\phi_1, \dots, \phi_{n-1}) = 1 \quad (9)$$

where  $d\sigma$  denotes integration over the unit sphere  $S^{n-1}$  in  $\mathbb{R}^n$ . Finally,  $\Lambda_a$  is a normalization and adjustment factor, needed because scaling by a factor of  $a$  changes the volume of the sector on which  $\chi_{a,\vec{\theta}}$  is supported:

$$\Lambda_a(\phi_1) := a^{(n+1)/4} \left( \frac{\sin(\phi_1/\sqrt{a})\sqrt{a}}{\sin(\phi_1)} \right)^{(n-2)/2}. \quad (10)$$

Note that, when  $\phi_1$  is small,  $\Lambda_a(\phi_1) \approx a^{(n+1)/4}$ . This is the main point where defining curvelets over  $\mathbb{R}^n$  is more complicated than over  $\mathbb{R}^2$ ; note that in dimension  $n = 2$ ,  $\Lambda_a(\phi_1) = a^{(n+1)/4} = a^{3/4}$  exactly. We remark that a simpler approach would be to use a constant normalization factor that only depends on  $a$  and not  $\phi_1$ ; however, our more complicated construction will be more convenient in the later sections of this paper.

We now state some basic properties of the curvelet transform. First, the curvelet transform works primarily on the high-frequency components of  $f$ , which correspond to fine-scale elements ( $a$  small). The constant factor  $\lambda$ , mentioned above, sets the low-frequency cutoff value, which corresponds to the coarsest scale ( $a = 1$ ). For convenience, here we assume that  $f$  has no low-frequency components below the cutoff value. In practice, when  $f$  has such low-frequency components, the curvelet transform leaves them unchanged, and simply returns them as a residual function  $f_{\text{res}}$ .

Next, we define the reference measure

$$d\mu(a, \vec{b}, \vec{\theta}) := \frac{da \, d\vec{b} \, d\sigma(\vec{\theta})}{a^{n+1}}. \quad (11)$$

This weights the contributions of  $\Gamma_f(a, \vec{b}, \vec{\theta})$  differently according to the scale  $a$ . Intuitively, this means that  $(a, \vec{b}, \vec{\theta})$  should be sampled in a certain way. To see this, write

$$d\mu(a, \vec{b}, \vec{\theta}) = \frac{da}{a} \frac{d\vec{b}}{a^{(n+1)/2}} \frac{d\sigma(\vec{\theta})}{a^{(n-1)/2}}. \quad (12)$$

Note that  $\frac{da}{a} = d(\log a)$ , suggesting that we should sample  $\log(a)$  at uniform intervals; we should sample  $\vec{b}$  on a grid in  $\mathbb{R}^n$  whose cells have size  $a \times (\sqrt{a})^{n-1}$ ; and we should sample  $\vec{\theta}$  on a mesh on  $S^{n-1}$  whose cells have size  $(\sqrt{a})^{n-1}$ . This is consistent with the tiling of

the frequency domain shown in Figure 2. (Later, when we construct the discrete curvelet transform, we will use this sampling trick for  $a$  and  $\vec{\theta}$ , in place of the reference measure.)

Then we have the following theorems:

**Theorem 1** *Suppose that  $\hat{f}(\vec{k}) = 0$  for all  $|\vec{k}| < 1/\lambda$ . Then we can recover  $f$  from its curvelet transform  $\Gamma_f$ :*

$$f(\vec{x}) = \int_{a < 1} \Gamma_f(a, \vec{b}, \vec{\theta}) \gamma_{a, \vec{b}, \vec{\theta}}(\vec{x}) d\mu(a, \vec{b}, \vec{\theta}). \quad (13)$$

**Theorem 2** *Suppose that  $\hat{f}(\vec{k}) = 0$  for all  $|\vec{k}| < 1/\lambda$ . Then the curvelet transform preserves the  $L^2$  norm:*

$$\int_{\mathbb{R}^n} |f(\vec{x})|^2 d\vec{x} = \int_{a < 1} |\Gamma_f(a, \vec{b}, \vec{\theta})|^2 d\mu(a, \vec{b}, \vec{\theta}). \quad (14)$$

These are straightforward generalizations (to the case of  $\mathbb{R}^n$ ) of results in [6]. We sketch the proofs below:

First, for any  $a$  and  $\vec{\theta}$ , let us define

$$g_{a, \vec{\theta}}(\vec{x}) := \int_{\mathbb{R}^n} \langle \gamma_{a, \vec{b}, \vec{\theta}}, f \rangle \gamma_{a, \vec{b}, \vec{\theta}}(\vec{x}) d\vec{b}. \quad (15)$$

We claim that

$$\hat{g}_{a, \vec{\theta}}(\vec{k}) = |\chi_{a, \vec{\theta}}(\vec{k})|^2 \hat{f}(\vec{k}). \quad (16)$$

To see this, write

$$\langle \gamma_{a, \vec{b}, \vec{\theta}}, f \rangle = \int_{\mathbb{R}^n} \gamma_{a, \vec{b}, \vec{\theta}}^*(\vec{y} - \vec{b}) f(\vec{y}) d\vec{y} = (\tilde{\gamma}_{a, \vec{b}, \vec{\theta}}^* * f)(\vec{b}),$$

where we define

$$\tilde{\gamma}_{a, \vec{b}, \vec{\theta}}(\vec{x}) = \gamma_{a, \vec{b}, \vec{\theta}}(-\vec{x}).$$

Thus we can write  $g_{a, \vec{\theta}}(\vec{x})$  as

$$g_{a, \vec{\theta}}(\vec{x}) = \int_{\mathbb{R}^n} \gamma_{a, \vec{b}, \vec{\theta}}(\vec{x} - \vec{b}) (\tilde{\gamma}_{a, \vec{b}, \vec{\theta}}^* * f)(\vec{b}) d\vec{b} = (\gamma_{a, \vec{b}, \vec{\theta}} * \tilde{\gamma}_{a, \vec{b}, \vec{\theta}}^* * f)(\vec{x}).$$

Taking the Fourier transform, we get

$$\hat{g}_{a, \vec{\theta}}(\vec{k}) = \hat{\gamma}_{a, \vec{b}, \vec{\theta}}(\vec{k}) (\tilde{\gamma}_{a, \vec{b}, \vec{\theta}}^*)^\wedge(\vec{k}) \hat{f}(\vec{k}) = |\hat{\gamma}_{a, \vec{b}, \vec{\theta}}(\vec{k})|^2 \hat{f}(\vec{k}),$$

using the fact that

$$(\tilde{\gamma}_{a, \vec{b}, \vec{\theta}}^*)^\wedge(\vec{k}) = \int_{\mathbb{R}^n} \gamma_{a, \vec{b}, \vec{\theta}}^*(-\vec{x}) e^{-2\pi i \vec{k} \cdot \vec{x}} d\vec{x} = \int_{\mathbb{R}^n} \gamma_{a, \vec{b}, \vec{\theta}}^*(\vec{x}) e^{2\pi i \vec{k} \cdot \vec{x}} d\vec{x} = (\hat{\gamma}_{a, \vec{b}, \vec{\theta}}(\vec{k}))^*.$$

This proves equation (16).

Next, we claim that, for all  $|\vec{k}| \geq 1/\lambda$ ,

$$\int_0^1 \int_{S^{n-1}} |\chi_{a, \vec{\theta}}(\vec{k})|^2 d\sigma(\vec{\theta}) \frac{da}{a^{n+1}} = 1. \quad (17)$$

To see this, proceed as follows. Fix  $\vec{k}$ , and write  $\vec{\theta}$  in spherical coordinates centered around  $\vec{k}$ , such that  $\theta_1$  is the angle between  $\vec{\theta}$  and  $\vec{k}$ . Then we have

$$\chi_{a, \vec{\theta}}(\vec{k}) = W(\lambda a |\vec{k}|) V(\theta_1 / \sqrt{a}) a^{(n+1)/4} \left( \frac{\sin(\theta_1 / \sqrt{a}) \sqrt{a}}{\sin(\theta_1)} \right)^{(n-2)/2}.$$



Then substitute into the integral:

$$\begin{aligned}
& \int_0^1 \int_{S^{n-1}} |\chi_{a,\vec{\theta}}(\vec{k})|^2 d\sigma(\vec{\theta}) \frac{da}{a^{n+1}} \\
&= \int_0^1 \int_{S^{n-1}} W(\lambda a |\vec{k}|)^2 V(\theta_1/\sqrt{a})^2 a^{(n+1)/2} \left( \frac{\sin(\theta_1/\sqrt{a})}{\sin(\theta_1)} \right)^{n-2} a^{(n-2)/2} d\sigma(\vec{\theta}) \frac{da}{a^{n+1}} \\
&= \int_0^1 \int_{S^{n-1}} W(\lambda a |\vec{k}|)^2 V(\theta_1/\sqrt{a})^2 \sin^{n-2}(\theta_1/\sqrt{a}) d\theta_1 d\sigma(\theta_2, \dots, \theta_{n-1}) \frac{da}{a^{3/2}}.
\end{aligned}$$

Note that  $V(\theta_1/\sqrt{a})$  is nonzero only when  $\theta_1 \in [0, \pi\sqrt{a}]$ , so we can restrict the integral to this range. Then change variables,  $\theta'_1 = \theta_1/\sqrt{a}$ , to get:

$$\begin{aligned}
& \int_0^1 \int_{S^{n-1}} |\chi_{a,\vec{\theta}}(\vec{k})|^2 d\sigma(\vec{\theta}) \frac{da}{a^{n+1}} \\
&= \int_0^1 \int_{S^{n-1}} W(\lambda a |\vec{k}|)^2 V(\theta'_1)^2 \sin^{n-2}(\theta'_1) d\theta'_1 \sqrt{a} d\sigma(\theta_2, \dots, \theta_{n-1}) \frac{da}{a^{3/2}} \\
&= \int_0^1 \int_{S^{n-1}} W(\lambda a |\vec{k}|)^2 V(\theta_1)^2 d\sigma(\vec{\theta}) \frac{da}{a} \\
&= \int_0^{\lambda|\vec{k}|} W(a)^2 \frac{da}{a} \int_{S^{n-1}} V(\theta_1)^2 d\sigma(\vec{\theta}) \\
&= 1,
\end{aligned}$$

using the admissibility conditions. This proves equation (17).

We now prove Theorem 1. We write

$$\begin{aligned}
& \int_{a < 1} \Gamma_f(a, \vec{b}, \vec{\theta}) \gamma_{a,\vec{b},\vec{\theta}}(\vec{x}) d\mu(a, \vec{b}, \vec{\theta}) \\
&= \int_0^1 \int_{S^{n-1}} \int_{\mathbb{R}^n} \langle \gamma_{a,\vec{b},\vec{\theta}}, f \rangle \gamma_{a,\vec{b},\vec{\theta}}(\vec{x}) d\vec{b} d\sigma(\vec{\theta}) \frac{da}{a^{n+1}} \\
&= \int_0^1 \int_{S^{n-1}} g_{a,\vec{\theta}}(\vec{x}) d\sigma(\vec{\theta}) \frac{da}{a^{n+1}},
\end{aligned}$$

and we claim that this equals  $f(\vec{x})$ . Taking the Fourier transform, we get

$$\int_0^1 \int_{S^{n-1}} \hat{g}_{a,\vec{\theta}}(\vec{k}) d\sigma(\vec{\theta}) \frac{da}{a^{n+1}},$$

and we claim that this equals  $\hat{f}(\vec{k})$ . Using equations (16) and (17), we rewrite this integral as:

$$\int_0^1 \int_{S^{n-1}} |\chi_{a,\vec{\theta}}(\vec{k})|^2 \hat{f}(\vec{k}) d\sigma(\vec{\theta}) \frac{da}{a^{n+1}} = \hat{f}(\vec{k}).$$

(The last equality holds because of (17) when  $|\vec{k}| \geq 1/\lambda$ , and because  $\hat{f}(\vec{k}) = 0$  when  $|\vec{k}| < 1/\lambda$ .) This proves Theorem 1.

Finally, we prove Theorem 2. We write

$$\int_{a < 1} |\Gamma_f(a, \vec{b}, \vec{\theta})|^2 d\mu(a, \vec{b}, \vec{\theta}) = \int_0^1 \int_{S^{n-1}} \int_{\mathbb{R}^n} |\langle \gamma_{a,\vec{b},\vec{\theta}}, f \rangle|^2 d\vec{b} d\sigma(\vec{\theta}) \frac{da}{a^{n+1}}.$$

We rewrite the innermost integral, applying some of the identities used to prove (16):

$$\begin{aligned}
\int_{\mathbb{R}^n} |\langle \gamma_{a, \vec{b}, \vec{\theta}}, f \rangle|^2 d\vec{b} &= \int_{\mathbb{R}^n} |(\tilde{\gamma}_{a, \vec{0}, \vec{\theta}}^* * f)(\vec{b})|^2 d\vec{b} \\
&= \int_{\mathbb{R}^n} |(\tilde{\gamma}_{a, \vec{0}, \vec{\theta}}^* \hat{f})(\vec{k})|^2 d\vec{k} \\
&= \int_{\mathbb{R}^n} |(\hat{\gamma}_{a, \vec{0}, \vec{\theta}}(\vec{k}))^* \hat{f}(\vec{k})|^2 d\vec{k} \\
&= \int_{\mathbb{R}^n} |\chi_{a, \vec{\theta}}(\vec{k})|^2 |\hat{f}(\vec{k})|^2 d\vec{k}.
\end{aligned}$$

Substituting in, and using (17), we get:

$$\begin{aligned}
&\int_{a < 1} |\Gamma_f(a, \vec{b}, \vec{\theta})|^2 d\mu(a, \vec{b}, \vec{\theta}) \\
&= \int_0^1 \int_{S^{n-1}} \int_{\mathbb{R}^n} |\chi_{a, \vec{\theta}}(\vec{k})|^2 |\hat{f}(\vec{k})|^2 d\vec{k} d\sigma(\vec{\theta}) \frac{da}{a^{n+1}} \\
&= \int_{\mathbb{R}^n} \int_0^1 \int_{S^{n-1}} |\chi_{a, \vec{\theta}}(\vec{k})|^2 d\sigma(\vec{\theta}) \frac{da}{a^{n+1}} |\hat{f}(\vec{k})|^2 d\vec{k} \\
&= \int_{\mathbb{R}^n} |\hat{f}(\vec{k})|^2 d\vec{k} = \int_{\mathbb{R}^n} |f(\vec{x})|^2 d\vec{x}.
\end{aligned}$$

This proves Theorem 2.

### 3 The curvelet transform of a radial function

Let  $f$  be a radial function,  $f(\vec{x}) = f_0(|\vec{x}|)$ . Its Fourier transform is also radial,  $\hat{f}(\vec{k}) = F_0(|\vec{k}|)$ , where

$$F_0(\rho) = \frac{2\pi}{\rho^{(n-2)/2}} \int_0^\infty J_{(n-2)/2}(2\pi\rho r) f_0(r) r^{n/2} dr, \quad (18)$$

and  $J$  is a Bessel function (see, e.g., [22]). We assume that  $f$  is normalized so that  $\int_{\mathbb{R}^n} |f(\vec{x})|^2 d\vec{x} = 1$ .

When  $f$  is radial,  $\Gamma_f$  has the following symmetries:

$$\Gamma_f(a, \vec{b}, \vec{\theta}) = \Gamma_f(a, -\vec{b}, -\vec{\theta}), \quad (19)$$

and for any rotation  $R$ ,

$$\Gamma_f(a, \vec{b}, \vec{\theta}) = \Gamma_f(a, R\vec{b}, R\vec{\theta}). \quad (20)$$

$|\Gamma_f(a, \vec{b}, \vec{\theta})|^2 d\mu(a, \vec{b}, \vec{\theta})$  can be interpreted as a probability density over the different scales, locations and directions  $(a, \vec{b}, \vec{\theta})$ . In this section we will develop some general tools for understanding where this probability mass is concentrated.

We make a particular choice for the radial and angular windows. These windows are  $C^1$  smooth, which is necessary in our analysis of the variance of  $\vec{b}$ . First, the radial window  $W$ :

$$W(r) = \begin{cases} C_w \sin(\pi \log r)^2, & 1/e \leq r \leq 1, \\ 0, & \text{otherwise,} \end{cases} \quad (21)$$

$$C_w = \sqrt{8/3}. \quad (22)$$

Next, the angular window  $V$ :

$$V(t) = \begin{cases} C_v \cos(t)^2, & 0 \leq t \leq \pi/2, \\ 0, & \text{otherwise,} \end{cases} \quad (23)$$

$$C_v = \sqrt{\frac{2(n+2)n}{3S_0}}. \quad (24)$$

### 3.1 The probability of observing a scale $a$

First, we claim that the probability of observing a fine-scale element  $a$  is related to the decay of  $\hat{f}$  away from the origin:

$$\Pr[a \leq \eta] = \int_{a \leq \eta} |\Gamma_f(a, \vec{b}, \vec{\theta})|^2 d\mu(a, \vec{b}, \vec{\theta}) \geq \int_{|\vec{k}| \geq 1/(\lambda\eta)} |\hat{f}(\vec{k})|^2 d\vec{k}. \quad (25)$$

This follows from the same argument used to prove Theorem 2. In the case of a radial function, we write this as:

$$\Pr[a \leq \eta] \geq S_0 \int_{1/(\lambda\eta)}^{\infty} F_0(\rho)^2 \rho^{n-1} d\rho, \quad (26)$$

where  $S_0 = \frac{2\pi^{n/2}}{\Gamma(n/2)}$  is the surface area of the sphere  $S^{n-1} \subset \mathbb{R}^n$ .

### 3.2 The location $\vec{b}$ and direction $\vec{\theta}$

We claim that the location  $\vec{b}$  has expectation value  $\vec{0}$ . To see this, write:

$$\begin{aligned} \mathbb{E}(b_j) &= \int b_j |\Gamma_f(a, \vec{b}, \vec{\theta})|^2 d\mu(a, \vec{b}, \vec{\theta}) \\ &= \int_{S^{n-1}} \int_0^1 \int_{\mathbb{R}^n} b_j |\Gamma_f(a, \vec{b}, \vec{\theta})|^2 d\vec{b} \frac{da}{a^{n+1}} d\sigma(\vec{\theta}) \\ &= \int_{S^{n-1}} \int_0^1 \int_{\mathbb{R}^n} -b_j |\Gamma_f(a, \vec{b}, \vec{\theta})|^2 d\vec{b} \frac{da}{a^{n+1}} d\sigma(\vec{\theta}) \\ &= \mathbb{E}(-b_j), \end{aligned}$$

using equation (19) and a change of variables; thus  $\mathbb{E}(b_j) = 0$ . Note that this remains true when we condition on the value of  $a$ .

Also, we claim that the direction  $\vec{\theta}$  is uniformly distributed. To see this, let  $\vec{\theta}_0, \vec{\theta}_1 \in S^{n-1}$ , and write:

$$\begin{aligned} \mathbb{P}(\vec{\theta} = \vec{\theta}_0) &= \int_{\vec{\theta}=\vec{\theta}_0} |\Gamma_f(a, \vec{b}, \vec{\theta})|^2 d\mu(a, \vec{b}, \vec{\theta}) \\ &= \int_0^1 \int_{\mathbb{R}^n} |\Gamma_f(a, \vec{b}, \vec{\theta}_0)|^2 d\vec{b} \frac{da}{a^{n+1}} \\ &= \int_0^1 \int_{\mathbb{R}^n} |\Gamma_f(a, \vec{b}, \vec{\theta}_1)|^2 d\vec{b} \frac{da}{a^{n+1}} \\ &= \mathbb{P}(\vec{\theta} = \vec{\theta}_1), \end{aligned}$$

using equation (20) and a change of variables; thus the distribution is uniform. Note that this remains true when we condition on the value of  $a$ , and when we condition on the value of  $\vec{b} \cdot \vec{\theta}$  (since this preserves the rotational symmetry).

### 3.3 The variance of $\vec{b}$

Finally, we seek to bound the variance of  $\vec{b}$ , in the directions perpendicular to  $\vec{\theta}$ , as well as parallel to  $\vec{\theta}$ .

The variance of  $\vec{b}$  perpendicular to  $\vec{\theta}$  is:

$$\mathbb{E}(\vec{b}^T(I - \vec{\theta}\vec{\theta}^T)\vec{b}) = \int_{S^{n-1}} \int_0^1 \int_{\mathbb{R}^n} (\vec{b}^T(I - \vec{\theta}\vec{\theta}^T)\vec{b}) |\Gamma_f(a, \vec{b}, \vec{\theta})|^2 d\vec{b} \frac{da}{a^{n+1}} d\sigma(\vec{\theta}). \quad (27)$$

We can simplify this by taking advantage of rotational symmetry. Fix a vector  $\vec{u} = (1, 0, \dots, 0)$ , and for each  $\vec{\theta}$ , let  $R$  be a rotation that maps  $\vec{\theta}$  to  $\vec{u}$ . Then

$$\mathbb{E}(\vec{b}^T(I - \vec{\theta}\vec{\theta}^T)\vec{b}) = \int_{S^{n-1}} \int_0^1 \int_{\mathbb{R}^n} (R(\vec{b})^T(I - \vec{u}\vec{u}^T)R(\vec{b})) |\Gamma_f(a, R(\vec{b}), \vec{u})|^2 d\vec{b} \frac{da}{a^{n+1}} d\sigma(\vec{\theta}). \quad (28)$$

Then change variables  $\vec{b} \mapsto R^{-1}(\vec{b})$ . The integrand is now independent of  $\vec{\theta}$ , so we can do the  $\vec{\theta}$  integral. We get:

$$\mathbb{E}(\vec{b}^T(I - \vec{\theta}\vec{\theta}^T)\vec{b}) = S_0 \int_0^1 \int_{\mathbb{R}^n} (\vec{b}^T(I - \vec{u}\vec{u}^T)\vec{b}) |\Gamma_f(a, \vec{b}, \vec{u})|^2 d\vec{b} \frac{da}{a^{n+1}}. \quad (29)$$

We now introduce some new notation,

$$\Phi_{a, \vec{\theta}}(\vec{b}) := \Gamma_f(a, \vec{b}, \vec{\theta}), \quad (30)$$

to emphasize that we view this as a function of  $\vec{b}$ . By equation (3), the Fourier transform of  $\Phi_{a, \vec{\theta}}$  is given by

$$\hat{\Phi}_{a, \vec{\theta}}(\vec{k}) = \hat{f}(\vec{k}) \chi_{a, \vec{\theta}}(\vec{k}). \quad (31)$$

And we have:

$$\mathbb{E}(\vec{b}^T(I - \vec{\theta}\vec{\theta}^T)\vec{b}) = S_0 \int_0^1 \int_{\mathbb{R}^n} (\vec{b}^T(I - \vec{u}\vec{u}^T)\vec{b}) |\Phi_{a, \vec{u}}(\vec{b})|^2 d\vec{b} \frac{da}{a^{n+1}}. \quad (32)$$

Let  $I_K$  denote the innermost integral in the above expression. Then

$$I_K = \sum_{j=2}^n \int_{\mathbb{R}^n} |b_j|^2 |\Phi_{a, \vec{u}}(\vec{b})|^2 d\vec{b}. \quad (33)$$

Using Plancherel's theorem, and symmetry with respect to rotations around the  $\vec{u}$  axis,

$$\begin{aligned} I_K &= \sum_{j=2}^n \int_{\mathbb{R}^n} \left| \frac{1}{2\pi i} \frac{\partial}{\partial k_j} \hat{\Phi}_{a, \vec{u}}(\vec{k}) \right|^2 d\vec{k} \\ &= \frac{n-1}{(2\pi)^2} \int_{\mathbb{R}^n} \left| \frac{\partial}{\partial k_2} \hat{\Phi}_{a, \vec{u}}(\vec{k}) \right|^2 d\vec{k}. \end{aligned} \quad (34)$$

Now, using spherical coordinates  $\vec{k} = (r, \phi_1, \dots, \phi_{n-1})$ , we write  $\hat{\Phi}_{a, \vec{u}}(\vec{k})$  as a product of a radial part and an angular part:

$$\hat{\Phi}_{a, \vec{u}}(\vec{k}) = L(r)M(\phi_1), \quad (35)$$

where

$$L(r) = F_0(r)W(\lambda ar), \quad M(\phi_1) = V(\phi_1/\sqrt{a})\Lambda_a(\phi_1). \quad (36)$$

Then we have

$$\frac{\partial}{\partial k_2} \hat{\Phi}_{a, \vec{u}}(\vec{k}) = L'(r)M(\phi_1) \frac{\partial r}{\partial k_2} + L(r)M'(\phi_1) \frac{\partial \phi_1}{\partial k_2}, \quad (37)$$

where

$$\frac{\partial r}{\partial k_2} = \sin \phi_1 \cos \phi_2, \quad \frac{\partial \phi_1}{\partial k_2} = \frac{\cos \phi_1 \cos \phi_2}{r}. \quad (38)$$

Now we can expand out the following integral: (note that  $\hat{\Phi}_{a,\vec{u}}(\vec{k})$  is real)

$$\begin{aligned} \int_{\mathbb{R}^n} \left| \frac{\partial}{\partial k_2} \hat{\Phi}_{a,\vec{u}}(\vec{k}) \right|^2 d\vec{k} &= \int_{S^{n-1}} \int_0^\infty \left( L'(r)M(\phi_1) \sin \phi_1 \cos \phi_2 \right. \\ &\quad \left. + L(r)M'(\phi_1)r^{-1} \cos \phi_1 \cos \phi_2 \right)^2 r^{n-1} dr d\sigma(\vec{\phi}) \\ &= I_{Ar}I_{A1}I_2 + 2I_{Br}I_{B1}I_2 + I_{Cr}I_{C1}I_2, \end{aligned} \quad (39)$$

where we define

$$I_{Ar} = \int_0^\infty L'(r)^2 r^{n-1} dr \quad (40)$$

$$I_{A1} = \int_0^\pi M(\phi_1)^2 \sin^n \phi_1 d\phi_1 \quad (41)$$

$$I_2 = \int_{S^{n-2}} \cos^2 \phi_2 d\sigma(\phi_2, \dots, \phi_{n-1}) \quad (42)$$

$$I_{Br} = \int_0^\infty L'(r)L(r)r^{n-2} dr \quad (43)$$

$$I_{B1} = \int_0^\pi M'(\phi_1)M(\phi_1) \cos \phi_1 \sin^{n-1} \phi_1 d\phi_1 \quad (44)$$

$$I_{Cr} = \int_0^\infty L(r)^2 r^{n-3} dr \quad (45)$$

$$I_{C1} = \int_0^\pi M'(\phi_1)^2 \cos^2 \phi_1 \sin^{n-2} \phi_1 d\phi_1. \quad (46)$$

Thus we can write the variance of  $\vec{b}$  perpendicular to  $\vec{\theta}$  as:

$$\mathbb{E}(\vec{b}^T(I - \vec{\theta}\vec{\theta}^T)\vec{b}) = \frac{n-1}{(2\pi)^2} S_0 \int_0^1 \left( I_{Ar}I_{A1}I_2 + 2I_{Br}I_{B1}I_2 + I_{Cr}I_{C1}I_2 \right) \frac{da}{a^{n+1}}. \quad (47)$$

A similar formula gives the variance conditioned on observing  $a \leq \eta$ :

$$\begin{aligned} \mathbb{E}(\vec{b}^T(I - \vec{\theta}\vec{\theta}^T)\vec{b} \mid a \leq \eta) \\ = \frac{1}{\Pr[a \leq \eta]} \frac{n-1}{(2\pi)^2} S_0 \int_0^\eta \left( I_{Ar}I_{A1}I_2 + 2I_{Br}I_{B1}I_2 + I_{Cr}I_{C1}I_2 \right) \frac{da}{a^{n+1}}. \end{aligned} \quad (48)$$

We would then like to bound the various integrals appearing on the right hand side.

### 3.3.1

We begin with the integral  $\int_0^\eta I_{Br}I_{B1}I_2 da/a^{n+1}$ . A straightforward calculation shows that

$$I_2 = \frac{1}{n-1} \int_{S^{n-2}} d\sigma(\phi_2, \dots, \phi_{n-1}). \quad (49)$$

We can simplify  $I_{B1}$ , by integrating by parts:

$$\begin{aligned} I_{B1} &= \frac{1}{2} M(\phi_1)^2 \cos \phi_1 \sin^{n-1} \phi_1 \Big|_0^\pi - \int_0^\pi \frac{1}{2} M(\phi_1)^2 (-\sin^n \phi_1 + (n-1) \cos^2 \phi_1 \sin^{n-2} \phi_1) d\phi_1 \\ &= - \int_0^\pi \frac{1}{2} M(\phi_1)^2 (-1 + n \cos^2 \phi_1) \sin^{n-2} \phi_1 d\phi_1. \end{aligned}$$

Substituting in the definition of  $M(\phi_1)$ , changing variables, and using the fact that  $V$  is supported on the interval  $[0, \pi/2]$ , we get:

$$\begin{aligned}
I_{B1} &= - \int_0^\pi \frac{1}{2} V(\phi_1/\sqrt{a})^2 a^{(2n-1)/2} \left( \frac{\sin(\phi_1/\sqrt{a})}{\sin \phi_1} \right)^{n-2} (-1 + n \cos^2 \phi_1) \sin^{n-2} \phi_1 d\phi_1 \\
&= - \int_0^\pi \frac{1}{2} V(\phi_1/\sqrt{a})^2 a^{(2n-1)/2} \sin(\phi_1/\sqrt{a})^{n-2} (-1 + n \cos^2 \phi_1) d\phi_1 \\
&= - \int_0^{\pi/\sqrt{a}} \frac{1}{2} V(\omega_1)^2 a^n \sin^{n-2} \omega_1 (-1 + n \cos^2(\omega_1 \sqrt{a})) d\omega_1 \\
&= \int_0^{\pi/2} \frac{1}{2} V(\omega_1)^2 a^n \sin^{n-2} \omega_1 (1 - n \cos^2(\omega_1 \sqrt{a})) d\omega_1, \\
|I_{B1}| &\leq \frac{1}{2} a^n (n-1) \int_0^{\pi/2} V(\omega_1)^2 \sin^{n-2} \omega_1 d\omega_1.
\end{aligned}$$

Combining this with  $I_2$ , we get:

$$|I_{B1} I_2| \leq \frac{1}{2} a^n \int_{S^{n-1}} V(\omega_1)^2 d\sigma(\omega_1, \phi_2, \dots, \phi_{n-1}) = \frac{1}{2} a^n. \quad (50)$$

Next, we can simplify  $I_{Br}$ , by integrating by parts:

$$\begin{aligned}
I_{Br} &= \frac{1}{2} L(r)^2 r^{n-2} \Big|_0^\infty - \int_0^\infty \frac{1}{2} L(r)^2 (n-2) r^{n-3} dr \\
&= - \int_0^\infty \frac{1}{2} L(r)^2 (n-2) r^{n-3} dr
\end{aligned}$$

Combining this with  $I_{B1}$  and  $I_2$ , substituting in the definition of  $L(r)$ , and exchanging the integrals, we get:

$$\begin{aligned}
\left| \int_0^\eta I_{Br} I_{B1} I_2 \frac{da}{a^{n+1}} \right| &\leq \int_0^\eta |I_{Br}| \frac{1}{2} \frac{da}{a} \\
&= \int_0^\eta \int_0^\infty \frac{1}{2} L(r)^2 (n-2) r^{n-3} dr \frac{1}{2} \frac{da}{a} \\
&= \int_0^\eta \int_0^\infty \frac{1}{2} F_0(r)^2 W(\lambda ar)^2 (n-2) r^{n-3} dr \frac{1}{2} \frac{da}{a} \\
&\leq \int_0^\infty \frac{1}{2} F_0(r)^2 \int_0^\eta W(\lambda ar)^2 \frac{1}{2} \frac{da}{a} (n-2) r^{n-3} dr.
\end{aligned}$$

By the definition of  $W$ ,

$$\int_0^\eta W(\lambda ar)^2 \frac{1}{2} \frac{da}{a} = \int_0^{\lambda \eta r} W(\alpha)^2 \frac{1}{2} \frac{d\alpha}{\alpha} \leq \frac{1}{2}, \quad (51)$$

and vanishes when  $r \leq 1/(\lambda \eta e)$ . Thus we have:

$$\boxed{\left| \int_0^\eta I_{Br} I_{B1} I_2 \frac{da}{a^{n+1}} \right| \leq \frac{1}{4} (n-2) \int_{1/(\lambda \eta e)}^\infty F_0(r)^2 r^{n-3} dr.} \quad (52)$$

### 3.3.2

Next, consider the integral  $\int_0^\eta I_{Ar} I_{A1} I_2 da/a^{n+1}$ . We already have a bound for  $I_2$ . For  $I_{A1}$ , we write:

$$\begin{aligned}
I_{A1} &= \int_0^\pi V(\phi_1/\sqrt{a})^2 a^{(2n-1)/2} \left( \frac{\sin(\phi_1/\sqrt{a})}{\sin \phi_1} \right)^{n-2} \sin^n \phi_1 d\phi_1 \\
&= \int_0^{\pi/\sqrt{a}} V(\omega_1)^2 a^n \sin^{n-2} \omega_1 \sin^2(\omega_1 \sqrt{a}) d\omega_1.
\end{aligned}$$

Using the fact that  $V$  is supported on  $[0, \pi/2]$ , and the simple bound  $\sin^2(\omega_1\sqrt{a}) \leq \omega_1^2 a \leq \frac{\pi^2}{4}a$ , we get:

$$0 \leq I_{A1} \leq \int_0^{\pi/2} V(\omega_1)^2 a^n \sin^{n-2} \omega_1 d\omega_1 \frac{\pi^2}{4} a.$$

Combining with  $I_2$ , we get:

$$0 \leq I_{A1} I_2 \leq \frac{\pi^2}{4} \frac{a^{n+1}}{n-1} \int_{S^{n-1}} V(\omega_1)^2 d\sigma(\omega_1, \phi_2, \dots, \phi_{n-1}) = \frac{\pi^2}{4} \frac{a^{n+1}}{n-1}. \quad (53)$$

We now turn to  $I_{Ar}$ . First, combining with  $I_{A1}$  and  $I_2$ , we have

$$0 \leq \int_0^\eta I_{Ar} I_{A1} I_2 \frac{da}{a^{n+1}} \leq \int_0^\eta I_{Ar} da \cdot \frac{\pi^2}{4(n-1)}. \quad (54)$$

We can upper-bound  $I_{Ar}$  as follows. Note that, for any two  $L^2$  functions, the Cauchy-Schwarz inequality implies that

$$\|f + g\|^2 = \|f\|^2 + 2\langle f, g \rangle + \|g\|^2 \leq \|f\|^2 + 2\|f\|\|g\| + \|g\|^2 \leq 2\|f\|^2 + 2\|g\|^2; \quad (55)$$

in the last step we used the arithmetic-geometric mean inequality,  $\sqrt{ab} \leq \frac{a+b}{2}$  for  $a, b \geq 0$ , with  $a = \|f\|^2$  and  $b = \|g\|^2$ . Thus we can write

$$\begin{aligned} 0 \leq I_{Ar} &= \int_0^\infty \left( F_0'(r)W(\lambda ar) + F_0(r)W'(\lambda ar)\lambda a \right)^2 r^{n-1} dr \\ &= \|G_1 + G_2\|^2 \leq 2\|G_1\|^2 + 2\|G_2\|^2, \end{aligned} \quad (56)$$

where we define

$$G_1(r) = F_0'(r)W(\lambda ar)r^{(n-1)/2} \quad (57)$$

$$G_2(r) = F_0(r)W'(\lambda ar)\lambda ar^{(n-1)/2}. \quad (58)$$

Thus we have

$$\boxed{0 \leq \int_0^\eta I_{Ar} I_{A1} I_2 \frac{da}{a^{n+1}} \leq \left( \int_0^\eta \|G_1\|^2 da + \int_0^\eta \|G_2\|^2 da \right) \cdot \frac{\pi^2}{2(n-1)}}. \quad (59)$$

We then want to upper-bound the integrals  $\int_0^\eta \|G_1\|^2 da$  and  $\int_0^\eta \|G_2\|^2 da$ .

For the first one, we have:

$$\begin{aligned} \int_0^\eta \|G_1\|^2 da &= \int_0^\eta \int_0^\infty F_0'(r)^2 W(\lambda ar)^2 r^{n-1} dr da \\ &= \int_0^\infty F_0'(r)^2 \int_0^\eta W(\lambda ar)^2 da r^{n-1} dr. \end{aligned}$$

Using the fact that  $W$  is supported on  $[1/e, 1]$ , we can write

$$\int_0^\eta W(\lambda ar)^2 da = \int_0^{\lambda\eta r} W(\alpha)^2 d\alpha \frac{1}{\lambda r} \leq \int_0^{\lambda\eta r} W(\alpha)^2 \frac{d\alpha}{\alpha} \frac{1}{\lambda r} \leq \frac{1}{\lambda r}, \quad (60)$$

and vanishes when  $r \leq 1/(\lambda\eta e)$ . Hence,

$$\boxed{\int_0^\eta \|G_1\|^2 da \leq \frac{1}{\lambda} \int_{1/(\lambda\eta e)}^\infty F_0'(r)^2 r^{n-2} dr}. \quad (61)$$

For the second integral, we have:

$$\begin{aligned}\int_0^\eta \|G_2\|^2 da &= \int_0^\eta \int_0^\infty F_0(r)^2 W'(\lambda ar)^2 \lambda^2 a^2 r^{n-1} dr da \\ &= \int_0^\infty F_0(r)^2 \int_0^\eta W'(\lambda ar)^2 \lambda^2 a^2 da r^{n-1} dr.\end{aligned}$$

Note that the derivative of  $W$  is given by

$$W'(r) = \begin{cases} C_w \sin(2\pi \log r) \pi / r, & 1/e \leq r \leq 1, \\ 0, & \text{otherwise,} \end{cases} \quad (62)$$

where  $C_w = \sqrt{8/3}$ . So we can write

$$\int_0^\eta W'(\lambda ar)^2 \lambda^2 a^2 da = \int_0^{\lambda \eta r} W'(\alpha)^2 \alpha^2 d\alpha \frac{1}{\lambda r^3} \leq \int_{1/e}^1 C_w^2 (\pi/\alpha)^2 \alpha^2 d\alpha \frac{1}{\lambda r^3} = \frac{8}{3} \pi^2 (1 - \frac{1}{e}) \frac{1}{\lambda r^3}, \quad (63)$$

and vanishes when  $r \leq 1/(\lambda \eta e)$ . Hence,

$$\boxed{\int_0^\eta \|G_2\|^2 da \leq \frac{8}{3} \pi^2 (1 - \frac{1}{e}) \frac{1}{\lambda} \int_{1/(\lambda \eta e)}^\infty F_0(r)^2 r^{n-4} dr.} \quad (64)$$

### 3.3.3

Finally, we consider the integral  $\int_0^\eta I_{C_r} I_{C_1} I_2 da / a^{n+1}$ . We already have a bound for  $I_2$ . For  $I_{C_1}$  we can write:

$$\begin{aligned}0 \leq I_{C_1} &= \int_0^\pi \left( V'(\phi_1/\sqrt{a})(1/\sqrt{a}) \Lambda_a(\phi_1) + V(\phi_1/\sqrt{a}) \Lambda'_a(\phi_1) \right)^2 \cos^2 \phi_1 \sin^{n-2} \phi_1 d\phi_1 \\ &= \|U_1 + U_2\|^2 \leq 2\|U_1\|^2 + 2\|U_2\|^2,\end{aligned} \quad (65)$$

where we define

$$U_1(\phi_1) = V'(\phi_1/\sqrt{a})(1/\sqrt{a}) \Lambda_a(\phi_1) \cos \phi_1 \sin^{(n-2)/2} \phi_1 \quad (66)$$

$$U_2(\phi_1) = V(\phi_1/\sqrt{a}) \Lambda'_a(\phi_1) \cos \phi_1 \sin^{(n-2)/2} \phi_1. \quad (67)$$

Then

$$0 \leq I_{C_1} I_2 \leq 2\|U_1\|^2 I_2 + 2\|U_2\|^2 I_2. \quad (68)$$

We now evaluate  $\|U_1\|^2$  and  $\|U_2\|^2$ .

For  $\|U_1\|^2$ , we can write

$$\begin{aligned}\|U_1\|^2 &= \int_0^\pi V'(\phi_1/\sqrt{a})^2 a^{-1} a^{(2n-1)/2} \left( \frac{\sin(\phi_1/\sqrt{a})}{\sin(\phi_1)} \right)^{n-2} \cos^2 \phi_1 \sin^{n-2} \phi_1 d\phi_1 \\ &= \int_0^\pi V'(\phi_1/\sqrt{a})^2 a^{(2n-3)/2} \sin^{n-2}(\phi_1/\sqrt{a}) \cos^2 \phi_1 d\phi_1 \\ &= \int_0^{\pi/\sqrt{a}} V'(\omega_1)^2 a^{n-1} \sin^{n-2} \omega_1 \cos^2(\omega_1 \sqrt{a}) d\omega_1 \\ &\leq a^{n-1} \int_0^{\pi/2} V'(\omega_1)^2 \sin^{n-2} \omega_1 d\omega_1.\end{aligned}$$

The derivative of  $V$  is given by

$$V'(t) = \begin{cases} -2C_v \cos(t) \sin(t), & 0 \leq t \leq \pi/2, \\ 0, & \text{otherwise,} \end{cases} \quad (69)$$



where  $C_v = \sqrt{\frac{2(n+2)n}{3S_0}}$ . Using these formulas and ([1], eqn. 4.3.127), a straightforward calculation shows that

$$\int_0^{\pi/2} V'(\omega_1)^2 \sin^{n-2} \omega_1 d\omega_1 = \frac{4n}{3S_0} \left(1 - \frac{1}{n}\right) \int_0^{\pi} \sin^{n-2} \omega_1 d\omega_1. \quad (70)$$

So we have

$$\|U_1\|^2 \leq a^{n-1} \cdot \frac{4n}{3S_0} \left(1 - \frac{1}{n}\right) \int_0^{\pi} \sin^{n-2} \omega_1 d\omega_1.$$

Combining with  $I_2$ , we get

$$0 \leq \|U_1\|^2 I_2 \leq a^{n-1} \cdot \frac{4n}{3S_0} \left(1 - \frac{1}{n}\right) \cdot \frac{1}{n-1} \int_{S^{n-1}} d\sigma(\omega_1, \phi_2, \dots, \phi_{n-1}) = \frac{4}{3} a^{n-1}. \quad (71)$$

Next we evaluate  $\|U_2\|^2$ . The derivative of  $\Lambda_a$  is given by:

$$\Lambda'_a(\phi_1) = a^{(2n-1)/4} \binom{n-2}{2} \left( \frac{\sin(\phi_1/\sqrt{a})}{\sin(\phi_1)} \right)^{(n-4)/2} \left( \frac{\cos(\phi_1/\sqrt{a})}{\sqrt{a} \sin(\phi_1)} - \frac{\sin(\phi_1/\sqrt{a}) \cos(\phi_1)}{\sin^2(\phi_1)} \right), \quad (72)$$

hence

$$U_2(\phi_1) = V(\phi_1/\sqrt{a}) a^{(2n-1)/4} \binom{n-2}{2} \sin^{(n-4)/2}(\phi_1/\sqrt{a}) \left( \frac{\cos(\phi_1/\sqrt{a})}{\sqrt{a}} - \frac{\sin(\phi_1/\sqrt{a}) \cos(\phi_1)}{\sin(\phi_1)} \right) \cos \phi_1,$$

and

$$\begin{aligned} \|U_2\|^2 &= \int_0^{\pi} V(\phi_1/\sqrt{a})^2 a^{(2n-1)/2} \binom{n-2}{2}^2 \sin^{n-4}(\phi_1/\sqrt{a}) \left( \frac{\cos(\phi_1/\sqrt{a})}{\sqrt{a}} - \frac{\sin(\phi_1/\sqrt{a}) \cos(\phi_1)}{\sin(\phi_1)} \right)^2 \cos^2 \phi_1 d\phi_1 \\ &= \int_0^{\pi/\sqrt{a}} V(\omega_1)^2 a^n \binom{n-2}{2}^2 \sin^{n-4}(\omega_1) \left( \frac{\cos(\omega_1)}{\sqrt{a}} - \frac{\sin(\omega_1) \cos(\omega_1 \sqrt{a})}{\sin(\omega_1 \sqrt{a})} \right)^2 \cos^2(\omega_1 \sqrt{a}) d\omega_1. \end{aligned}$$

Recall that  $V$  is supported on  $[0, \pi/2]$ . For  $\omega_1$  in this range, we have the following crude bound: (using [1], eqn. 4.3.81)

$$\left| \frac{\cos(\omega_1)}{\sqrt{a}} - \frac{\sin(\omega_1) \cos(\omega_1 \sqrt{a})}{\sin(\omega_1 \sqrt{a})} \right| \leq \frac{1}{\sqrt{a}} + \frac{\sin(\omega_1)}{\sin(\omega_1 \sqrt{a})} \cdot \frac{\sin(\omega_1 \sqrt{a})}{\omega_1 \sqrt{a}} \leq \frac{1}{\sqrt{a}} + \frac{1}{\sqrt{a}}.$$

Also, we have  $\cos^2(\omega_1 \sqrt{a}) \leq 1$ . Hence,

$$\begin{aligned} \|U_2\|^2 &\leq \int_0^{\pi/2} V(\omega_1)^2 a^n \binom{n-2}{2}^2 \sin^{n-4}(\omega_1) \left(\frac{2}{\sqrt{a}}\right)^2 d\omega_1 \\ &= 4a^{n-1} \binom{n-2}{2}^2 \int_0^{\pi/2} V(\omega_1)^2 \sin^{n-4} \omega_1 d\omega_1. \end{aligned}$$

Note that

$$\int_0^{\pi/2} V(\omega_1)^2 \sin^{n-4} \omega_1 d\omega_1 = \left(1 + \frac{5}{n-3}\right) \int_0^{\pi/2} V(\omega_1)^2 \sin^{n-2} \omega_1 d\omega_1, \quad (73)$$

using the definition of  $V$ , and integration by parts.

So we have:

$$\|U_2\|^2 \leq 4a^{n-1} \binom{n-2}{2}^2 \left(1 + \frac{5}{n-3}\right) \int_0^{\pi/2} V(\omega_1)^2 \sin^{n-2} \omega_1 d\omega_1.$$

Combining with  $I_2$ , we get:

$$\begin{aligned} 0 \leq \|U_2\|^2 I_2 &\leq 4a^{n-1} \left(\frac{n-2}{2}\right)^2 \left(1 + \frac{5}{n-3}\right) \frac{1}{n-1} \int_{S^{n-1}} V(\omega_1)^2 d\sigma(\omega_1, \phi_2, \dots, \phi_{n-1}) \\ &\leq a^{n-1} (n-2) \left(1 + \frac{5}{n-3}\right). \end{aligned} \quad (74)$$

So, by substituting into (68), we have

$$0 \leq I_{C1} I_2 \leq 2 \cdot \frac{4}{3} a^{n-1} + 2 \cdot a^{n-1} (n-2) \left(1 + \frac{5}{n-3}\right). \quad (75)$$

Finally, we turn to  $I_{Cr}$ . Combining it with  $I_{C1}$  and  $I_2$ , we have

$$0 \leq \int_0^\eta I_{Cr} I_{C1} I_2 \frac{da}{a^{n+1}} \leq \left(\frac{8}{3} + 2(n-2) \left(1 + \frac{5}{n-3}\right)\right) \int_0^\eta I_{Cr} \frac{da}{a^2}.$$

We can bound the integral on the right hand side as follows.

$$\begin{aligned} \int_0^\eta I_{Cr} \frac{da}{a^2} &= \int_0^\eta \int_0^\infty F_0(r)^2 W(\lambda ar)^2 r^{n-3} dr \frac{da}{a^2} \\ &= \int_0^\infty F_0(r)^2 \int_0^\eta W(\lambda ar)^2 \frac{da}{a^2} r^{n-3} dr. \end{aligned}$$

Using the fact that  $W$  is supported on  $[1/e, 1]$ ,

$$\int_0^\eta W(\lambda ar)^2 \frac{da}{a^2} = \int_0^{\lambda \eta r} W(\alpha)^2 \frac{d\alpha}{\alpha^2} \lambda r \leq \int_0^{\lambda \eta r} W(\alpha)^2 \frac{d\alpha}{\alpha} e \lambda r \leq e \lambda r, \quad (76)$$

and vanishes when  $r \leq 1/(\lambda \eta e)$ . Hence

$$\int_0^\eta I_{Cr} \frac{da}{a^2} \leq e \lambda \int_{1/(\lambda \eta e)}^\infty F_0(r)^2 r^{n-2} dr.$$

$$0 \leq \int_0^\eta I_{Cr} I_{C1} I_2 \frac{da}{a^{n+1}} \leq \left(\frac{8}{3} + 2(n-2) \left(1 + \frac{5}{n-3}\right)\right) e \lambda \int_{1/(\lambda \eta e)}^\infty F_0(r)^2 r^{n-2} dr. \quad (77)$$

### 3.4 The variance of $\vec{b}$ parallel to $\vec{\theta}$

Finally, we seek to bound the variance of  $\vec{b}$ , in the direction parallel to  $\vec{\theta}$ . The analysis is similar to the previous section.

The variance of  $\vec{b}$  parallel to  $\vec{\theta}$  is:

$$\mathbb{E}((\vec{b} \cdot \vec{\theta})^2) = \int_{S^{n-1}} \int_0^1 \int_{\mathbb{R}^n} (\vec{b} \cdot \vec{\theta})^2 |\Gamma_f(a, \vec{b}, \vec{\theta})|^2 d\vec{b} \frac{da}{a^{n+1}} d\sigma(\vec{\theta}). \quad (78)$$

We can simplify this by taking advantage of rotational symmetry. Fix a vector  $\vec{u} = (1, 0, \dots, 0)$ , and for each  $\vec{\theta}$ , let  $R$  be a rotation that maps  $\vec{\theta}$  to  $\vec{u}$ . Then

$$\mathbb{E}((\vec{b} \cdot \vec{\theta})^2) = \int_{S^{n-1}} \int_0^1 \int_{\mathbb{R}^n} (R(\vec{b}) \cdot \vec{u})^2 |\Gamma_f(a, R(\vec{b}), \vec{u})|^2 d\vec{b} \frac{da}{a^{n+1}} d\sigma(\vec{\theta}). \quad (79)$$

Then change variables  $\vec{b} \mapsto R^{-1}(\vec{b})$ . The integrand is now independent of  $\vec{\theta}$ , so we can do the  $\vec{\theta}$  integral. We get:

$$\mathbb{E}((\vec{b} \cdot \vec{\theta})^2) = S_0 \int_0^1 \int_{\mathbb{R}^n} b_1^2 |\Gamma_f(a, \vec{b}, \vec{u})|^2 d\vec{b} \frac{da}{a^{n+1}}. \quad (80)$$

We now introduce some new notation,

$$\Phi_{a,\vec{\theta}}(\vec{b}) := \Gamma_f(a, \vec{b}, \vec{\theta}), \quad (81)$$

to emphasize that we view this as a function of  $\vec{b}$ . By equation (3), the Fourier transform of  $\Phi_{a,\vec{\theta}}$  is given by

$$\hat{\Phi}_{a,\vec{\theta}}(\vec{k}) = \hat{f}(\vec{k})\chi_{a,\vec{\theta}}(\vec{k}). \quad (82)$$

And we have, by Plancherel's theorem:

$$\begin{aligned} E((\vec{b} \cdot \vec{\theta})^2) &= S_0 \int_0^1 \int_{\mathbb{R}^n} b_1^2 |\Phi_{a,\vec{u}}(\vec{b})|^2 d\vec{b} \frac{da}{a^{n+1}} \\ &= S_0 \int_0^1 \int_{\mathbb{R}^n} \left| \frac{1}{2\pi i} \frac{\partial}{\partial k_1} \hat{\Phi}_{a,\vec{u}}(\vec{k}) \right|^2 d\vec{k} \frac{da}{a^{n+1}}. \end{aligned} \quad (83)$$

Now, using spherical coordinates  $\vec{k} = (r, \phi_1, \dots, \phi_{n-1})$ , we write  $\hat{\Phi}_{a,\vec{u}}(\vec{k})$  as a product of a radial part and an angular part:

$$\hat{\Phi}_{a,\vec{u}}(\vec{k}) = L(r)M(\phi_1), \quad (84)$$

where

$$L(r) = F_0(r)W(\lambda ar), \quad M(\phi_1) = V(\phi_1/\sqrt{a})\Lambda_a(\phi_1). \quad (85)$$

Then we have

$$\frac{\partial}{\partial k_1} \hat{\Phi}_{a,\vec{u}}(\vec{k}) = L'(r)M(\phi_1) \frac{\partial r}{\partial k_1} + L(r)M'(\phi_1) \frac{\partial \phi_1}{\partial k_1}, \quad (86)$$

where

$$\frac{\partial r}{\partial k_1} = \cos \phi_1, \quad \frac{\partial \phi_1}{\partial k_1} = -\frac{\sin \phi_1}{r}. \quad (87)$$

Now we can expand out the following integral: (note that  $\hat{\Phi}_{a,\vec{u}}(\vec{k})$  is real)

$$\begin{aligned} \int_{\mathbb{R}^n} \left| \frac{\partial}{\partial k_1} \hat{\Phi}_{a,\vec{u}}(\vec{k}) \right|^2 d\vec{k} &= \int_{S^{n-1}} \int_0^\infty \left( L'(r)M(\phi_1) \cos \phi_1 \right. \\ &\quad \left. - L(r)M'(\phi_1)r^{-1} \sin \phi_1 \right)^2 r^{n-1} dr d\sigma(\vec{\phi}) \\ &= K_{Ar}K_{A1}K_2 - 2K_{Br}K_{B1}K_2 + K_{Cr}K_{C1}K_2, \end{aligned} \quad (88)$$

where we define

$$K_{Ar} = \int_0^\infty L'(r)^2 r^{n-1} dr \quad (89)$$

$$K_{A1} = \int_0^\pi M(\phi_1)^2 \cos^2 \phi_1 \sin^{n-2} \phi_1 d\phi_1 \quad (90)$$

$$K_2 = \int_{S^{n-2}} d\sigma(\phi_2, \dots, \phi_{n-1}) \quad (91)$$

$$K_{Br} = \int_0^\infty L'(r)L(r)r^{n-2} dr \quad (92)$$

$$K_{B1} = \int_0^\pi M'(\phi_1)M(\phi_1) \cos \phi_1 \sin^{n-1} \phi_1 d\phi_1 \quad (93)$$

$$K_{Cr} = \int_0^\infty L(r)^2 r^{n-3} dr \quad (94)$$

$$K_{C1} = \int_0^\pi M'(\phi_1)^2 \sin^n \phi_1 d\phi_1. \quad (95)$$

Thus we can write the variance of  $\vec{b}$  parallel to  $\vec{\theta}$  as:

$$\mathbb{E}((\vec{b} \cdot \vec{\theta})^2) = \frac{S_0}{(2\pi)^2} \int_0^1 \left( K_{Ar} K_{A1} K_2 - 2K_{Br} K_{B1} K_2 + K_{Cr} K_{C1} K_2 \right) \frac{da}{a^{n+1}}. \quad (96)$$

A similar formula gives the variance conditioned on observing  $a \leq \eta$ :

$$\begin{aligned} \mathbb{E}((\vec{b} \cdot \vec{\theta})^2 | a \leq \eta) \\ = \frac{1}{\Pr[a \leq \eta]} \frac{S_0}{(2\pi)^2} \int_0^\eta \left( K_{Ar} K_{A1} K_2 - 2K_{Br} K_{B1} K_2 + K_{Cr} K_{C1} K_2 \right) \frac{da}{a^{n+1}}. \end{aligned} \quad (97)$$

We would then like to bound the various integrals appearing on the right hand side.

### 3.4.1

We begin with the integral  $\int_0^\eta K_{Br} K_{B1} K_2 da/a^{n+1}$ .

Note that  $K_2 = (n-1)I_2$ , while  $K_{B1} = I_{B1}$  and  $K_{Br} = I_{Br}$ . Using the argument from the previous section, we have:

$$\left| \int_0^\eta K_{Br} K_{B1} K_2 \frac{da}{a^{n+1}} \right| \leq \frac{1}{4}(n-1)(n-2) \int_{1/(\lambda\eta e)}^\infty F_0(r)^2 r^{n-3} dr. \quad (98)$$

### 3.4.2

Next, consider the integral  $\int_0^\eta K_{Ar} K_{A1} K_2 da/a^{n+1}$ . We already have a bound for  $K_2$ . For  $K_{A1}$ , we write:

$$\begin{aligned} K_{A1} &= \int_0^\pi V(\phi_1/\sqrt{a})^2 \Lambda_a(\phi_1)^2 \cos^2 \phi_1 \sin^{n-2} \phi_1 d\phi_1 \\ &= \int_0^\pi V(\phi_1/\sqrt{a})^2 a^{(2n-1)/2} \left( \frac{\sin(\phi_1/\sqrt{a})}{\sin \phi_1} \right)^{n-2} \cos^2 \phi_1 \sin^{n-2} \phi_1 d\phi_1 \\ &= \int_0^{\pi/\sqrt{a}} V(\omega_1)^2 a^n \sin^{n-2} \omega_1 \cos^2(\omega_1 \sqrt{a}) d\omega_1. \end{aligned}$$

Using the fact that  $V$  is supported on  $[0, \pi/2]$ , and the simple bound  $\cos^2(\omega_1 \sqrt{a}) \leq 1$ , we get:

$$0 \leq K_{A1} \leq \int_0^{\pi/2} V(\omega_1)^2 a^n \sin^{n-2} \omega_1 d\omega_1.$$

Combining with  $K_2$ , we get:

$$0 \leq K_{A1} K_2 \leq a^n \int_{S^{n-1}} V(\omega_1)^2 d\sigma(\omega_1, \phi_2, \dots, \phi_{n-1}) = a^n. \quad (99)$$

We now turn to  $K_{Ar}$ . First, combining with  $K_{A1}$  and  $K_2$ , we have

$$0 \leq \int_0^\eta K_{Ar} K_{A1} K_2 \frac{da}{a^{n+1}} \leq \int_0^\eta K_{Ar} \frac{da}{a}. \quad (100)$$

Note that  $K_{Ar} = I_{Ar}$ , so we can upper-bound  $K_{Ar}$  as in the previous section:

$$0 \leq K_{Ar} \leq 2\|G_1\|^2 + 2\|G_2\|^2, \quad (101)$$

where we define

$$G_1(r) = F_0'(r)W(\lambda ar)r^{(n-1)/2} \quad (102)$$

$$G_2(r) = F_0(r)W'(\lambda ar)\lambda ar^{(n-1)/2}. \quad (103)$$

Thus we have

$$\boxed{0 \leq \int_0^\eta K_{Ar} K_{A1} K_2 \frac{da}{a^{n+1}} \leq 2 \left( \int_0^\eta \|G_1\|^2 \frac{da}{a} + \int_0^\eta \|G_2\|^2 \frac{da}{a} \right)}. \quad (104)$$

We then want to upper-bound the integrals  $\int_0^\eta \|G_1\|^2 da/a$  and  $\int_0^\eta \|G_2\|^2 da/a$ .

For the first one, we have:

$$\begin{aligned} \int_0^\eta \|G_1\|^2 \frac{da}{a} &= \int_0^\eta \int_0^\infty F_0'(r)^2 W(\lambda ar)^2 r^{n-1} dr \frac{da}{a} \\ &= \int_0^\infty F_0'(r)^2 \int_0^\eta W(\lambda ar)^2 \frac{da}{a} r^{n-1} dr. \end{aligned}$$

Using equation (51), we get:

$$\boxed{\int_0^\eta \|G_1\|^2 \frac{da}{a} \leq \int_{1/(\lambda\eta e)}^\infty F_0'(r)^2 r^{n-1} dr.} \quad (105)$$

For the second integral, we have:

$$\begin{aligned} \int_0^\eta \|G_2\|^2 \frac{da}{a} &= \int_0^\eta \int_0^\infty F_0(r)^2 W'(\lambda ar)^2 \lambda^2 a^2 r^{n-1} dr \frac{da}{a} \\ &= \int_0^\infty F_0(r)^2 \int_0^\eta W'(\lambda ar)^2 \lambda^2 a da r^{n-1} dr. \end{aligned}$$

Recall that the derivative of  $W$  is given by equation (62). So we can write

$$\int_0^\eta W'(\lambda ar)^2 \lambda^2 a da = \int_0^{\lambda\eta r} W'(\alpha)^2 \alpha d\alpha \frac{1}{r^2} \leq \int_{1/e}^1 C_w^2 (\pi/\alpha)^2 \alpha d\alpha \frac{1}{r^2} = \frac{8}{3} \pi^2 \frac{1}{r^2}, \quad (106)$$

and vanishes when  $r \leq 1/(\lambda\eta e)$ . Hence,

$$\boxed{\int_0^\eta \|G_2\|^2 \frac{da}{a} \leq \frac{8}{3} \pi^2 \int_{1/(\lambda\eta e)}^\infty F_0(r)^2 r^{n-3} dr.} \quad (107)$$

### 3.4.3

Finally, we consider the integral  $\int_0^\eta K_{Cr} K_{C1} K_2 da/a^{n+1}$ . We already have a bound for  $K_2$ . For  $K_{C1}$  we can write:

$$\begin{aligned} 0 \leq K_{C1} &= \int_0^\pi \left( V'(\phi_1/\sqrt{a})(1/\sqrt{a})\Lambda_a(\phi_1) + V(\phi_1/\sqrt{a})\Lambda'_a(\phi_1) \right)^2 \sin^n \phi_1 d\phi_1 \\ &= \|\tilde{U}_1 + \tilde{U}_2\|^2 \leq 2\|\tilde{U}_1\|^2 + 2\|\tilde{U}_2\|^2, \end{aligned} \quad (108)$$

where we define

$$\tilde{U}_1(\phi_1) = V'(\phi_1/\sqrt{a})(1/\sqrt{a})\Lambda_a(\phi_1) \sin^{n/2} \phi_1 \quad (109)$$

$$\tilde{U}_2(\phi_1) = V(\phi_1/\sqrt{a})\Lambda'_a(\phi_1) \sin^{n/2} \phi_1. \quad (110)$$

Then

$$0 \leq K_{C1} K_2 \leq 2\|\tilde{U}_1\|^2 K_2 + 2\|\tilde{U}_2\|^2 K_2. \quad (111)$$

We now evaluate  $\|\tilde{U}_1\|^2$  and  $\|\tilde{U}_2\|^2$ .

For  $\|\tilde{U}_1\|^2$ , we can write

$$\begin{aligned}
\|\tilde{U}_1\|^2 &= \int_0^\pi V'(\phi_1/\sqrt{a})^2 a^{-1} a^{(2n-1)/2} \left( \frac{\sin(\phi_1/\sqrt{a})}{\sin(\phi_1)} \right)^{n-2} \sin^n \phi_1 d\phi_1 \\
&= \int_0^\pi V'(\phi_1/\sqrt{a})^2 a^{(2n-3)/2} \sin^{n-2}(\phi_1/\sqrt{a}) \sin^2 \phi_1 d\phi_1 \\
&= \int_0^{\pi/\sqrt{a}} V'(\omega_1)^2 a^{n-1} \sin^{n-2} \omega_1 \sin^2(\omega_1 \sqrt{a}) d\omega_1 \\
&\leq \frac{\pi^2}{4} a^n \int_0^{\pi/2} V'(\omega_1)^2 \sin^{n-2} \omega_1 d\omega_1.
\end{aligned}$$

(In the last step we used the bound  $\sin^2(\omega_1 \sqrt{a}) \leq \omega_1^2 a \leq \frac{\pi^2}{4} a$ .)

Then, using equation (70), we have

$$\|\tilde{U}_1\|^2 \leq \frac{\pi^2}{4} a^n \cdot \frac{4n}{3S_0} \left(1 - \frac{1}{n}\right) \int_0^\pi \sin^{n-2} \omega_1 d\omega_1.$$

Combining with  $K_2$ , we get

$$0 \leq \|\tilde{U}_1\|^2 K_2 \leq \frac{\pi^2}{4} a^n \cdot \frac{4n}{3S_0} \left(1 - \frac{1}{n}\right) \cdot \int_{S_{n-1}} d\sigma(\omega_1, \phi_2, \dots, \phi_{n-1}) = \frac{\pi^2}{3} a^n (n-1). \quad (112)$$

Next we evaluate  $\|\tilde{U}_2\|^2$ . The derivative of  $\Lambda_a$  is given by equation (72), hence

$$\tilde{U}_2(\phi_1) = V(\phi_1/\sqrt{a}) a^{(2n-1)/4} \left(\frac{n-2}{2}\right) \sin^{(n-4)/2}(\phi_1/\sqrt{a}) \left( \frac{\cos(\phi_1/\sqrt{a})}{\sqrt{a}} - \frac{\sin(\phi_1/\sqrt{a}) \cos(\phi_1)}{\sin(\phi_1)} \right) \sin \phi_1,$$

and

$$\begin{aligned}
\|\tilde{U}_2\|^2 &= \int_0^\pi V(\phi_1/\sqrt{a})^2 a^{(2n-1)/2} \left(\frac{n-2}{2}\right)^2 \sin^{n-4}(\phi_1/\sqrt{a}) \left( \frac{\cos(\phi_1/\sqrt{a})}{\sqrt{a}} - \frac{\sin(\phi_1/\sqrt{a}) \cos(\phi_1)}{\sin(\phi_1)} \right)^2 \sin^2 \phi_1 d\phi_1 \\
&= \int_0^{\pi/\sqrt{a}} V(\omega_1)^2 a^n \left(\frac{n-2}{2}\right)^2 \sin^{n-4}(\omega_1) \left( \frac{\cos(\omega_1)}{\sqrt{a}} - \frac{\sin(\omega_1) \cos(\omega_1 \sqrt{a})}{\sin(\omega_1 \sqrt{a})} \right)^2 \sin^2(\omega_1 \sqrt{a}) d\omega_1.
\end{aligned}$$

Recall that  $V$  is supported on  $[0, \pi/2]$ . For  $\omega_1$  in this range, we have the following crude bound: (using [1], eqn. 4.3.81)

$$\left| \frac{\cos(\omega_1)}{\sqrt{a}} - \frac{\sin(\omega_1) \cos(\omega_1 \sqrt{a})}{\sin(\omega_1 \sqrt{a})} \right| \leq \frac{1}{\sqrt{a}} + \frac{\sin(\omega_1)}{\sin(\omega_1 \sqrt{a})} \cdot \frac{\sin(\omega_1 \sqrt{a})}{\omega_1 \sqrt{a}} \leq \frac{1}{\sqrt{a}} + \frac{1}{\sqrt{a}}.$$

Also, we have  $\sin^2(\omega_1 \sqrt{a}) \leq \omega_1^2 a \leq \frac{\pi^2}{4} a$ . Hence,

$$\begin{aligned}
\|\tilde{U}_2\|^2 &\leq \int_0^{\pi/2} V(\omega_1)^2 a^n \left(\frac{n-2}{2}\right)^2 \sin^{n-4}(\omega_1) \left(\frac{2}{\sqrt{a}}\right)^2 \frac{\pi^2}{4} a d\omega_1 \\
&= \pi^2 a^n \left(\frac{n-2}{2}\right)^2 \int_0^{\pi/2} V(\omega_1)^2 \sin^{n-4} \omega_1 d\omega_1.
\end{aligned}$$

By equation (73), we have:

$$\|\tilde{U}_2\|^2 \leq \pi^2 a^n \left(\frac{n-2}{2}\right)^2 \left(1 + \frac{5}{n-3}\right) \int_0^{\pi/2} V(\omega_1)^2 \sin^{n-2} \omega_1 d\omega_1.$$

Combining with  $K_2$ , we get:

$$\begin{aligned}
0 \leq \|\tilde{U}_2\|^2 K_2 &\leq \pi^2 a^n \left(\frac{n-2}{2}\right)^2 \left(1 + \frac{5}{n-3}\right) \int_{S_{n-1}} V(\omega_1)^2 d\sigma(\omega_1, \phi_2, \dots, \phi_{n-1}) \\
&\leq \frac{\pi^2}{4} a^n (n-2)^2 \left(1 + \frac{5}{n-3}\right).
\end{aligned} \quad (113)$$

So, by substituting into (111), we have

$$0 \leq K_{C_1}K_2 \leq 2 \cdot \frac{\pi^2}{3}a^n(n-1) + 2 \cdot \frac{\pi^2}{4}a^n(n-2)^2\left(1 + \frac{5}{n-3}\right). \quad (114)$$

Finally, we turn to  $K_{C_r}$ . Combining it with  $K_{C_1}$  and  $K_2$ , we have

$$0 \leq \int_0^\eta K_{C_r}K_{C_1}K_2 \frac{da}{a^{n+1}} \leq \left(\frac{2\pi^2}{3}(n-1) + \frac{\pi^2}{2}(n-2)^2\left(1 + \frac{5}{n-3}\right)\right) \int_0^\eta K_{C_r} \frac{da}{a}.$$

We can bound the integral on the right hand side as follows.

$$\begin{aligned} \int_0^\eta K_{C_r} \frac{da}{a} &= \int_0^\eta \int_0^\infty F_0(r)^2 W(\lambda ar)^2 r^{n-3} dr \frac{da}{a} \\ &= \int_0^\infty F_0(r)^2 \int_0^\eta W(\lambda ar)^2 \frac{da}{a} r^{n-3} dr. \end{aligned}$$

Using equation (51), we get

$$\int_0^\eta K_{C_r} \frac{da}{a} \leq \int_{1/(\lambda\eta e)}^\infty F_0(r)^2 r^{n-3} dr.$$

$$0 \leq \int_0^\eta K_{C_r}K_{C_1}K_2 \frac{da}{a^{n+1}} \leq \left(\frac{2\pi^2}{3}(n-1) + \frac{\pi^2}{2}(n-2)^2\left(1 + \frac{5}{n-3}\right)\right) \int_{1/(\lambda\eta e)}^\infty F_0(r)^2 r^{n-3} dr.$$

(115)

## 4 The Ball in $\mathbb{R}^n$

Let  $B$  be a ball in  $\mathbb{R}^n$ . In this section we will analyze the curvelet transform of the function

$$f(\vec{x}) = \begin{cases} 1/\sqrt{\text{vol}(B)} & \text{if } \vec{x} \in B, \\ 0 & \text{otherwise.} \end{cases} \quad (116)$$

This is the wavefunction one gets by quantum-sampling over the ball  $B$ . We will prove bounds on the distribution of probability mass resulting from the curvelet transform. This will eventually lead to a single-shot measurement procedure for estimating the center of the ball (see Section 7).

Note that the curvelet transform behaves in a simple way when we translate the function  $f$ : if  $g(\vec{x}) = f(\vec{x} - \vec{z})$ , then using equation (3), we see that

$$\Gamma_g(a, \vec{b}, \vec{\theta}) = \int_{\mathbb{R}^n} \hat{f}(\vec{k}) e^{-2\pi i \vec{k} \cdot \vec{z}} \chi_{a, \vec{\theta}}(\vec{k}) e^{2\pi i \vec{k} \cdot \vec{b}} d\vec{k} = \Gamma_f(a, \vec{b} - \vec{z}, \vec{\theta}). \quad (117)$$

Thus, without loss of generality, we can assume that the ball  $B$  is centered at the origin. In this case  $f$  is a radial function, and we can use the results from the previous section.

So let the ball  $B$  be centered at the origin, with radius  $\beta$ . We write  $f(\vec{x}) = f_0(|\vec{x}|)$ , where

$$f_0(r) = \begin{cases} C & \text{if } r \leq \beta, \\ 0 & \text{otherwise,} \end{cases} \quad (118)$$

and  $C = 1/\sqrt{\text{vol}(B)} = (S_0\beta^n/n)^{-1/2}$ , where  $S_0$  is the surface area of the unit sphere  $S^{n-1}$

in  $\mathbb{R}^n$ . Then the Fourier transform of  $f$  is given by  $\hat{f}(\vec{k}) = F_0(|\vec{k}|)$ , where

$$\begin{aligned}
F_0(\rho) &= \frac{2\pi C}{\rho^{(n-2)/2}} \int_0^\beta J_{(n-2)/2}(2\pi\rho r) r^{n/2} dr \\
&= \frac{2\pi C}{\rho^{(n-2)/2}} \int_0^{2\pi\rho\beta} J_{(n-2)/2}(s) s^{n/2} ds \frac{1}{(2\pi\rho)^{(n+2)/2}} \\
&= \frac{2\pi C}{\rho^{(n-2)/2}} J_{n/2}(s) s^{n/2} \Big|_{s=0}^{s=2\pi\rho\beta} \frac{1}{(2\pi\rho)^{(n+2)/2}} \\
&= \frac{C}{\rho^{n/2}} \beta^{n/2} J_{n/2}(2\pi\rho\beta) \\
&= \sqrt{\frac{n}{S_0}} \frac{1}{\rho^{n/2}} J_{n/2}(2\pi\rho\beta),
\end{aligned} \tag{119}$$

using equation (18), and the identity  $\frac{d}{dz}(z^\nu J_\nu(z)) = z^\nu J_{\nu-1}(z)$  (see [1], eqn. (9.1.30)).

We will study the curvelet transform  $\Gamma_f(a, \vec{b}, \vec{\theta})$  on  $\mathbb{R}^n$ , for  $n \geq 4$ . We use the window functions  $W$  and  $V$  specified in Section 3. We set the parameter  $\lambda$  to be

$$\lambda = 2\pi\beta e/n. \tag{120}$$

We show the following:

**Theorem 3** *Almost all of the power in  $\hat{f}$  is located at frequencies  $|\vec{k}| \geq 1/\lambda$ :*

$$\int_{|\vec{k}| \leq 1/\lambda} |\hat{f}(\vec{k})|^2 d\vec{k} < \frac{1}{\pi n}. \tag{121}$$

For any  $\eta \leq 1/e^2$ , the probability of observing a fine-scale element  $a \leq \eta$  is lower-bounded by:

$$\Pr[a \leq \eta] \geq \frac{e\eta}{14} \left(1 - \frac{1}{n}\right). \tag{122}$$

Furthermore, if  $\eta \leq (1/e^2)(1 - \frac{2}{n+2})$ , then the variance of  $\vec{b}$ , in the directions orthogonal / parallel to  $\vec{\theta}$ , conditioned on  $a \leq \eta$ , is upper-bounded by:

$$E(\vec{b}^T (I - \vec{\theta}\vec{\theta}^T) \vec{b} \mid a \leq \eta) \leq \eta \beta^2 (1908 + O(\frac{1}{n})), \tag{123}$$

$$E((\vec{b} \cdot \vec{\theta})^2 \mid a \leq \eta) \leq \beta^2 (121 + O(\frac{1}{n})). \tag{124}$$

## 4.1 The low-frequency components

First, we claim that almost all the power in  $\hat{f}$  is located at frequencies above some threshold  $1/\lambda$ . This justifies our use of the curvelet transform, and theorems 1 and 2, for an appropriate choice of the parameter  $\lambda$ .

We start by proving an upper-bound on the integral  $\int_0^z t^{-1} J_\nu(t)^2 dt$ , for  $\nu > 0$ . Note that ([1], eqn. (9.1.62))

$$|J_\nu(t)| \leq \frac{(\frac{1}{2}t)^\nu}{\nu!} \quad (\nu \geq -\frac{1}{2}, t \geq 0). \tag{125}$$

Also ([1], eqn. (6.1.38)),

$$\nu! > \sqrt{2\pi\nu}^{\nu+\frac{1}{2}} e^{-\nu} \quad (\nu > 0). \tag{126}$$

Hence

$$|J_\nu(t)| < \frac{(\frac{1}{2}t)^\nu}{\sqrt{2\pi\nu}^{\nu+\frac{1}{2}} e^{-\nu}} = \frac{1}{\sqrt{2\pi\nu}} \left(\frac{te}{2\nu}\right)^\nu, \tag{127}$$



and

$$\int_0^z t^{-1} J_\nu(t)^2 dt < \int_0^z \frac{1}{t} \frac{1}{2\pi\nu} \left(\frac{te}{2\nu}\right)^{2\nu} dt = \frac{1}{2\pi\nu} \left(\frac{e}{2\nu}\right)^{2\nu} \frac{1}{2\nu} t^{2\nu} \Big|_0^z = \frac{1}{4\pi\nu^2} \left(\frac{ez}{2\nu}\right)^{2\nu}. \quad (128)$$

This upper bound is useful when  $z \leq 2\nu/e$ .

We can now calculate the amount of power contained in the low-frequency components of  $f$ :

$$\begin{aligned} \int_{|\vec{k}| \leq z} |\hat{f}(\vec{k})|^2 d\vec{k} &= \int_0^z \frac{n}{S_0} \frac{1}{\rho^n} J_{n/2}(2\pi\rho\beta)^2 \cdot S_0 \rho^{n-1} d\rho \\ &= n \int_0^{2\pi\beta z} t^{-1} J_{n/2}(t)^2 \cdot dt \\ &< n \frac{1}{\pi n^2} \left(\frac{2\pi\beta ez}{n}\right)^n. \end{aligned} \quad (129)$$

Setting  $z = n/(2\pi\beta e)$ , we get

$$\int_{|\vec{k}| \leq n/(2\pi\beta e)} |\hat{f}(\vec{k})|^2 d\vec{k} < \frac{1}{\pi n}. \quad (130)$$

So the region  $\{|\vec{k}| \leq n/(2\pi\beta e)\}$  contains at most a  $1/(\pi n)$  fraction of the total power. Accordingly, we set the parameter  $\lambda$  to be

$$\boxed{\lambda = 2\pi\beta e/n.} \quad (131)$$

## 4.2 The decay of $J_\nu(x)$

We now prove some technical lemmas on the decay of  $J_\nu(x)$  for  $x \geq 2\nu$ ,  $\nu \geq 1/2$ . These follow from classical results on Bessel functions [1, 23], though some care is required near the transition region at  $x \approx \nu$ . In particular, the usual asymptotic expansions for  $J_\nu(x)$  only work when  $x \geq \nu^2$ , or when  $x = \alpha\nu$  for some fixed constant  $\alpha$ . For our purposes, we use an asymptotic expansion of  $J_\nu(x)^2 + Y_\nu(x)^2$ , that behaves well when  $x \geq \nu$ .

### 4.2.1

We start by quoting the following result from ([23], p.447). Define

$$M_\nu(x) = \sqrt{J_\nu(x)^2 + Y_\nu(x)^2}. \quad (132)$$

Then for all  $x \geq \nu \geq 1/2$ ,

$$\frac{2}{\pi x} < M_\nu(x)^2 < \frac{2}{\pi\sqrt{x^2 - \nu^2}}. \quad (133)$$

This immediately implies an upper bound on  $J_\nu(x)^2$ , for all  $x \geq 2\nu$ ,  $\nu \geq 1/2$ :

$$J_\nu(x)^2 \leq M_\nu(x)^2 < \frac{2}{\pi\sqrt{x^2 - \nu^2}} \leq \frac{2}{\pi x} \cdot \frac{2}{\sqrt{3}}. \quad (134)$$

### 4.2.2

We next prove a lower bound on  $|J_\nu(x)|$ , for  $x$  within certain intervals. Note that  $J_\nu(x)$  is large at a zero of  $Y_\nu(x)$ . We will show that (1) the zeroes of  $Y_\nu(x)$  are not too far apart, and (2)  $J_\nu(x)$  is large in a neighborhood around each zero of  $Y_\nu(x)$ .

To see this, note that  $J_\nu(x)$  and  $Y_\nu(x)$  can be written in terms of a modulus and phase,

$$J_\nu(x) = M_\nu(x) \cos \theta_\nu(x), \quad (135)$$

$$Y_\nu(x) = M_\nu(x) \sin \theta_\nu(x), \quad (136)$$

where  $M_\nu(x)$  is as defined above, and  $\theta_\nu(x)$  satisfies the equation

$$\theta'_\nu(x) = \frac{2}{\pi x M_\nu(x)^2} \quad (137)$$

(see [1], eqn. 9.2.21, and [23], p.514). This implies lower and upper bounds on  $\theta'_\nu(x)$ , for all  $x \geq 2\nu$ :

$$\frac{\sqrt{3}}{2} < \theta'_\nu(x) < 1. \quad (138)$$

First, we claim that for any  $t \geq 2\nu$ , the interval  $[t, t + \frac{2\pi}{\sqrt{3}}]$  contains a zero of  $Y_\nu(x)$ . To see this, write the following, for any  $\delta \geq 0$ :

$$\theta_\nu(x + \delta) = \theta_\nu(x) + \int_x^{x+\delta} \theta'_\nu(y) dy \geq \theta_\nu(x) + \frac{\sqrt{3}}{2} \delta.$$

So  $\theta_\nu(t + \frac{2\pi}{\sqrt{3}}) \geq \theta_\nu(t) + \pi$ . So  $\theta_\nu(x)$  must equal an integer multiple of  $\pi$  for some  $x \in [t, t + \frac{2\pi}{\sqrt{3}}]$ ; and  $Y_\nu(x)$  must vanish at that point. This proves our first claim.

Second, let  $\phi$  be a zero of  $Y_\nu(x)$ , satisfying  $\phi \geq 2\nu$ . We claim that, for any  $\delta \in [-\pi/2, \pi/2]$ ,

$$|J_\nu(\phi + \delta)| \geq M_\nu(\phi + \delta) \cos \delta. \quad (139)$$

To see this, write

$$|J_\nu(\phi + \delta)| = M_\nu(\phi + \delta) |\cos \theta_\nu(\phi + \delta)| = M_\nu(\phi + \delta) |\cos |\theta_\nu(\phi + \delta) - \theta_\nu(\phi)||.$$

(The last step follows because  $\theta_\nu(\phi)$  is an integer multiple of  $\pi$ .) Then note that

$$|\theta_\nu(\phi + \delta) - \theta_\nu(\phi)| = \left| \int_\phi^{\phi+\delta} \theta'_\nu(y) dy \right| \leq |\delta|.$$

Hence we have

$$|\cos |\theta_\nu(\phi + \delta) - \theta_\nu(\phi)|| \geq |\cos |\delta|| = \cos \delta.$$

This proves our second claim.

### 4.2.3

Finally, we prove the following lower bound on a sum of squares of Bessel functions:

Let  $\nu_1, \dots, \nu_m \in [1/2, \nu_{\max}]$ . Let  $t \geq 2\nu_{\max}$ . Then there exists some  $t' \in [t - \frac{\pi}{2}, t + \frac{2\pi}{\sqrt{3}} + \frac{\pi}{2}]$  such that

$$\sum_{k=1}^m J_{\nu_k}(t')^2 \geq \frac{m}{7t'}. \quad (140)$$

Proof: Essentially, we will show that there must exist a point  $t'$  where a constant fraction of the functions  $J_{\nu_k}(t')^2$  ( $k = 1, \dots, m$ ) are large simultaneously.

Define the interval  $I = [t, t + \frac{2\pi}{\sqrt{3}}]$ . For each  $k = 1, \dots, m$ ,  $I$  contains a zero of  $Y_{\nu_k}(x)$ , call it  $\phi_k$ . Now define the function

$$\chi_k(x) = \begin{cases} \cos^2(x - \phi_k) & \text{if } \phi_k - \frac{\pi}{2} \leq x \leq \phi_k + \frac{\pi}{2}, \\ 0 & \text{otherwise.} \end{cases}$$

Note that

$$J_{\nu_k}(x)^2 \geq M_{\nu_k}(x)^2 \chi_k(x) > \frac{2}{\pi x} \chi_k(x).$$

Furthermore, define the function

$$u(x) = \sum_{k=1}^m \chi_k(x),$$

and note that

$$\sum_{k=1}^m J_{\nu_k}(x)^2 \geq \frac{2}{\pi x} u(x).$$

Define the interval  $I' = [t - \frac{\pi}{2}, t + \frac{2\pi}{\sqrt{3}} + \frac{\pi}{2}]$ ; this interval contains the support of all of the functions  $\chi_k(x)$  ( $k = 1, \dots, m$ ). Then write

$$\int_{I'} u(x) dx = \sum_{k=1}^m \int_{\phi_k - (\pi/2)}^{\phi_k + (\pi/2)} \chi_k(x) dx = m \cdot \frac{\pi}{2}.$$

So there must exist a point  $t' \in I'$  such that

$$u(t') \geq \frac{1}{|I'|} \int_{I'} u(x) dx \geq \frac{1}{7} \cdot m \cdot \frac{\pi}{2} = \frac{\pi}{14} m,$$

and the claim follows.

### 4.3 The probability of observing a scale $a$

Next we claim that  $\hat{f}$  has a heavy tail. This implies that we will observe fine-scale elements ( $a$  small) with significant probability.

Again, we start by proving a lower bound on  $\int_z^\infty t^{-1} J_\nu(t)^2 dt$ , when  $\nu$  is of the form  $m$  or  $m + (1/2)$  (where  $m$  is an integer),  $\nu \geq 1$ , and  $z \geq 2\nu$ . We will show that:

$$\int_z^\infty t^{-1} J_\nu(t)^2 dt \geq \left(1 - \frac{1}{2\nu}\right) \frac{1}{7(z + 5.20)}. \quad (141)$$

First, consider the case of  $\nu = m$ . We assume  $m \geq 1$  and  $z \geq 2m$ . Using ([1], eqn. 11.3.36), we can write

$$\begin{aligned} \int_z^\infty t^{-1} J_\nu(t)^2 dt &= \int_z^\infty t^{-1} J_m(t)^2 dt \\ &= -\frac{1}{2m} \left( J_0(t)^2 + J_m(t)^2 + 2 \sum_{k=1}^{m-1} J_k(t)^2 \right) \Big|_z^\infty \\ &= \frac{1}{2m} \left( J_0(z)^2 + J_m(z)^2 + 2 \sum_{k=1}^{m-1} J_k(z)^2 \right) \\ &\geq \frac{1}{2m} \left( J_m(z)^2 + 2 \sum_{k=1}^{m-1} J_k(z)^2 \right). \end{aligned}$$

Then, using the lemma from the previous section, we get the following, for some  $z' \in [z, z + 5.20]$ :

$$\int_z^\infty t^{-1} J_\nu(t)^2 dt \geq \frac{1}{2m} \frac{2m-1}{7z'} \geq \left(1 - \frac{1}{2\nu}\right) \frac{1}{7(z + 5.20)}. \quad (142)$$

Next, consider the case  $\nu = m + (1/2)$ . We assume  $m \geq 1$  and  $z \geq 2m + 1$ . Using ([1], eqn. 11.3.36), we can write

$$\begin{aligned} \int_z^\infty t^{-1} J_\nu(t)^2 dt &= \int_z^\infty t^{-1} J_{m+(1/2)}(t)^2 dt \\ &= \frac{1}{2m+1} \int_z^\infty t^{-1} J_{1/2}(t)^2 dt - \frac{1}{2m+1} \left( J_{1/2}(t)^2 + J_{m+(1/2)}(t)^2 + 2 \sum_{k=1}^{m-1} J_{k+(1/2)}(t)^2 \right) \Big|_z^\infty \\ &\geq \frac{1}{2m+1} \left( J_{1/2}(z)^2 + J_{m+(1/2)}(z)^2 + 2 \sum_{k=1}^{m-1} J_{k+(1/2)}(z)^2 \right). \end{aligned}$$

Then, using the lemma from the previous section, we get the following, for some  $z' \in [z, z + 5.20]$ :

$$\int_z^\infty t^{-1} J_\nu(t)^2 dt \geq \frac{1}{2m+1} \frac{2m}{7z'} \geq \left(1 - \frac{1}{2\nu}\right) \frac{1}{7(z+5.20)}. \quad (143)$$

We now proceed to lower-bound the probability of observing a fine-scale element  $a$ . The following bound holds for any  $n \geq 2$  and any  $\eta \leq 1/e^2$ .

$$\begin{aligned} \Pr[a \leq \eta] &\geq \int_{|\vec{k}| \geq 1/(\lambda\eta)} |\hat{f}(\vec{k})|^2 d\vec{k} \\ &= \int_{1/(\lambda\eta)}^\infty \frac{n}{S_0} \rho^{-n} J_{n/2}(2\pi\rho\beta)^2 \cdot S_0 \rho^{n-1} d\rho \\ &= n \int_{2\pi\beta/(\lambda\eta)}^\infty t^{-1} J_{n/2}(t)^2 dt \\ &= n \int_{n/(e\eta)}^\infty t^{-1} J_{n/2}(t)^2 dt, \end{aligned}$$

where in the last step we used the definition  $\lambda = 2\pi\beta e/n$ . Then, by equation (141), and using the fact that  $n/(e\eta) \geq 2e \geq 5.43$ , we get

$$\Pr[a \leq \eta] \geq n \left(1 - \frac{1}{n}\right) \frac{1}{7\left(\frac{n}{e\eta} + 5.20\right)} \geq n \left(1 - \frac{1}{n}\right) \frac{1}{14\frac{n}{e\eta}} = \frac{e\eta}{14} \left(1 - \frac{1}{n}\right). \quad (144)$$

$$\boxed{\Pr[a \leq \eta] \geq \frac{e\eta}{14} \left(1 - \frac{1}{n}\right)}. \quad (145)$$

#### 4.4 The variance of $\vec{b}$ orthogonal to $\vec{\theta}$

First, we give a simple upper bound on integrals of the form

$$\int_z^\infty t^{-k} J_\nu(t)^2 dt,$$

for  $k \geq 1$ ,  $z \geq 2\nu$  and  $\nu \geq 1/2$ . This follows from equation (134):

$$\begin{aligned} \int_z^\infty t^{-k} J_\nu(t)^2 dt &\leq \int_z^\infty t^{-k} \frac{2}{\pi t} \frac{2}{\sqrt{3}} dt \\ &= \frac{4}{\pi\sqrt{3}} \int_z^\infty t^{-k-1} dt = \frac{4}{\pi\sqrt{3}} \left( -1/k \right) t^{-k} \Big|_z^\infty = \frac{4}{\pi\sqrt{3}k} z^{-k}. \end{aligned} \quad (146)$$

We use this to upper-bound the integral

$$\int_{1/(\lambda\eta e)}^{\infty} F_0(r)^2 r^{n-k} dr,$$

for  $k \geq 1$  and  $\eta \leq 1/e^2$ . We write the following: (recall the definition  $\lambda = 2\pi\beta e/n$ , which implies  $2\pi\beta/(\lambda\eta e) = n/(\eta e^2)$ )

$$\begin{aligned} \int_{1/(\lambda\eta e)}^{\infty} F_0(r)^2 r^{n-k} dr &= \frac{n}{S_0} \int_{1/(\lambda\eta e)}^{\infty} J_{n/2}(2\pi\beta r)^2 r^{-k} dr \\ &= \frac{n}{S_0} \int_{2\pi\beta/(\lambda\eta e)}^{\infty} J_{n/2}(t)^2 t^{-k} dt \cdot (2\pi\beta)^{k-1} \\ &\leq \frac{n}{S_0} \frac{4}{\pi\sqrt{3}k} \left(\frac{\eta e^2}{n}\right)^k \cdot (2\pi\beta)^{k-1}. \end{aligned} \quad (147)$$

Using a similar argument, we can upper-bound the integral

$$\int_{1/(\lambda\eta e)}^{\infty} F'_0(r)^2 r^{n-k} dr,$$

for  $k \geq 1$  and  $\eta \leq \frac{n}{n+2}(1/e^2)$ . First, note that

$$F'_0(r) = -\sqrt{\frac{n}{S_0}} r^{-n/2} J_{(n/2)+1}(2\pi\beta r)(2\pi\beta). \quad (148)$$

(To see this, write  $F_0(r) = \sqrt{\frac{n}{S_0}}(2\pi\beta)^{n/2} g(2\pi\beta r)$ , where  $g(x) = x^{-n/2} J_{n/2}(x)$ . Then  $F'_0(r) = \sqrt{\frac{n}{S_0}}(2\pi\beta)^{n/2} g'(2\pi\beta r)(2\pi\beta)$ , where  $g'(x) = -x^{-n/2} J_{(n/2)+1}(x)$ , see [1] eqn. 9.1.30.) Then we write the following: (recall the definition  $\lambda = 2\pi\beta e/n$ , which implies  $2\pi\beta/(\lambda\eta e) = n/(\eta e^2)$ )

$$\begin{aligned} \int_{1/(\lambda\eta e)}^{\infty} F'_0(r)^2 r^{n-k} dr &= \frac{n}{S_0} \int_{1/(\lambda\eta e)}^{\infty} J_{(n/2)+1}(2\pi\beta r)^2 r^{-k} dr \cdot (2\pi\beta)^2 \\ &= \frac{n}{S_0} \int_{2\pi\beta/(\lambda\eta e)}^{\infty} J_{(n/2)+1}(t)^2 t^{-k} dt \cdot (2\pi\beta)^{k+1} \\ &\leq \frac{n}{S_0} \frac{4}{\pi\sqrt{3}k} \left(\frac{\eta e^2}{n}\right)^k \cdot (2\pi\beta)^{k+1}. \end{aligned} \quad (149)$$

We now combine this with the results of section 3, to show a bound on the variance of  $\vec{b}$  perpendicular to  $\vec{\theta}$ , conditioned on  $a \leq \eta$ .

Substituting into equations (52), (59) and (77), we get:

$$\begin{aligned} \left| \int_0^\eta I_{Br} I_{B1} I_2 \frac{da}{a^{n+1}} \right| &\leq \frac{25}{S_0} \frac{\eta^3}{n} (2\pi\beta)^2, \\ 0 \leq \int_0^\eta I_{Ar} I_{A1} I_2 \frac{da}{a^{n+1}} &\leq \frac{5}{n-1} \left( \frac{8}{S_0} \eta^2 (2\pi\beta)^2 + \frac{3600}{S_0} \frac{\eta^4}{n^2} (2\pi\beta)^2 \right), \\ 0 \leq \int_0^\eta I_{Cr} I_{C1} I_2 \frac{da}{a^{n+1}} &\leq \left( 1 + \frac{5}{n-3} \right) \frac{320}{S_0} \frac{\eta^2}{n} (2\pi\beta)^2. \end{aligned}$$

Substituting into equation (48), and using (145), we get:

$$\begin{aligned} E(\vec{b}^T (I - \vec{\theta}\vec{\theta}^T) \vec{b} \mid a \leq \eta) &\leq \frac{5 \cdot 20}{\eta} \left( 1 + \frac{1}{n-1} \right) \beta^2 \left( 360\eta^2 + \frac{1600}{n-3} \eta^2 + 50\eta^3 + \frac{18000}{n^2} \eta^4 \right) \\ &\leq (1 + O(\frac{1}{n})) \beta^2 \eta \left( 1872 + 260\eta + O(\frac{1}{n}) \right). \end{aligned} \quad (150)$$

Using our assumption that  $\eta \leq 1/e^2$ , we can rewrite this as

$$\boxed{E(\vec{b}^T(I - \vec{\theta}\vec{\theta}^T)\vec{b} \mid a \leq \eta) \leq \eta\beta^2(1908 + O(\frac{1}{n}))}. \quad (151)$$

#### 4.5 The variance of $\vec{b}$ parallel to $\vec{\theta}$

We also get a bound on the variance of  $\vec{b}$  parallel to  $\vec{\theta}$ , conditioned on  $a \leq \eta$ .

Substituting into equations (98), (104) and (115), we get:

$$\begin{aligned} \left| \int_0^\eta K_{Br}K_{B1}K_2 \frac{da}{a^{n+1}} \right| &\leq \frac{25}{S_0} \eta^3 (2\pi\beta)^2, \\ 0 \leq \int_0^\eta K_{Ar}K_{A1}K_2 \frac{da}{a^{n+1}} &\leq \frac{12}{S_0} \eta (2\pi\beta)^2 + \frac{5300}{S_0} \frac{\eta^3}{n^2} (2\pi\beta)^2, \\ 0 \leq \int_0^\eta K_{Cr}K_{C1}K_2 \frac{da}{a^{n+1}} &\leq \frac{700}{S_0} \frac{\eta^3}{n} (2\pi\beta)^2 + \frac{500}{S_0} \eta^3 \left(1 + \frac{5}{n-3}\right) (2\pi\beta)^2. \end{aligned}$$

Substituting into equation (97), and using (145), we get:

$$\begin{aligned} E((\vec{b} \cdot \vec{\theta})^2 \mid a \leq \eta) &\leq \frac{5.20}{\eta} \left(1 + \frac{1}{n-1}\right) \beta^2 \left(12\eta + 100\eta^3 \left(\frac{53}{n^2} + \frac{1}{2} + \frac{7}{n} + 5 + \frac{25}{n-3}\right)\right) \\ &\leq (1 + O(\frac{1}{n})) \beta^2 \left(63 + 3120\eta^2 + O(\frac{1}{n})\right). \end{aligned} \quad (152)$$

Using our assumption that  $\eta \leq 1/e^2$ , we can rewrite this as

$$\boxed{E((\vec{b} \cdot \vec{\theta})^2 \mid a \leq \eta) \leq \beta^2(121 + O(\frac{1}{n}))}. \quad (153)$$

## 5 Spherical Shells

We now consider the curvelet transform of a function supported on a spherical shell in  $\mathbb{R}^n$ . We will prove bounds on the distribution of probability mass, showing that the curvelet transform reveals information about the center of the spherical shell, just as it did with the ball, but with a significant improvement: we can find the center with accuracy that scales with the *thickness* of the shell. Even if the shell has very large radius, if it is also very thin (i.e., its inner and outer surfaces are close together), then we can find its center very accurately.

We will use these results in Section 7, to design a quantum algorithm for an oracle problem, finding the center of a radial function. We will give evidence that the quantum algorithm requires a constant number of queries and polynomial time, whereas known classical algorithms for the same problem require a polynomial number of queries and polynomial time.

Without loss of generality, we can assume the shell is centered at the origin (see Section 4). So consider the following function on  $\mathbb{R}^n$ ,

$$f(\vec{x}) = \begin{cases} C, & \text{if } \beta < |\vec{x}| \leq \beta + \delta, \\ 0, & \text{otherwise,} \end{cases} \quad (154)$$

where  $C = 1/\sqrt{(\beta + \delta)^n B_0 - \beta^n B_0}$ , and  $B_0$  is the volume of the unit ball in  $\mathbb{R}^n$ . This represents a uniform superposition over a spherical shell centered at the origin, with inner radius  $\beta$  and thickness  $\delta$ . We call this a spherical shell with “square” cross-section.

This is the exactly the kind of state that appears in our quantum algorithm. However, it is difficult to analyze, as its Fourier transform involves a linear combination of two Bessel

functions oscillating at different rates. We will give a heuristic explanation of why this state lets us find the center with precision proportional to  $\delta$ . Then we will give a more rigorous argument, for spherical shells that have ‘‘Gaussian’’ cross-sections—these functions are similar to the above, but they are analytically tractable.

We can write  $f = h - g$ , where  $h$  is  $C$  times the indicator function of a ball of radius  $\beta + \delta$  around the origin, and  $g$  is  $C$  times the indicator function of a ball of radius  $\beta$  around the origin. Then its Fourier transform is  $\hat{f} = \hat{h} - \hat{g}$ , where  $\hat{h}$  and  $\hat{g}$  are calculated as in Section 4. We can write this as:  $\hat{f}(\vec{k}) = F_0(|\vec{k}|)$ ,

$$F_0(\rho) = \frac{C}{\rho^{n/2}}(\beta + \delta)^{n/2} J_{n/2}(2\pi(\beta + \delta)\rho) - \frac{C}{\rho^{n/2}}\beta^{n/2} J_{n/2}(2\pi\beta\rho). \quad (155)$$

We are interested in the case where  $\delta \ll \beta$ . Note that interference between the two Bessel functions begins to play a major role when  $\rho \gtrsim 1/(2\pi\delta)$ . We claim that  $F_0(\rho)$  decays quite slowly, out to distance  $1/(2\pi\delta)$ .

It will be convenient to define

$$K(\beta) = \beta^{n/2} J_{n/2}(2\pi\beta\rho), \quad (156)$$

so we have

$$F_0(\rho) = \frac{C}{\rho^{n/2}}(K(\beta + \delta) - K(\beta)). \quad (157)$$

We can approximate  $F_0(\rho)$  by a simpler expression. First, when  $\delta \ll \beta$ , we can write  $C$  as follows:

$$C \approx \frac{1}{\sqrt{n\beta^{n-1}\delta B_0}} = \sqrt{\frac{\beta}{n\delta}} \frac{1}{\sqrt{\beta^n B_0}}. \quad (158)$$

Also, when  $\delta$  is sufficiently small (we will elaborate on this point later),

$$F_0(\rho) \approx \frac{C}{\rho^{n/2}} \delta K'(\beta). \quad (159)$$

A straightforward calculation (see [1], equation 9.1.30) shows that

$$K'(\beta) = (2\pi\rho)\beta^{n/2} J_{(n/2)-1}(2\pi\beta\rho). \quad (160)$$

Note that  $K'(\beta)$  is roughly  $2\pi\rho$  times larger than  $K(\beta)$ , so we expect the approximation to be accurate when  $\delta \lesssim 1/(2\pi\rho)$ , or equivalently, when  $\rho \lesssim 1/(2\pi\delta)$ . Combining the above equations, we get the following approximation for  $F_0(\rho)$ :

$$\begin{aligned} F_0(\rho) &\approx \sqrt{\frac{\beta}{n\delta}} \frac{1}{\sqrt{\beta^n B_0}} \cdot \frac{1}{\rho^{n/2}} \delta \cdot (2\pi\rho)\beta^{n/2} J_{(n/2)-1}(2\pi\beta\rho) \\ &= \sqrt{\frac{\beta\delta}{S_0}} \frac{2\pi}{\rho^{(n/2)-1}} J_{(n/2)-1}(2\pi\beta\rho), \end{aligned} \quad (161)$$

where  $S_0$  is the surface area of the sphere in  $\mathbb{R}^n$  (note that  $B_0 = S_0/n$ ).

Compared to the Fourier transform of the ball (Section 4), this function decays more slowly, out to distance  $1/(2\pi\delta)$ . Thus, when we apply the curvelet transform, with significant probability, we can observe fine-scale elements  $a \leq \eta$ , where  $\eta$  shrinks with  $\delta$ . This suggests that a very thin spherical shell (i.e.,  $\delta$  very small) allows us to find the center with very high precision.

Now we take a different approach to the problem: we consider functions that approximate the spherical shell, but are easier to analyze. This will lead to a more rigorous version of the above claim.

First, consider a shell with infinitesimal thickness. Let  $q$  be the measure supported on the sphere of radius  $\beta$  around the origin, and obtained by restricting the usual volume measure on  $\mathbb{R}^n$ . Note that

$$\int_{\mathbb{R}^n} q(\vec{x}) d\vec{x} = \beta^{n-1} S_0, \quad (162)$$

where  $S_0$  is the surface area of the unit sphere. We can write  $q$  in terms of the Dirac delta function,

$$q(\vec{x}) = q_0(|\vec{x}|), \quad q_0(r) = \delta(r - \beta). \quad (163)$$

Then the Fourier transform  $\hat{q}$  is given by

$$\hat{q}(\vec{k}) = Q_0(|\vec{k}|), \quad Q_0(\rho) = \frac{2\pi}{\rho^{(n/2)-1}} J_{(n/2)-1}(2\pi\beta\rho) \beta^{n/2}. \quad (164)$$

This resembles the Fourier transform of the ball, except that it decays more slowly. Thus there is more probability mass in the high-frequency regions, which correspond to finer scales—this is the intuitive reason why our algorithm can find the center more precisely.

However, the function  $q$  is not a realistic model of our quantum state, because its  $L^2$  norm is infinite, and because it does not account for the finite thickness of the spherical shell. Both of these problems can be fixed by convolving  $q$  with a smooth bump function  $g$  of width  $\delta$  (e.g., a Gaussian). We describe this next.

Let

$$f = g * q. \quad (165)$$

Then  $f$  has finite  $L^2$  norm (see, e.g., Young’s convolution theorem), and it represents a superposition over a spherical shell with thickness  $\delta$  (though the function is not quite uniform over the shell, and does not immediately drop to 0 as one moves away from the shell). Note that over the frequency domain,

$$\hat{f} = \hat{g} \cdot \hat{q}, \quad (166)$$

where  $\hat{g}$  is a smoothly decaying function of width  $1/\delta$ . Intuitively, this “cuts off” the frequencies above  $1/\delta$ . So, when we perform the curvelet transform, the finest scale we can measure will be proportional to  $\delta$ , hence we can find the center with accuracy proportional to  $\delta$ .

We will analyze the case where  $g$  is a Gaussian of width  $\delta$ :

$$g(\vec{x}) = \delta^{-n/2} \exp(-\pi|\vec{x}|^2/\delta^2), \quad (167)$$

$$\hat{g}(\vec{k}) = \delta^{n/2} \exp(-\pi\delta^2|\vec{k}|^2). \quad (168)$$

We call this a spherical shell with “Gaussian” cross-section. It is more convenient to write the normalization factor for  $f$  separately, so we write

$$f = C_f g * q, \quad (169)$$

$$\hat{f} = C_f \hat{g} \cdot \hat{q}. \quad (170)$$

Clearly,  $f$  is a radial function, and so is  $\hat{f}$ ,

$$\hat{f}(\vec{k}) = F_0(|\vec{k}|), \quad F_0(\rho) = C_f \cdot \delta^{n/2} \frac{2\pi}{\rho^{(n/2)-1}} \beta^{n/2} \cdot \exp(-\pi\delta^2\rho^2) \cdot J_{(n/2)-1}(2\pi\beta\rho). \quad (171)$$

Note that this is quite similar to equation (161), when we substitute in the upper and lower bounds on  $C_f$  (to be given later in this section). This suggests that the spherical shell with “square” cross-section can indeed be approximated by one with “Gaussian” cross-section.

We will prove bounds on the curvelet transform of a spherical shell with “Gaussian” cross-section. We will use the continuous curvelet transform, with the same window functions as in Section 4. We use a slightly different scaling parameter,

$$\lambda = \frac{2\pi\beta e}{n-2}. \quad (172)$$



We assume that the dimension  $n$  is at least 4, and we assume that the thickness of the shell is small compared to the radius,

$$\delta = \varepsilon\beta, \quad \varepsilon \leq \min\left(\frac{6}{(n-2)^2}, \frac{1}{n+2}, \frac{1}{\varepsilon n}\right). \quad (173)$$

(Note that for these values of  $n$ ,  $\frac{1}{\varepsilon n} \leq \frac{1}{n+2}$ , so the middle condition is actually redundant.) Note that we can write  $F_0(\rho)$  as follows, substituting in  $\delta = \varepsilon\beta$ :

$$F_0(\rho) = C_f \cdot \varepsilon^{n/2} \frac{2\pi}{\rho^{(n/2)-1}} \beta^n \cdot \exp(-\pi\varepsilon^2\beta^2\rho^2) \cdot J_{(n/2)-1}(2\pi\beta\rho). \quad (174)$$

Under these assumptions, we prove the following:

**Theorem 4** *Almost all of the power in  $\hat{f}$  is located at frequencies  $|\vec{k}| \geq 1/\lambda$ :*

$$\int_{|\vec{k}| \leq 1/\lambda} |\hat{f}(\vec{k})|^2 d\vec{k} \leq \frac{\varepsilon}{5}. \quad (175)$$

Let  $\eta_c = \varepsilon(n-2)/e$ . The probability of observing a fine-scale element  $a \leq \eta_c$  is lower-bounded by:

$$\Pr[a \leq \eta_c] > 0.045. \quad (176)$$

Furthermore, the variance of  $\vec{b}$ , in the directions orthogonal / parallel to  $\vec{\theta}$ , conditioned on  $a \leq \eta_c$ , is upper-bounded by:

$$E(\vec{b}^T(I - \vec{\theta}\vec{\theta}^T)\vec{b} \mid a \leq \eta_c) \leq (n-1)\varepsilon\beta^2(507 + O(\frac{1}{n})), \quad (177)$$

$$E((\vec{b} \cdot \vec{\theta})^2 \mid a \leq \eta_c) \leq \beta^2(23 + O(\frac{1}{n^2})). \quad (178)$$

## 5.1 The normalization factor $C_f$

We begin by proving upper and lower bounds on the normalization factor  $C_f$ . The following identity will be useful: (this follows from the definition of  $F_0(\rho)$  and a change of variables)

$$\int_{\alpha}^{\alpha'} F_0(\rho)^2 \rho^{n-1} d\rho = C_f^2 \varepsilon^n \beta^{2n-2} \int_{2\pi\beta\alpha}^{2\pi\beta\alpha'} \exp(-\frac{1}{2\pi}\varepsilon^2 t^2) J_{(n/2)-1}(t)^2 t dt. \quad (179)$$

Then the  $L^2$  norm of  $\hat{f}(\vec{k})$  is given by:

$$\begin{aligned} \int_{\mathbb{R}^n} |\hat{f}(\vec{k})|^2 d\vec{k} &= S_0 \int_0^\infty F_0(\rho)^2 \rho^{n-1} d\rho \\ &= S_0 C_f^2 \varepsilon^n \beta^{2n-2} \int_0^\infty \exp(-\frac{1}{2\pi}\varepsilon^2 t^2) J_{(n/2)-1}(t)^2 t dt \\ &= S_0 C_f^2 \varepsilon^n \beta^{2n-2} (N_1 + N_2), \end{aligned} \quad (180)$$

where we split the integral into two parts,

$$N_1 = \int_0^{n-2} \exp(-\frac{1}{2\pi}\varepsilon^2 t^2) J_{(n/2)-1}(t)^2 t dt, \quad (181)$$

$$N_2 = \int_{n-2}^\infty \exp(-\frac{1}{2\pi}\varepsilon^2 t^2) J_{(n/2)-1}(t)^2 t dt. \quad (182)$$

We now prove upper bounds on  $N_1$  and  $N_2$ . For  $N_1$ , using trivial upper bounds on  $\exp(-x^2)$  and  $J_\nu(x)^2$  (see [1], eqn. 9.1.60), we get:

$$N_1 \leq \int_0^{n-2} \frac{1}{2} t dt = \frac{1}{4}(n-2)^2. \quad (183)$$

For  $N_2$ , using the upper bound on  $J_\nu(x)^2$  from equation (134), we get:

$$\begin{aligned}
N_2 &\leq \int_{n-2}^{\infty} \exp(-\frac{1}{2\pi}\varepsilon^2 t^2) \frac{4}{\pi\sqrt{3}} dt \\
&= \frac{4}{\pi\sqrt{3}} \sqrt{2\pi} \frac{1}{\varepsilon} \int_{\frac{1}{\sqrt{2\pi}}\varepsilon(n-2)}^{\infty} \exp(-\tau^2) d\tau \\
&\leq \frac{4}{\pi\sqrt{3}} \sqrt{2\pi} \frac{1}{\varepsilon} \frac{\sqrt{\pi}}{2} = 2\sqrt{\frac{2}{3}} \frac{1}{\varepsilon}.
\end{aligned} \tag{184}$$

Substituting into (180), we get

$$\int_{\mathbb{R}^n} |\hat{f}(\vec{k})|^2 d\vec{k} \leq S_0 C_f^2 \varepsilon^n \beta^{2n-2} (\frac{1}{4}(n-2)^2 + 2\sqrt{\frac{2}{3}} \frac{1}{\varepsilon}).$$

We assumed  $\varepsilon \leq \frac{6}{(n-2)^2}$ , and it is easy to check that this implies  $\frac{1}{4}(n-2)^2 \leq 2\sqrt{\frac{2}{3}} \frac{1}{\varepsilon}$ . Thus

$$\int_{\mathbb{R}^n} |\hat{f}(\vec{k})|^2 d\vec{k} \leq S_0 C_f^2 \varepsilon^n \beta^{2n-2} \cdot 4\sqrt{\frac{2}{3}} \frac{1}{\varepsilon}.$$

Setting the left side equal to 1 implies a lower bound on  $C_f^2$ :

$$\boxed{C_f^2 \geq \frac{1}{S_0 \varepsilon^{n-1} \beta^{2n-2}} \cdot \frac{1}{4} \sqrt{\frac{3}{2}}.} \tag{185}$$

Next we show lower bounds on  $N_1$  and  $N_2$ . For  $N_1$  we have a trivial lower bound,

$$N_1 \geq 0. \tag{186}$$

For  $N_2$ , we use the lower bound  $J_\nu(x)^2 > \frac{2}{\pi x} \cos^2(\theta_\nu(x))$  (see equations (135) and (133)). For convenience, we define  $\theta(x) = \theta_\nu(x)$ , suppressing the  $\nu$  subscript. We get:

$$N_2 \geq \frac{2}{\pi} \int_{n-2}^{\infty} \exp(-\frac{1}{2\pi}\varepsilon^2 t^2) \cos^2(\theta(t)) dt. \tag{187}$$

Note that  $\theta(t)$  is a monotone increasing function (equation (138)), hence it is one-to-one and has a well-defined inverse. We make a change of variables,  $\tau = \theta(t)$ ,  $t = \theta^{-1}(\tau)$ :

$$N_2 \geq \frac{2}{\pi} \int_{\theta(n-2)}^{\infty} \exp(-\frac{1}{2\pi}\varepsilon^2 (\theta^{-1}(\tau))^2) \cos^2 \tau \cdot (\theta^{-1})'(\tau) d\tau. \tag{188}$$

Note that, whenever  $\tau = \theta(t)$ , we have  $(\theta^{-1})'(\tau) = \frac{1}{\theta'(t)}$ . Hence, by equation (138),

$$1 < (\theta^{-1})'(\tau) < \frac{2}{\sqrt{3}}, \quad \text{for } \tau \geq \theta(n-2). \tag{189}$$

Also note that

$$\begin{aligned}
\theta^{-1}(\tau) &= \theta^{-1}(\theta(n-2)) + \int_{\theta(n-2)}^{\tau} (\theta^{-1})'(x) dx \\
&\leq n-2 + \frac{2}{\sqrt{3}}(\tau - \theta(n-2)).
\end{aligned} \tag{190}$$

Substituting in, we get:

$$N_2 \geq \frac{2}{\pi} \int_{\theta(n-2)}^{\infty} \exp(-\frac{1}{2\pi}\varepsilon^2 \cdot (n-2 + \frac{2}{\sqrt{3}}(\tau - \theta(n-2)))^2) \cos^2 \tau d\tau. \tag{191}$$

We will use the following simple fact: if a function  $f$  is nonnegative and monotone decreasing on the interval  $[\alpha, \infty)$ , then

$$\int_{\alpha}^{\infty} f(x) \cos^2 x dx \geq \frac{1}{2} \int_{\alpha+\pi}^{\infty} f(x) dx. \quad (192)$$

This follows because

$$\begin{aligned} \int_{\alpha}^{\infty} f(x) \cos^2 x dx &= \sum_{k=0}^{\infty} \int_{\alpha+k\pi}^{\alpha+(k+1)\pi} f(x) \cos^2 x dx \\ &\geq \sum_{k=0}^{\infty} f(\alpha + (k+1)\pi) \int_{\alpha+k\pi}^{\alpha+(k+1)\pi} \cos^2 x dx \\ &= \sum_{k=0}^{\infty} f(\alpha + (k+1)\pi) \frac{\pi}{2} \\ &= \sum_{k=0}^{\infty} f(\alpha + (k+1)\pi) \frac{1}{2} \int_{\alpha+(k+1)\pi}^{\alpha+(k+2)\pi} dx \\ &\geq \sum_{k=0}^{\infty} \frac{1}{2} \int_{\alpha+(k+1)\pi}^{\alpha+(k+2)\pi} f(x) dx \\ &= \frac{1}{2} \int_{\alpha+\pi}^{\infty} f(x) dx. \end{aligned} \quad (193)$$

Using the above fact, and a change of variables, we get

$$\begin{aligned} N_2 &\geq \frac{1}{\pi} \int_{\theta(n-2)+\pi}^{\infty} \exp\left(-\frac{1}{2\pi}\varepsilon^2 \cdot \left(n-2 + \frac{2}{\sqrt{3}}(\tau - \theta(n-2))\right)^2\right) d\tau \\ &= \frac{\sqrt{3}}{2\pi} \int_{n-2+\frac{2\pi}{\sqrt{3}}}^{\infty} \exp\left(-\frac{1}{2\pi}\varepsilon^2 x^2\right) dx \\ &= \frac{\sqrt{3}}{\sqrt{2\pi}} \frac{1}{\varepsilon} \int_{\frac{1}{\sqrt{2\pi}}\varepsilon(n-2+\frac{2\pi}{\sqrt{3}})}^{\infty} \exp(-y^2) dy. \end{aligned} \quad (194)$$

Recall that we assumed  $\varepsilon \leq \frac{1}{n+2}$ . This implies  $\frac{1}{\sqrt{2\pi}}\varepsilon(n-2+\frac{2\pi}{\sqrt{3}}) \leq \frac{1}{\sqrt{2\pi}}$ . So, substituting in and integrating numerically, we get that

$$N_2 \geq \frac{\sqrt{3}}{\sqrt{2\pi}} \frac{1}{\varepsilon} \int_{\frac{1}{\sqrt{2\pi}}}^{\infty} \exp(-y^2) dy \geq \frac{1}{4\varepsilon}. \quad (195)$$

Substituting into (180), we get that

$$\int_{\mathbb{R}^n} |\hat{f}(\vec{k})|^2 d\vec{k} \geq S_0 C_f^2 \varepsilon^n \beta^{2n-2} \left(0 + \frac{1}{4\varepsilon}\right) = S_0 C_f^2 \varepsilon^{n-1} \beta^{2n-2} \cdot \frac{1}{4}. \quad (196)$$

Setting the left side equal to 1 implies an upper bound on  $C_f^2$ :

$$\boxed{C_f^2 \leq \frac{4}{S_0 \varepsilon^{n-1} \beta^{2n-2}}}. \quad (197)$$

## 5.2 The low-frequency components

Next, we show that  $\hat{f}(\vec{k})$  has very little power at low frequencies, corresponding to coarse scales  $a \geq 1$ . This justifies our use of the curvelet transform, which effectively ignores these low-frequency components (recall Theorems 1 and 2).

The total amount of power at frequencies less than  $z$  (for any  $z \geq 0$ ) is given by:

$$\begin{aligned} \int_{|\vec{k}| \leq z} |\hat{f}(\vec{k})|^2 d\vec{k} &= S_0 \int_0^z F_0(\rho)^2 \rho^{n-1} d\rho \\ &= S_0 C_f^2 \varepsilon^n \beta^{2n-2} \int_0^{2\pi\beta z} \exp\left(-\frac{1}{2\pi}\varepsilon^2 t^2\right) J_{(n/2)-1}(t)^2 t dt. \end{aligned} \quad (198)$$

(We used equation (179).) Using a trivial upper bound  $\exp(-x^2) \leq 1$ , and the upper bound for  $J_\nu(x)$  (when  $x$  is small) from equation (127), we get:

$$\begin{aligned} \int_{|\vec{k}| \leq z} |\hat{f}(\vec{k})|^2 d\vec{k} &\leq S_0 C_f^2 \varepsilon^n \beta^{2n-2} \int_0^{2\pi\beta z} \frac{1}{\pi(n-2)} \left(\frac{te}{n-2}\right)^{n-2} t dt \\ &= S_0 C_f^2 \varepsilon^n \beta^{2n-2} \cdot \frac{e^{n-2}}{\pi(n-2)^{n-1}} \cdot \frac{1}{n} (2\pi\beta z)^n. \end{aligned} \quad (199)$$

Using our upper bound on  $C_f^2$  (equation (197)), we get

$$\begin{aligned} \int_{|\vec{k}| \leq z} |\hat{f}(\vec{k})|^2 d\vec{k} &\leq 4\varepsilon \cdot \frac{e^{n-2}}{\pi(n-2)^{n-1}} \cdot \frac{1}{n} (2\pi\beta z)^n \\ &\leq \frac{4\varepsilon}{\pi e^2} \cdot \frac{e^n}{(n-2)^n} \cdot (2\pi\beta z)^n. \end{aligned} \quad (200)$$

Now, fix  $z = 1/\lambda$ , where  $\lambda = \frac{2\pi\beta e}{n-2}$ . Then we have

$$\boxed{\int_{|\vec{k}| \leq 1/\lambda} |\hat{f}(\vec{k})|^2 d\vec{k} \leq \frac{4\varepsilon}{\pi e^2} \leq \frac{\varepsilon}{5}.} \quad (201)$$

Recall that we assumed  $\varepsilon \leq \frac{1}{n+2}$ . So the frequencies below  $1/\lambda$  only constitute a small fraction of the total probability mass. This justifies our use of the curvelet transform, with this choice of the parameter  $\lambda$ .

### 5.3 The probability of measuring a fine-scale element

We give a lower bound on the probability of measuring the scale variable to be small,  $a \leq \eta$ . We assume  $\eta \leq 1/e$ ; later, we will be interested in a particular value of  $\eta$ ,

$$\eta_c = \frac{\varepsilon(n-2)}{e}. \quad (202)$$

We will show that  $a \leq \eta_c$  with at least constant probability.

First, we write  $\Pr[a \leq \eta]$  as follows, using equations (26) and (179):

$$\begin{aligned} \Pr[a \leq \eta] &\geq S_0 \int_{1/(\lambda\eta)}^\infty F_0(\rho)^2 \rho^{n-1} d\rho \\ &= S_0 C_f^2 \varepsilon^n \beta^{2n-2} \int_{2\pi\beta/(\lambda\eta)}^\infty \exp\left(-\frac{1}{2\pi}\varepsilon^2 t^2\right) J_{(n/2)-1}(t)^2 t dt. \end{aligned} \quad (203)$$

The lower limit of integration can be simplified, by substituting in the definition of  $\lambda$ ,

$$\frac{2\pi\beta}{\lambda\eta} = \frac{2\pi\beta}{\eta} \cdot \frac{n-2}{2\pi\beta e} = \frac{n-2}{\eta e} \geq n-2. \quad (204)$$

This integral is similar to the integral  $N_2$  which we encountered earlier (equation (182)). We can get a lower bound using the same technique (equations (187) - (194)); this leads to:

$$\Pr[a \leq \eta] \geq S_0 C_f^2 \varepsilon^n \beta^{2n-2} \cdot \frac{\sqrt{3}}{\sqrt{2\pi}} \frac{1}{\varepsilon} \int_{\frac{1}{\sqrt{2\pi}}\varepsilon\left(\frac{n-2}{\eta e} + \frac{2\pi}{\sqrt{3}}\right)}^\infty \exp(-y^2) dy. \quad (205)$$

Now, we specialize to the case  $\eta = \eta_c$ . The lower limit of integration can be written as

$$\begin{aligned} \frac{1}{\sqrt{2\pi}}\varepsilon\left(\frac{n-2}{\eta e} + \frac{2\pi}{\sqrt{3}}\right) &= \frac{1}{\sqrt{2\pi}} + \frac{1}{\sqrt{2\pi}}\varepsilon\frac{2\pi}{\sqrt{3}} \\ &\leq \frac{1}{\sqrt{2\pi}} + \frac{1}{\sqrt{2\pi}} = \sqrt{\frac{2}{\pi}}, \end{aligned} \quad (206)$$

where the last inequality follows because  $\varepsilon \leq \frac{1}{n+2} \leq \frac{1}{5} < \frac{\sqrt{3}}{2\pi}$ . Thus we can lower-bound our integral as follows:

$$\begin{aligned} \Pr[a \leq \eta_c] &\geq S_0 C_f^2 \varepsilon^n \beta^{2n-2} \cdot \frac{\sqrt{3}}{\sqrt{2\pi}} \frac{1}{\varepsilon} \int_{\sqrt{2/\pi}}^{\infty} \exp(-y^2) dy \\ &> S_0 C_f^2 \varepsilon^n \beta^{2n-2} \cdot \frac{0.15}{\varepsilon} \\ &= (0.15) S_0 C_f^2 \varepsilon^{n-1} \beta^{2n-2}. \end{aligned} \quad (207)$$

Now, using our lower bound for  $C_f^2$  (equation (185)), we get:

$$\boxed{\Pr[a \leq \eta_c] \geq (0.15) \cdot \frac{1}{4} \sqrt{\frac{3}{2}} > 0.045.} \quad (208)$$

## 5.4 Some more integrals

Our next goal is to bound the variance of  $\vec{b}$ . We begin by proving upper bounds on certain integrals involving  $F_0(r)$  and  $F'_0(r)$ . Then, in the following two sections, we will bound the variance of  $\vec{b}$  in the directions orthogonal and parallel to  $\vec{\theta}$ .

First, we consider integrals of the following form, where  $k \geq 1$ :

$$\int_{\alpha}^{\infty} F_0(r)^2 r^{n-k} dr. \quad (209)$$

Using the definition of  $F_0(r)$ , and a change of variables,

$$\int_{\alpha}^{\infty} F_0(r)^2 r^{n-k} dr = C_f^2 \varepsilon^n (2\pi)^{k-1} \beta^{2n+k-3} \int_{2\pi\beta\alpha}^{\infty} \exp(-\frac{1}{2\pi}\varepsilon^2 t^2) J_{(n/2)-1}(t)^2 \frac{dt}{t^{k-2}}.$$

We will upper-bound this integral, assuming that  $\alpha \geq \frac{n-2}{2\pi\beta}$ . First, using equation (134), we have  $J_{(n/2)-1}(t)^2 \leq \frac{4}{\pi\sqrt{3}} \frac{1}{t}$ , and we get:

$$\int_{\alpha}^{\infty} F_0(r)^2 r^{n-k} dr \leq C_f^2 \varepsilon^n (2\pi)^{k-1} \beta^{2n+k-3} \cdot \frac{4}{\pi\sqrt{3}} \int_{2\pi\beta\alpha}^{\infty} \exp(-\frac{1}{2\pi}\varepsilon^2 t^2) \frac{dt}{t^{k-1}}.$$

Next, we use a simple inequality:  $t^{k-1} \geq (2\pi\beta\alpha)^{k-1}$ , whenever  $t \geq 2\pi\beta\alpha$ . Thus,

$$\int_{\alpha}^{\infty} F_0(r)^2 r^{n-k} dr \leq C_f^2 \varepsilon^n \beta^{2n-2} \cdot \frac{4}{\pi\sqrt{3}} \frac{1}{\alpha^{k-1}} \int_{2\pi\beta\alpha}^{\infty} \exp(-\frac{1}{2\pi}\varepsilon^2 t^2) dt.$$

The integral on the right hand side can be bounded as follows:

$$\int_{2\pi\beta\alpha}^{\infty} \exp(-\frac{1}{2\pi}\varepsilon^2 t^2) dt = \int_{\frac{1}{\sqrt{2\pi}}\varepsilon \cdot 2\pi\beta\alpha}^{\infty} \exp(-\tau^2) d\tau \cdot \sqrt{2\pi} \frac{1}{\varepsilon} \leq \frac{\sqrt{\pi}}{2} \cdot \sqrt{2\pi} \frac{1}{\varepsilon} = \frac{\pi}{\sqrt{2}} \frac{1}{\varepsilon}.$$

Substituting in, we get:

$$\boxed{\int_{\alpha}^{\infty} F_0(r)^2 r^{n-k} dr \leq C_f^2 \varepsilon^{n-1} \beta^{2n-2} \cdot \frac{4}{\sqrt{6}} \frac{1}{\alpha^{k-1}}.} \quad (210)$$

Next, we consider integrals of the following form, where  $k = 1, 2$ :

$$\int_{\alpha}^{\infty} F_0'(r)^2 r^{n-k} dr. \quad (211)$$

In order to calculate  $F_0'(r)$ , we write  $F_0(r)$  in the following form:

$$F_0(r) = C_f \varepsilon^{n/2} (2\pi) \beta^n \cdot (2\pi\beta)^{(n/2)-1} \cdot H(r) \cdot K(2\pi\beta r),$$

where

$$H(x) = \exp(-\pi\varepsilon^2\beta^2x^2), \quad K(x) = \frac{1}{x^{(n/2)-1}} J_{(n/2)-1}(x).$$

Then  $F_0'(r)$  can be written as

$$F_0'(r) = F_0^{(a)}(r) + F_0^{(b)}(r),$$

where

$$\begin{aligned} F_0^{(a)}(r) &= C_f \varepsilon^{n/2} (2\pi) \beta^n \cdot (2\pi\beta)^{(n/2)-1} \cdot H'(r) \cdot K(2\pi\beta r), \\ F_0^{(b)}(r) &= C_f \varepsilon^{n/2} (2\pi) \beta^n \cdot (2\pi\beta)^{(n/2)-1} \cdot H(r) \cdot K'(2\pi\beta r)(2\pi\beta). \end{aligned}$$

We can expand this out. Note that (see [1], equation (9.1.30))

$$H'(x) = \exp(-\pi\varepsilon^2\beta^2x^2)(-2\pi\varepsilon^2\beta^2x), \quad K'(x) = -\frac{1}{x^{(n/2)-1}} J_{n/2}(x).$$

Substituting in, we get

$$\begin{aligned} F_0^{(a)}(r) &= C_f \varepsilon^{n/2} (2\pi) \beta^n \frac{1}{r^{(n/2)-1}} \cdot \exp(-\pi\varepsilon^2\beta^2r^2)(-2\pi\varepsilon^2\beta^2r) J_{(n/2)-1}(2\pi\beta r), \\ F_0^{(b)}(r) &= C_f \varepsilon^{n/2} (2\pi) \beta^n \frac{1}{r^{(n/2)-1}} \cdot \exp(-\pi\varepsilon^2\beta^2r^2)(-1) J_{n/2}(2\pi\beta r)(2\pi\beta). \end{aligned}$$

Thus  $F_0'(r)$  is given by:

$$F_0'(r) = C_f \varepsilon^{n/2} (2\pi) \beta^n \frac{1}{r^{(n/2)-1}} \exp(-\pi\varepsilon^2\beta^2r^2) \cdot \left( -2\pi\varepsilon^2\beta^2r J_{(n/2)-1}(2\pi\beta r) - 2\pi\beta J_{n/2}(2\pi\beta r) \right). \quad (212)$$

Substituting into our integral, and performing a change of variables, we get:

$$\int_{\alpha}^{\infty} F_0'(r)^2 r^{n-k} dr = C_f^2 \varepsilon^n (2\pi)^{k-1} \beta^{2n+k-3} \int_{2\pi\beta\alpha}^{\infty} \exp(-\frac{1}{2\pi}\varepsilon^2t^2) \left( \varepsilon^2\beta t J_{(n/2)-1}(t) + 2\pi\beta J_{n/2}(t) \right)^2 \frac{dt}{t^{k-2}}. \quad (213)$$

We will upper-bound this integral, assuming that  $\alpha \geq \frac{n}{2\pi\beta}$ . First, using equation (134), we have  $J_{n/2}(t)^2 \leq \frac{4}{\pi\sqrt{3}} \frac{1}{t}$ , and similarly for  $J_{(n/2)-1}(t)^2$ . So we get:

$$\int_{\alpha}^{\infty} F_0'(r)^2 r^{n-k} dr \leq C_f^2 \varepsilon^n (2\pi)^{k-1} \beta^{2n+k-3} \int_{2\pi\beta\alpha}^{\infty} \exp(-\frac{1}{2\pi}\varepsilon^2t^2) \left( \varepsilon^2\beta t + 2\pi\beta \right)^2 \left( \frac{4}{\pi\sqrt{3}} \frac{1}{t} \right) \frac{dt}{t^{k-2}}. \quad (214)$$

Changing variables and rearranging, we get:

$$\begin{aligned} & \int_{\alpha}^{\infty} F_0'(r)^2 r^{n-k} dr \\ & \leq C_f^2 \varepsilon^n (2\pi)^{k-1} \beta^{2n+k-3} \int_{\sqrt{2\pi\varepsilon\beta\alpha}}^{\infty} \exp(-\tau^2) (\sqrt{2\pi\varepsilon\beta\tau} + 2\pi\beta)^2 \frac{4}{\pi\sqrt{3}} \frac{d\tau}{\tau^{k-1}} \cdot \left( \frac{1}{\sqrt{2\pi}} \varepsilon \right)^{k-2} \\ & = C_f^2 \varepsilon^n (2\pi)^{k-1} \beta^{2n+k-3} \cdot \frac{4}{\pi\sqrt{3}} \left( \frac{1}{\sqrt{2\pi}} \varepsilon \right)^{k-2} \int_{\sqrt{2\pi\varepsilon\beta\alpha}}^{\infty} \exp(-\tau^2) (2\pi\varepsilon^2\beta^2\tau^2 + 2(2\pi)^{3/2}\varepsilon\beta^2\tau + (2\pi)^2\beta^2) \frac{d\tau}{\tau^{k-1}} \\ & = C_f^2 \varepsilon^{n+k-2} \sqrt{2\pi}^k \beta^{2n+k-1} \cdot \frac{4}{\pi\sqrt{3}} \int_{\sqrt{2\pi\varepsilon\beta\alpha}}^{\infty} \exp(-\tau^2) (2\pi\varepsilon^2\tau^2 + 2(2\pi)^{3/2}\varepsilon\tau + (2\pi)^2) \frac{d\tau}{\tau^{k-1}}. \end{aligned} \quad (215)$$

We can handle integrals of the form

$$\int_a^\infty \exp(-\tau^2) \frac{d\tau}{\tau^\ell} \quad (216)$$

as follows. When  $\ell \geq 0$ , we have

$$\int_a^\infty \exp(-\tau^2) \frac{d\tau}{\tau^\ell} \leq \frac{1}{a^\ell} \int_a^\infty \exp(-\tau^2) d\tau \leq \frac{1}{a^\ell} \cdot \frac{\sqrt{\pi}}{2}. \quad (217)$$

When  $\ell = -1$ , we have

$$\int_a^\infty \exp(-\tau^2) \tau d\tau \leq \int_0^\infty \exp(-\tau^2) \tau d\tau = -\frac{1}{2} \exp(-\tau^2) \Big|_0^\infty = \frac{1}{2}. \quad (218)$$

When  $\ell = -2$ , we have

$$\int_a^\infty \exp(-\tau^2) \tau^2 d\tau \leq \int_0^\infty \exp(-\tau^2) \tau^2 d\tau = -\frac{1}{2} \exp(-\tau^2) \tau \Big|_0^\infty - \int_0^\infty -\frac{1}{2} \exp(-\tau^2) d\tau = \frac{\sqrt{\pi}}{4} < 0.45. \quad (219)$$

Now, consider the case of  $k = 2$ :

$$\begin{aligned} & \int_\alpha^\infty F'_0(r)^2 r^{n-2} dr \\ & \leq C_f^2 \varepsilon^n (2\pi) \beta^{2n+1} \cdot \frac{4}{\pi\sqrt{3}} \int_{\sqrt{2\pi\varepsilon\beta\alpha}}^\infty \exp(-\tau^2) (2\pi\varepsilon^2\tau^2 + 2(2\pi)^{3/2}\varepsilon\tau + (2\pi)^2) \frac{d\tau}{\tau} \\ & \leq C_f^2 \varepsilon^n (2\pi) \beta^{2n+1} \cdot \frac{4}{\pi\sqrt{3}} \left( 2\pi\varepsilon^2 \cdot \frac{1}{2} + 2(2\pi)^{3/2}\varepsilon \cdot \frac{\sqrt{\pi}}{2} + (2\pi)^2 \cdot \frac{1}{\sqrt{2\pi\varepsilon\beta\alpha}} \frac{\sqrt{\pi}}{2} \right) \\ & = C_f^2 \varepsilon^n (2\pi) \beta^{2n+1} \cdot \frac{8}{\sqrt{3}} \left( \frac{1}{2}\varepsilon^2 + \sqrt{2\pi}\varepsilon + \frac{\pi}{\sqrt{2}} \frac{1}{\varepsilon\beta\alpha} \right). \end{aligned} \quad (220)$$

Now, consider the case of  $k = 1$ :

$$\begin{aligned} & \int_\alpha^\infty F'_0(r)^2 r^{n-1} dr \\ & \leq C_f^2 \varepsilon^{n-1} \sqrt{2\pi} \beta^{2n} \cdot \frac{4}{\pi\sqrt{3}} \int_{\sqrt{2\pi\varepsilon\beta\alpha}}^\infty \exp(-\tau^2) (2\pi\varepsilon^2\tau^2 + 2(2\pi)^{3/2}\varepsilon\tau + (2\pi)^2) d\tau \\ & \leq C_f^2 \varepsilon^{n-1} \sqrt{2\pi} \beta^{2n} \cdot \frac{4}{\pi\sqrt{3}} \left( 2\pi\varepsilon^2 \cdot \frac{\sqrt{\pi}}{4} + 2(2\pi)^{3/2}\varepsilon \cdot \frac{1}{2} + (2\pi)^2 \cdot \frac{\sqrt{\pi}}{2} \right) \\ & = C_f^2 \varepsilon^{n-1} \sqrt{2\pi} \beta^{2n} \cdot \frac{8}{\sqrt{3}} \left( \frac{\sqrt{\pi}}{4}\varepsilon^2 + \sqrt{2\pi}\varepsilon + \pi^{3/2} \right). \end{aligned} \quad (221)$$

## 5.5 The variance of $\vec{b}$ orthogonal to $\vec{\theta}$

We now bound the variance of  $\vec{b}$  orthogonal to  $\vec{\theta}$ , conditioned on observing  $a \leq \eta_c$ . Recall that  $\eta_c = \frac{\varepsilon(n-2)}{e}$ .

We start with the results of Section 3. From equation (52), we get:

$$\left| \int_0^\eta I_{Br} I_{B1} I_2 \frac{da}{a^{n+1}} \right| \leq \frac{1}{4} (n-2) \lambda \eta e \int_{1/(\lambda\eta e)}^\infty F_0(r)^2 r^{n-2} dr. \quad (222)$$

(We used the fact that  $1 \leq r \cdot \lambda\eta e$ , for all  $r$  in this interval.) From equations (59), (61) and (64), we get:

$$\begin{aligned} 0 \leq \int_0^\eta I_{Ar} I_{A1} I_2 \frac{da}{a^{n+1}} & \leq \frac{\pi^2}{2(n-1)} \cdot \frac{1}{\lambda} \int_{1/(\lambda\eta e)}^\infty F'_0(r)^2 r^{n-2} dr + \\ & \frac{\pi^2}{2(n-1)} \cdot 24e^2 \lambda \eta^2 \int_{1/(\lambda\eta e)}^\infty F_0(r)^2 r^{n-2} dr. \end{aligned} \quad (223)$$

(Again, we used the fact that  $1 \leq r \cdot \lambda \eta e$ , for all  $r$  in this interval.) From equation (77), we get:

$$0 \leq \int_0^\eta I_{Cr} I_{C1} I_2 \frac{da}{a^{n+1}} \leq 2(n+10)e\lambda \int_{1/(\lambda\eta e)}^\infty F_0(r)^2 r^{n-2} dr. \quad (224)$$

(We used the fact that  $\frac{8}{3} + 2(n-2)(1 + \frac{5}{n-3}) = \frac{8}{3} + 2(n+3 + \frac{5}{n-3}) \leq 2(n+10)$ , assuming  $n \geq 4$ .)

Now we fix  $\eta = \eta_c$ , and we upper-bound these integrals, using equations (210) and (220). (Note that, in order to apply these results, we must have  $\frac{1}{\lambda\eta_c e} \geq \frac{n}{2\pi\beta}$ . Recall that  $\lambda = \frac{2\pi\beta e}{n-2}$ , and  $\eta_c = \frac{\varepsilon(n-2)}{e}$ . Also, recall that we assumed  $\varepsilon \leq \frac{1}{en}$ . Then  $\frac{1}{\lambda\eta_c e} = \frac{1}{2\pi\beta\varepsilon e} \geq \frac{n}{2\pi\beta}$ , as desired.)

After some tedious calculation, we get:

$$\left| \int_0^{\eta_c} I_{Br} I_{B1} I_2 \frac{da}{a^{n+1}} \right| \leq (n-2) \cdot C_f^2 \varepsilon^{n-1} \beta^{2n-2} \cdot 120\varepsilon^2 \beta^2, \quad (225)$$

$$0 \leq \int_0^{\eta_c} I_{Ar} I_{A1} I_2 \frac{da}{a^{n+1}} \leq 5 \cdot C_f^2 \varepsilon^{n-1} \beta^{2n-2} \cdot \varepsilon \beta^2 (12000\varepsilon^2 + 9\varepsilon + 80), \quad (226)$$

$$0 \leq \int_0^{\eta_c} I_{Cr} I_{C1} I_2 \frac{da}{a^{n+1}} \leq C_f^2 \varepsilon^{n-1} \beta^{2n-2} \cdot 2600\varepsilon \beta^2 (1 + \frac{12}{n-2}). \quad (227)$$

Then, by combining these equations and using our assumption that  $\varepsilon \leq O(\frac{1}{n^2})$ , we get:

$$\begin{aligned} & \int_0^{\eta_c} \left( I_{Ar} I_{A1} I_2 + 2I_{Br} I_{B1} I_2 + I_{Cr} I_{C1} I_2 \right) \frac{da}{a^{n+1}} \\ & \leq C_f^2 \varepsilon^{n-1} \beta^{2n-2} \cdot \varepsilon \beta^2 (60000\varepsilon^2 + 45\varepsilon + 400 + 2(n-2)120\varepsilon + 2600(1 + \frac{12}{n-2})) \\ & \leq C_f^2 \varepsilon^{n-1} \beta^{2n-2} \cdot \varepsilon \beta^2 (400 + 2600 + O(\frac{1}{n})). \end{aligned} \quad (228)$$

Next, recall from equation (207) that:

$$\Pr[a \leq \eta_c] \geq (0.15) S_0 C_f^2 \varepsilon^{n-1} \beta^{2n-2}. \quad (229)$$

Finally, by substituting into equation (48) and simplifying, we get a bound on the variance of  $\vec{b}$ , in the subspace orthogonal to  $\vec{\theta}$ , conditioned on observing  $a \leq \eta_c$ :

$$\boxed{\mathbb{E}(\vec{b}^T (I - \vec{\theta}\vec{\theta}^T) \vec{b} \mid a \leq \eta_c) \leq (n-1)\varepsilon\beta^2(507 + O(\frac{1}{n}))}. \quad (230)$$

## 5.6 The variance of $\vec{b}$ parallel to $\vec{\theta}$

We now bound the variance of  $\vec{b}$  parallel to  $\vec{\theta}$ , conditioned on observing  $a \leq \eta_c$ . Recall that  $\eta_c = \frac{\varepsilon(n-2)}{e}$ .

We start with the results of Section 3. From equation (98), we get:

$$\left| \int_0^\eta K_{Br} K_{B1} K_2 \frac{da}{a^{n+1}} \right| \leq \frac{1}{4}(n-1)(n-2) \int_{1/(\lambda\eta e)}^\infty F_0(r)^2 r^{n-3} dr. \quad (231)$$

From equations (104), (105) and (107), we get:

$$\begin{aligned} 0 \leq \int_0^\eta K_{Ar} K_{A1} K_2 \frac{da}{a^{n+1}} & \leq 2 \int_{1/(\lambda\eta e)}^\infty F_0'(r)^2 r^{n-1} dr + \\ & 2 \cdot \frac{8}{3} \pi^2 \int_{1/(\lambda\eta e)}^\infty F_0(r)^2 r^{n-3} dr. \end{aligned} \quad (232)$$

From equation (115), we get:

$$0 \leq \int_0^\eta K_{Cr} K_{C1} K_2 \frac{da}{a^{n+1}} \leq \frac{\pi^2}{2}(n^2 + 3n + 3) \int_{1/(\lambda\eta e)}^\infty F_0(r)^2 r^{n-3} dr. \quad (233)$$



(We used the fact that  $\frac{2\pi^2}{3}(n-1) + \frac{\pi^2}{2}(n-2)^2(1 + \frac{5}{n-3}) = \frac{\pi^2}{2}(n^2 + \frac{7}{3}n - \frac{7}{3} + \frac{5}{n-3}) \leq \frac{\pi^2}{2}(n^2 + 3n + 3)$ , assuming  $n \geq 4$ .)

Now we fix  $\eta = \eta_c$ , and we upper-bound these integrals, using equations (210) and (221). (Note that, in order to apply these results, we must have  $\frac{1}{\lambda\eta_c e} \geq \frac{n}{2\pi\beta}$ . Recall that  $\lambda = \frac{2\pi\beta e}{n-2}$ , and  $\eta_c = \frac{\varepsilon(n-2)}{e}$ . Also, recall that we assumed  $\varepsilon \leq \frac{1}{en}$ . Then  $\frac{1}{\lambda\eta_c e} = \frac{1}{2\pi\beta\varepsilon} \geq \frac{n}{2\pi\beta}$ , as desired.)

After some tedious calculation, we get:

$$\left| \int_0^{\eta_c} K_{Br}K_{B1}K_2 \frac{da}{a^{n+1}} \right| \leq C_f^2 \varepsilon^{n-1} \beta^{2n-2} \cdot n^2 \cdot 120\varepsilon^2 \beta^2, \quad (234)$$

$$0 \leq \int_0^{\eta_c} K_{Ar}K_{A1}K_2 \frac{da}{a^{n+1}} \leq C_f^2 \varepsilon^{n-1} \beta^{2n-2} \cdot \beta^2 (25200\varepsilon^2 + 60\varepsilon + 132), \quad (235)$$

$$0 \leq \int_0^{\eta_c} K_{Cr}K_{C1}K_2 \frac{da}{a^{n+1}} \leq C_f^2 \varepsilon^{n-1} \beta^{2n-2} \cdot 2400(n^2 + 3n + 3)\varepsilon^2 \beta^2. \quad (236)$$

Then, by combining these equations and using our assumption that  $\varepsilon \leq O(\frac{1}{n^2})$ , we get:

$$\begin{aligned} & \int_0^{\eta_c} \left( K_{Ar}K_{A1}K_2 - 2K_{Br}K_{B1}K_2 + K_{Cr}K_{C1}K_2 \right) \frac{da}{a^{n+1}} \\ & \leq C_f^2 \varepsilon^{n-1} \beta^{2n-2} \cdot \beta^2 (25200\varepsilon^2 + 60\varepsilon + 132 + 2 \cdot 120n^2\varepsilon^2 + 2400(n^2 + 3n + 3)\varepsilon^2) \\ & \leq C_f^2 \varepsilon^{n-1} \beta^{2n-2} \cdot \beta^2 (132 + O(\frac{1}{n^2})). \end{aligned} \quad (237)$$

Next, recall from equation (207) that:

$$\Pr[a \leq \eta_c] \geq (0.15) S_0 C_f^2 \varepsilon^{n-1} \beta^{2n-2}. \quad (238)$$

Finally, by substituting into equation (97) and simplifying, we get a bound on the variance of  $\vec{b}$ , in the direction  $\vec{\theta}$ , conditioned on observing  $a \leq \eta_c$ :

$$\boxed{\mathbb{E}((\vec{b} \cdot \vec{\theta})^2 \mid a \leq \eta_c) \leq \beta^2 (23 + O(\frac{1}{n^2}))}. \quad (239)$$

## 6 A Fast Quantum Curvelet Transform

In this section we present a quantum curvelet transform, acting on superposition states, and we show how such a transform can be computed efficiently. First, we describe how the continuous curvelet transform can be discretized, using ideas known previously in the classical setting [4]. Then, we define the quantum curvelet transform. Here we encounter some new technical challenges: implementing this transform requires preparing certain superpositions of different scales and directions  $|a, \vec{\theta}\rangle$ . This seems hard for a generic choice of the window functions  $\chi_{a, \vec{\theta}}(\vec{k})$ . However, we construct two specific families of window functions, for which the quantum curvelet transform can be implemented efficiently. One family consists of indicator functions (“Haar” curvelets), which have poor analytic properties, but are extremely simple. The other family consists of certain “bump” functions, which have nicer smoothness properties, and more closely resemble the curvelets used in Sections 3, 4 and 5.

### 6.1 The Discrete Curvelet Transform

The discrete curvelet transform takes a function  $f(\vec{x})$  and returns a function  $\Gamma_f(a, \vec{b}, \vec{\theta})$ , where both functions are defined over finite domains. This is a discrete analogue of the continuous curvelet transform.

First, we describe the discrete Fourier transform. Recall that the continuous Fourier transform maps a function  $f$  on  $\mathbb{R}^n$  to a function  $\hat{f}$  on  $\mathbb{R}^n$ . We give a heuristic argument

that the discrete Fourier transform arises naturally when we restrict  $f$  to act on a bounded subset of  $\mathbb{R}^n$ , and sample it at discrete points.

Suppose that the support of  $f$  lies within the cube  $[-L, L]^n$ . Consider a new function  $f_1$ , which is defined on  $\mathbb{R}^n$ , agrees with  $f$  on  $[-L, L]^n$ , and is periodic with respect to the lattice  $(2L\mathbb{Z})^n$ . Then  $\hat{f}_1$  is defined on the dual lattice  $(\frac{1}{2L}\mathbb{Z})^n$ , and it agrees with  $\hat{f}$  on these points.

Next, we will sample the function  $f_1$  at points on the lattice  $(\sigma\mathbb{Z})^n$ , where  $\sigma = 2L/M$  for some large natural number  $M$ . This yields a function  $f_2$ , which is defined on  $(\sigma\mathbb{Z})^n \cap [-L, L]^n$ . Its Fourier transform  $\hat{f}_2$  is defined on  $(\frac{1}{2L}\mathbb{Z})^n \cap [-\frac{1}{2\sigma}, \frac{1}{2\sigma}]^n$ . We expect that  $f_2 \approx f_1$  and  $\hat{f}_2 \approx \hat{f}_1$ , provided that  $\hat{f}_1$  has most of its probability mass concentrated within distance  $\frac{1}{2\sigma}$  of the origin.

To summarize, the discrete Fourier transform is a good approximation to the continuous Fourier transform, provided that two conditions hold: (1) over the spatial domain,  $f$  has most of its probability mass concentrated within distance  $L$  of the origin; (2) over the frequency domain,  $\hat{f}$  has most of its probability mass concentrated within distance  $\frac{1}{2\sigma}$  of the origin.

For convenience, we introduce some notation:

$$Z = (\sigma\mathbb{Z})^n \cap [-L, L]^n, \quad \hat{Z} = (\frac{1}{2L}\mathbb{Z})^n \cap [-\frac{1}{2\sigma}, \frac{1}{2\sigma}]^n. \quad (240)$$

Then the discrete Fourier transform maps a function  $f$  on  $Z$  to a function  $\hat{f}$  on  $\hat{Z}$ , as follows:

$$\hat{f}(\vec{k}) = \sigma^n \sum_{\vec{x} \in Z} f(\vec{x}) e^{-2\pi i \vec{k} \cdot \vec{x}}, \quad (241)$$

$$f(\vec{x}) = (\frac{1}{2L})^n \sum_{\vec{k} \in \hat{Z}} \hat{f}(\vec{k}) e^{2\pi i \vec{k} \cdot \vec{x}}. \quad (242)$$

We now define the discrete curvelet transform. This follows the same approach that led to the continuous curvelet transform, but now we use a discrete Fourier transform and a discrete set of window functions.

For the ‘‘location’’ variables  $\vec{x}$  and  $\vec{b}$ , we let  $\vec{x}, \vec{b} \in Z$ . For the ‘‘scale’’ and ‘‘direction’’ variables  $a$  and  $\vec{\theta}$ , we choose them from a discrete set that corresponds to a ‘‘tiling’’ of frequency space. (We will discuss this tiling in further detail below.) The tiles correspond to the supports of the window functions  $\chi_{a, \vec{\theta}}(\vec{k})$ , and the window functions themselves satisfy the identity

$$\sum_{a, \vec{\theta}} \chi_{a, \vec{\theta}}(\vec{k})^2 = 1, \quad \forall \vec{k} \in \hat{Z}. \quad (243)$$

This ensures that the curvelet transform can be realized as a unitary operation on the space spanned by the states  $|\vec{k}, a, \vec{\theta}\rangle$ . The curvelet transform itself is given by

$$\Gamma_f(a, \vec{b}, \vec{\theta}) := (\frac{1}{2L})^n \sum_{\vec{k} \in \hat{Z}} \hat{f}(\vec{k}) \chi_{a, \vec{\theta}}(\vec{k}) e^{2\pi i \vec{k} \cdot \vec{b}}. \quad (244)$$

The tiling of frequency space can be constructed in many different ways, but they share a few basic features. Essentially, the ‘‘scale’’ variable  $a$  should take on values which are powers of 2, and the ‘‘direction’’ variable  $\vec{\theta}$  should take on values separated by angular distance  $\sqrt{a}$ . This yields tiles in frequency space that have length  $1/a$  in the radial direction and length  $1/\sqrt{a}$  in the other orthogonal directions. (See Figure 2 at the beginning of this paper.) This non-uniform sampling of  $a$  and  $\vec{\theta}$  plays the same role (in the discrete case) as the reference measure  $d\mu(a, \vec{b}, \vec{\theta})$  (in the continuous case).

To be more concrete, let  $a$  take on powers of two, between lower and upper cutoff values, that is,  $a \in \{2^{-s} \mid s \in \mathbb{Z}, s_{\text{coarse}} \leq s \leq s_{\text{fine}}\}$ . These coarse- and fine-scale cutoffs arise naturally when one approximates  $\mathbb{R}^n$  by a finite grid: the coarse-scale cutoff measures the size

of the domain, while the fine-scale cutoff measures the spacing between adjacent grid points. They can also be interpreted over frequency space, as low-frequency and high-frequency cutoffs.

We let  $\vec{\theta}$  take on discrete values from some set  $G_a$ , which depends on the scale  $a$ . Intuitively,  $G_a$  consists of points evenly distributed on the sphere  $S^{n-1}$ , with angular spacing  $\sqrt{a}$ . One can think of this as “splitting at every other step”: as one moves to finer and finer scales, at every two steps, the angular spacing between elements in  $G_a$  decreases by a factor of two (while  $a$  decreases by a factor of four).

A special case occurs when  $a$  is at the coarse-scale and fine-scale cutoff values. Here, we do not resolve different directions  $\vec{\theta}$ ; instead, we have a single window function whose support is a disk or an annulus, respectively. We denote this by  $\chi_{a,\vec{\theta}}(\vec{k})$  where  $\theta = \text{“undef”}$ .

Later in this section, we will give a detailed construction of one such tiling, and the corresponding window functions  $\chi_{a,\vec{\theta}}$ .

Note that an example of a discrete curvelet transform (over  $\mathbb{R}^2$  or  $\mathbb{R}^3$ ) can be found in [4]. There, the frequency space is partitioned into concentric cubes according to the scale  $a$ , and these are divided into wedges according to the direction  $\vec{\theta}$ . For our purposes, we will use a tiling based on concentric balls (in  $\mathbb{R}^n$ ), which more closely approximates the continuous curvelet transform defined in Section 2.

As a classical computation, the discrete curvelet transform can be implemented using the fast Fourier transform [4] (see in particular the “wrapping” method). We will use these ideas to implement a quantum curvelet transform. The following discussion will be self-contained; but for readers who are familiar with [4], we mention that we omit the “wrapping” step. Our transform produces curvelet coefficients that are somewhat oversampled, but this does not cause any problems in our situation.

## 6.2 A Fast Quantum Curvelet Transform

The quantum curvelet transform is the unitary operation that maps

$$\sum_{\vec{x}} f(\vec{x})|\vec{x}\rangle|0,\vec{0}\rangle \mapsto \sum_{a,\vec{b},\vec{\theta}} \Gamma_f(a,\vec{b},\vec{\theta})|\vec{b}\rangle|a,\vec{\theta}\rangle. \quad (245)$$

This can be achieved by applying the quantum Fourier transform (QFT), then the operation  $\mathcal{X}$  that maps

$$|\vec{k}\rangle|0,\vec{0}\rangle \mapsto |\vec{k}\rangle \sum_{a,\vec{\theta}} \chi_{a,\vec{\theta}}(\vec{k})|a,\vec{\theta}\rangle, \quad (246)$$

and then the inverse QFT. We want to compute this in time polynomial in  $n$  and  $\log(L/\sigma)$ . This is possible for the QFT, but it is not clear how to perform the operation  $\mathcal{X}$ , for a generic choice of the window functions  $\chi_{a,\vec{\theta}}(\vec{k})$ . In the following section we will construct two families of window functions, for which the operation  $\mathcal{X}$  (and hence the quantum curvelet transform) can be implemented efficiently.

## 6.3 Constructing the Window Functions $\chi_{a,\vec{\theta}}(\vec{k})$

We will construct two families of window functions  $\chi_{a,\vec{\theta}}(\vec{k})$ , for which the operation  $\mathcal{X}$  can be performed efficiently.

First, suppose we have some partition of the frequency domain into disjoint subsets,  $(\mathbb{Z}_M)^n = \bigcup_{a,\vec{\theta}} S_{a,\vec{\theta}}$ , such that given any point  $\vec{k} \in (\mathbb{Z}_M)^n$ , we can efficiently compute which set  $S_{a,\vec{\theta}}$  contains  $\vec{k}$ . Define the window functions to be the indicator functions for these sets,

$$\chi_{a,\vec{\theta}}(\vec{k}) = \begin{cases} 1, & \text{if } \vec{k} \in S_{a,\vec{\theta}}, \\ 0, & \text{otherwise.} \end{cases} \quad (247)$$

Then the operation  $\mathcal{X}$  can be implemented efficiently: it simply maps  $|\vec{k}\rangle|0, \vec{0}\rangle \mapsto |\vec{k}\rangle|a, \vec{\theta}\rangle$ , where  $a$  and  $\vec{\theta}$  denote the set  $S_{a, \vec{\theta}}$  that contains  $\vec{k}$ .

Unfortunately, these window functions are sharply discontinuous, so the resulting curvelets are not very well-localized in space. This makes them poorly suited for the applications proposed in this paper (recall that the results of Sections 3, 4 and 5 required window functions that were  $C^1$ -smooth).

Smooth window functions are more challenging to implement, because the supports of the functions  $\chi_{a, \vec{\theta}}(\vec{k})$  necessarily overlap. Thus, at a given point  $\vec{k}$ , the operation  $\mathcal{X}$  must create a superposition of many values of  $a$  and  $\vec{\theta}$ . These superpositions can be complicated: for instance, if we imagine that the tiling of frequency space looks (locally) like an array of  $n$ -dimensional cubes, then a significant amount of volume lies near the corners of the cubes, and each corner point touches  $2^n$  different cubes, so we would have to prepare superpositions of  $2^n$  different values of  $a$  and  $\vec{\theta}$ . This seems impossible for many choices of the window functions.

However, the above example also suggests a solution to the problem. We can use spherical coordinates, which look locally like Cartesian coordinates (except at the poles). If we define the window functions to be products of simpler functions, each depending on a single variable, then we can prepare these superpositions efficiently. We now demonstrate this construction.

First, recall the definition of spherical coordinates in  $\mathbb{R}^n$ : we have  $(r, \phi_1, \dots, \phi_{n-1})$ , where  $r \in [0, \infty)$ ,  $\phi_1, \dots, \phi_{n-2} \in [0, \pi] \cup \{\text{"undef"}\}$ , and  $\phi_{n-1} \in (-\pi, \pi] \cup \{\text{"undef"}\}$ . We use the value "undef" to represent points on the "poles" of the sphere, e.g., if  $\phi_j = 0$  or  $\pi$ , then  $\phi_{j+1} = \dots = \phi_{n-1} = \text{"undef"}$  (a similar situation arises when  $r = 0$ ).

Cartesian coordinates are written in terms of spherical coordinates as follows:

$$x_1 = r \cos \phi_1 \quad (\text{or } 0 \text{ if undefined}), \quad (248)$$

$$x_j = r \sin \phi_1 \cdots \sin \phi_{j-1} \cos \phi_j \quad (\text{or } 0 \text{ if undefined}) \quad (j = 2, \dots, n-1), \quad (249)$$

$$x_n = r \sin \phi_1 \cdots \sin \phi_{n-1} \quad (\text{or } 0 \text{ if undefined}). \quad (250)$$

The reverse mapping is given by:

$$r = \sqrt{x_1^2 + \cdots + x_n^2}, \quad (251)$$

$$\phi_1 = \arccos(x_1/r) \quad (\text{or "undef" if } r = 0), \quad (252)$$

$$\phi_j = \arccos(x_j / (r \sin \phi_1 \cdots \sin \phi_{j-1})) \quad (\text{or "undef" if } \phi_{j-1} \in \{0, \pi, \text{"undef"}\}) \quad (j = 2, \dots, n-2), \quad (253)$$

$$\phi_{n-1} = \text{sign}(x_n) \arccos(x_{n-1} / (r \sin \phi_1 \cdots \sin \phi_{n-2})) \quad (\text{or "undef" if } \phi_{n-2} \in \{0, \pi, \text{"undef"}\}). \quad (254)$$

Next we will define discrete values for the scale variable  $a$  and the direction variable  $\vec{\theta}$ . In the notation, it will be convenient to represent the scale variable by  $s$  instead of  $a$ , where

$$a = 2^{-s}. \quad (255)$$

We will then define window functions  $\chi_{s, \vec{\theta}}(\vec{k})$ . These will be products of radial and angular components (we write  $\vec{k} = (r, \vec{\phi})$  using spherical coordinates):

$$\chi_{s, \vec{\theta}}(\vec{k}) = w_s(\lambda r) v_{s, \vec{\theta}}(\vec{\phi}). \quad (256)$$

Here,  $\lambda$  is a parameter that sets the radial scaling. For future use, we define the function  $c: [0, \infty) \rightarrow \mathbb{R}$ ,

$$c(x) = \begin{cases} \cos x, & 0 \leq x \leq \pi/2, \\ 0, & x > \pi/2. \end{cases} \quad (257)$$

We begin with the scale variable  $a = 2^{-s}$ . We fix the cutoff values  $s_{min}, s_{max} \in \mathbb{Z}$ , where  $1 \leq s_{min} \leq s_{max}$ . Then we let  $s \in \{s_{min}, s_{min} + 1, \dots, s_{max}\} \cup \{\text{“coarse”}, \text{“fine”}\}$ .

We define radial window functions  $w_s(r)$  as follows:

$$w_s(r) = \begin{cases} c(\frac{\pi}{2}(2^s - r)/2^{s-1}), & 2^{s-1} \leq r \leq 2^s, \\ c(\frac{\pi}{2}(r - 2^s)/2^s), & 2^s \leq r \leq 2^{s+1}, \\ 0, & \text{otherwise,} \end{cases} \quad (258)$$

$$w_{\text{“coarse”}}(r) = \begin{cases} 1, & 0 \leq r \leq 2^{s_{min}-1}, \\ c(\frac{\pi}{2}(r - 2^{s_{min}-1})/2^{s_{min}-1}), & 2^{s_{min}-1} \leq r \leq 2^{s_{min}}, \\ 0, & r \geq 2^{s_{min}}, \end{cases} \quad (259)$$

$$w_{\text{“fine”}}(r) = \begin{cases} 0, & 0 \leq r \leq 2^{s_{max}}, \\ c(\frac{\pi}{2}(2^{s_{max}+1} - r)/2^{s_{max}}), & 2^{s_{max}} \leq r \leq 2^{s_{max}+1}, \\ 1, & r \geq 2^{s_{max}}. \end{cases} \quad (260)$$

It is easy to check that

$$\sum_s w_s(r)^2 = 1 \quad (\forall r \geq 0). \quad (261)$$

(Note that at any given point  $r$ , at most two of the functions  $w_s(r)$  are nonzero.)

We let the direction variable  $\vec{\theta}$  take on values in the set  $G_s(S^{n-1})$ . (Assume for the time being that  $s \notin \{\text{“coarse”}, \text{“fine”}\}$ ; we will handle those special cases later.) The set  $G_s(S^{n-1})$  contains grid points on the sphere  $S^{n-1}$ , defined using spherical coordinates, with angular spacing  $\pi/2^{\lceil s/2 \rceil} \approx \pi/\sqrt{2^s} = \pi\sqrt{a}$ . This set is defined recursively:

$$G_s(S^1) = \{\pi t/2^{\lceil s/2 \rceil} \mid t \in \mathbb{Z}, 0 \leq t \leq 2 \cdot 2^{\lceil s/2 \rceil} - 1\}, \quad (262)$$

$$G_s(S^k) = \{\pi t/2^{\lceil s/2 \rceil} \mid t \in \mathbb{Z}, 1 \leq t \leq 2^{\lceil s/2 \rceil} - 1\} \times G_s(S^{k-1}) \cup \{0, \pi\} \times \{\text{“undef”}\} \quad (k \geq 2). \quad (263)$$

(See Figure 3 for an example.)

We define angular window functions  $v_{s, \vec{\theta}}(\vec{\phi})$  as follows:

$$v_{s, \vec{\theta}}(\vec{\phi}) = \prod_{j=1}^{n-1} u_{s, \theta_j}(\phi_j), \quad (264)$$

where

$$u_{s, \theta_j}(\phi_j) = c(2^{\lceil s/2 \rceil} |\phi_j - \theta_j|/2). \quad (265)$$

This requires some further explanation.

Intuitively,  $u_{s, \theta_j}(\phi_j)$  is a one-dimensional “bump” function centered around  $\theta_j$ , and  $v_{s, \vec{\theta}}(\vec{\phi})$  is a product of these functions.

Note that, for the first  $n - 2$  coordinates  $j = 1, \dots, n - 2$ ,  $u_{s, \theta_j}(\phi_j)$  is defined on the interval  $[0, \pi]$ , whereas for the last coordinate  $j = n - 1$ ,  $u_{s, \theta_j}(\phi_j)$  is defined on the circle  $(-\pi, \pi]$ ; in this latter case, we interpret  $|\phi_j - \theta_j|$  as the shortest-path distance around the circle.

Also, in the definition of  $v_{s, \vec{\theta}}(\vec{\phi})$ , we simply omit those factors that have  $\theta_j = \text{“undef”}$  or  $\phi_j = \text{“undef”}$ . We claim that this is a natural thing to do, in that it yields a simple geometric picture. Intuitively,  $\theta_j = \text{“undef”}$  means that  $\vec{\theta}$  is located on a pole of the sphere, with some coordinate  $\theta_i$  ( $i < j$ ) equal to 0 or  $\pi$ . Then this construction produces a bump function that covers a circular region around the pole, and so does not depend on  $\phi_j$ . On the other hand, if  $\phi_j = \text{“undef”}$ , then  $\vec{\phi}$  is located on a pole of the sphere, with some coordinate  $\phi_i$  ( $i < j$ ) equal to 0 or  $\pi$ . If  $\theta_i \neq \phi_i$ , then  $u_{s, \theta_i}(\phi_i) = 0$ , hence  $v_{s, \vec{\theta}}(\vec{\phi}) = 0$ , independent of  $\phi_j$ . If  $\theta_i = \phi_i$ , then  $\vec{\theta}$  is located on a pole, hence  $v_{s, \vec{\theta}}(\vec{\phi})$  does not depend on  $\phi_j$ .

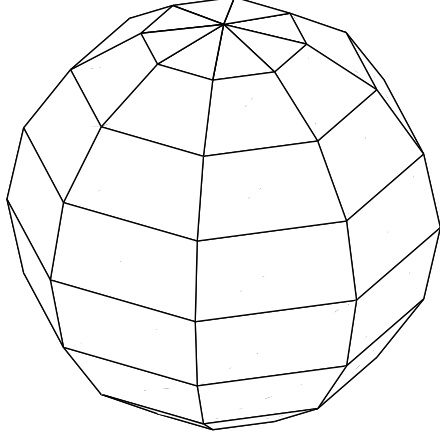


Figure 3: Grid points on the sphere  $S^2$ . Note that this example is slightly different from our construction — it does not use the same spacing between grid points for latitude and longitude.

Note that at least the first ( $j = 1$ ) factor will always be defined, since  $\theta_1$  is always defined whenever  $\vec{\theta} \in G_s(S^{n-1})$ , and  $\phi_1$  is always defined whenever  $\vec{k} \neq \vec{0}$  (we can ignore the case of  $\vec{k} = \vec{0}$ , because it is relevant only when  $s = \text{“coarse”}$ , in which case we will not use these angular windows).

Finally, in the special case where  $s = \text{“coarse”}$  or  $\text{“fine”}$ , we do not resolve any directions  $\vec{\theta}$ . Instead, we fix  $\vec{\theta} = \text{“undef”}$ , and we define the angular window to be trivial,  $v_{s,\vec{\theta}}(\vec{\phi}) = 1$ .

We now show how to perform the operation  $\mathcal{X}$  that maps

$$|\vec{k}\rangle|0, \vec{0}\rangle \mapsto |\vec{k}\rangle \sum_{s, \vec{\theta}} \chi_{s, \vec{\theta}}(\vec{k}) |s, \vec{\theta}\rangle. \quad (266)$$

We will do this by converting  $\vec{k}$  to spherical coordinates  $(r, \vec{\phi})$ , performing an operation  $\mathcal{X}'$  that creates the superposition over  $s$  and  $\vec{\theta}$ , then converting back to Cartesian coordinates:

$$\begin{aligned} |\vec{k}\rangle|0, \vec{0}\rangle|0, \vec{0}\rangle &\mapsto |\vec{k}\rangle|r, \vec{\phi}\rangle|0, \vec{0}\rangle \\ &\mapsto |\vec{k}\rangle|r, \vec{\phi}\rangle \sum_{s, \vec{\theta}} w_s(\lambda r) v_{s, \vec{\theta}}(\vec{\phi}) |s, \vec{\theta}\rangle \\ &= |\vec{k}\rangle|r, \vec{\phi}\rangle \sum_{s, \vec{\theta}} \chi_{s, \vec{\theta}}(\vec{k}) |s, \vec{\theta}\rangle \\ &\mapsto |\vec{k}\rangle|0, \vec{0}\rangle \sum_{s, \vec{\theta}} \chi_{s, \vec{\theta}}(\vec{k}) |s, \vec{\theta}\rangle. \end{aligned} \quad (267)$$

The operation  $\mathcal{X}'$  is implemented recursively, acting on the variables  $r, \phi_1, \dots, \phi_{n-1}$  one at a time:

// The “ $s$ ” register

If  $\lambda r < 2^{s_{min}}$ , then let  $s_1 = \text{“coarse”}$  and  $s_2 = s_{min}$ .

Else if  $\lambda r > 2^{s_{max}}$ , then let  $s_1 = s_{max}$  and  $s_2 = \text{“fine”}$ .

Else, let  $s_1 = \lfloor \lg(\lambda r) \rfloor$  and  $s_2 = \lceil \lg(\lambda r) \rceil$ .  
 If  $s_1 = s_2$ , then set the “s” register to  $|s_1\rangle$ .  
 Else, set the “s” register to  $w_{s_1}(\lambda r)|s_1\rangle + w_{s_2}(\lambda r)|s_2\rangle$ .

// The “ $\theta_1$ ” register  
 If  $s \in \{\text{“coarse”}, \text{“fine”}\}$ , then set the “ $\theta_1$ ” register to  $|\text{“undef”}\rangle$ .  
 Else, begin:  
 Let  $\tau_1 = (\pi/2^s)\lfloor \phi_1(2^s/\pi) \rfloor$  and  $\tau_2 = (\pi/2^s)\lceil \phi_1(2^s/\pi) \rceil$ .  
 If  $\tau_1 = \tau_2$ , then set the “ $\theta_1$ ” register to  $|\tau_1\rangle$ .  
 Else, set the “ $\theta_1$ ” register to  $u_{s,\tau_1}(\phi_1)|\tau_1\rangle + u_{s,\tau_2}(\phi_1)|\tau_2\rangle$ .  
 // Note,  $\phi_1 \neq \text{“undef”}$ , since otherwise we would have  $s = \text{“coarse”}$   
 // Note, if  $\phi_1 \in \{0, \pi\}$ , then  $\tau_1 = \tau_2$ , hence  $\theta_1 \in \{0, \pi\}$   
 End.  
 Recurse on the “ $\theta_2$ ” register.

// The “ $\theta_\ell$ ” register, for  $\ell = 2, \dots, n-2$   
 If  $\theta_{\ell-1} \in \{0, \pi, \text{“undef”}\}$ , then set the “ $\theta_\ell$ ” register to  $|\text{“undef”}\rangle$ .  
 Else, begin:  
 Let  $\tau_1 = (\pi/2^s)\lfloor \phi_\ell(2^s/\pi) \rfloor$  and  $\tau_2 = (\pi/2^s)\lceil \phi_\ell(2^s/\pi) \rceil$ .  
 If  $\tau_1 = \tau_2$ , then set the “ $\theta_\ell$ ” register to  $|\tau_1\rangle$ .  
 Else, set the “ $\theta_\ell$ ” register to  $u_{s,\tau_1}(\phi_\ell)|\tau_1\rangle + u_{s,\tau_2}(\phi_\ell)|\tau_2\rangle$ .  
 // Note,  $\phi_\ell \neq \text{“undef”}$ , since otherwise we would have, in some previous iteration  $k$ ,  
 //  $\phi_k \in \{0, \pi\}$ , hence  $\theta_k \in \{0, \pi\}$ , and  $\theta_{\ell-1} \in \{0, \pi, \text{“undef”}\}$   
 // Note, if  $\phi_\ell \in \{0, \pi\}$ , then  $\tau_1 = \tau_2$ , hence  $\theta_\ell \in \{0, \pi\}$   
 End.  
 Recurse on the “ $\theta_{\ell+1}$ ” register.

// The “ $\theta_{n-1}$ ” register  
 If  $\theta_{n-2} \in \{0, \pi, \text{“undef”}\}$ , then set the “ $\theta_{n-1}$ ” register to  $|\text{“undef”}\rangle$ .  
 Else, begin:  
 Let  $\tau_1 = (\pi/2^s)\lfloor \phi_{n-1}(2^s/\pi) \rfloor$  and  $\tau_2 = (\pi/2^s)\lceil \phi_{n-1}(2^s/\pi) \rceil$ .  
 If  $\tau_1 = \tau_2$ , then set the “ $\theta_{n-1}$ ” register to  $|\tau_1\rangle$ .  
 Else, set the “ $\theta_{n-1}$ ” register to  $\tilde{u}_{s,\tau_1}(\phi_{n-1})|\tau_1\rangle + \tilde{u}_{s,\tau_2}(\phi_{n-1})|\tau_2\rangle$ .  
 // Note,  $\phi_{n-1} \neq \text{“undef”}$ , since otherwise we would have, in some previous iteration  $k$ ,  
 //  $\phi_k \in \{0, \pi\}$ , hence  $\theta_k \in \{0, \pi\}$ , and  $\theta_{n-2} \in \{0, \pi, \text{“undef”}\}$   
 End.

This construction yields a fast quantum curvelet transform using smooth window functions. Note that we can carry out this construction using other choices of the function  $c(x)$ , which lead to different window functions  $\chi_{s,\vec{\theta}}(\vec{k})$ . We only need  $c(x)$  to satisfy the identity  $c(x)^2 + c(\frac{\pi}{2} - x)^2 = 1$  (for all  $0 \leq x \leq \pi/2$ ).

For instance, we can define

$$c(x) = \begin{cases} \cos(h(x)), & 0 \leq x \leq \pi/2, \\ 0, & x > \pi/2, \end{cases} \quad (268)$$

where  $h(x)$  is any increasing function that satisfies  $h(0) = 0$ ,  $h(\frac{\pi}{2}) = \frac{\pi}{2}$ , and  $h(\frac{\pi}{2} - x) = \frac{\pi}{2} - h(x)$  (for all  $0 \leq x \leq \pi/2$ ).

In particular, if we set  $h(x) = \frac{\pi}{2} \sin^2 x$ , then the resulting function  $c(x)$  is  $C^1$ -smooth. Thus we get window functions  $\chi_{s,\vec{\theta}}(\vec{k})$  that are  $C^1$ -smooth, and are qualitatively similar to the ones used in Sections 3-5 of this paper.

## 7 Quantum Algorithms using the Curvelet Transform

In this section we describe two applications of the quantum curvelet transform. The first is a single-shot measurement procedure for finding the center of a ball  $B$  in  $\mathbb{R}^n$ , given a quantum-sample state for  $B$ . This procedure runs in polynomial time, and finds the center of  $B$  with a certain precision and success probability that are *independent* of the dimension  $n$ . By comparison, classical sampling with a single point would achieve the same degree of precision with probability at most  $2^{-\Omega(n)}$ .

Next, we propose an oracle problem called “finding the center of a radial function,” and a quantum algorithm for solving this problem using the curvelet transform. We give a heuristic argument that suggests this algorithm can yield a quantum speed-up. In particular, we argue that it can find the center with a certain precision using  $O(1)$  oracle queries and polynomial time, whereas any classical algorithm seems to require  $\Omega(n)$  queries.

We describe and analyze these ideas over  $\mathbb{R}^n$ , but the algorithms themselves will work over a finite set of points  $G \subset \mathbb{R}^n$ , consisting of a discrete grid restricted to a finite region of space. (For instance, let  $G = (\sigma\mathbb{Z})^n \cap [-L, L]^n$ , which is a square lattice with spacing  $\sigma$  between adjacent points, restricted to the hypercube with side length  $2L$  centered at the origin.) This discrete approximation should not have a big effect, since the spacing between grid points can be exponentially small, and we can compute a quantum curvelet transform on  $(\mathbb{Z}_M)^n$  in time polynomial in  $n$  and  $\log(M)$ .

### 7.1 Single-shot measurement of a quantum-sample state

Consider the following problem:

Input: a natural number  $n$ , such that  $n \geq 4$ ;  
 a description of the set of grid points  $G = (\sigma\mathbb{Z})^n \cap [-L, L]^n$ ;  
 real numbers  $\beta$ ,  $R$  and  $\mu$ ;  
 a quantum state  $\frac{1}{\sqrt{|G \cap B|}} \sum_{\vec{x} \in G \cap B} |\vec{x}\rangle$ , where  $B$  is a ball in  $\mathbb{R}^n$  of radius  $\beta$ ,  
 centered at some unspecified point  $\vec{c}$ , such that  $\vec{c}$  lies within distance  $R$  of the origin.  
 Output: a point  $\vec{z}$  in  $\mathbb{R}^n$ , which lies within distance  $\mu$  of  $\vec{c}$ .

In light of our results in Section 4, we propose the following algorithm. Intuitively, this algorithm uses the curvelet transform to find a line that passes near the center of the ball, then guesses a random point along this line.

Let  $|\psi\rangle$  be the input quantum state.

Set  $\eta = \frac{1}{6} \frac{\mu^2}{\beta^2} \frac{1}{1908 + (Q_1/n)}$ , where  $Q_1$  is a certain constant (see below).

Apply the fast quantum curvelet transform, with the parameters set as follows:

$$\lambda = \frac{2\pi\beta e}{n}, s_{min} = 1, s_{max} = \lg \frac{1}{\eta} + 3.$$

Measure the scale  $a = 2^{-s}$ , location  $\vec{b}$  and direction  $\vec{\theta}$ .

If  $a > \eta$ , then return “no answer.”

Guess some  $u \in [-1, 1]$  uniformly at random.

Return the point  $\vec{b}' = \vec{b} + u(\sqrt{3}\beta\sqrt{121 + (Q_2/n)})\vec{\theta}$ , where  $Q_2$  is a certain constant (see below).

We are especially interested in instances where the error  $\mu$  is a constant fraction of the radius  $\beta$ , say,  $\mu = \nu\beta$ . We conjecture that, for any constant  $\nu$ , the algorithm solves these instances with constant probability. In particular, the success probability is independent of the dimension  $n$ . This is an interesting contrast to what happens in the classical case: if we choose a single point uniformly at random from the ball, then the success probability (i.e., the probability that the point will lie within distance  $\mu$  of the center) is  $\nu^n$ , which is exponentially small in  $n$ .

We now show how our results from Section 4 support this conjecture. Consider a “continuous” analogue of this algorithm, using the continuous curvelet transform over  $\mathbb{R}^n$ . We



will show that this algorithm succeeds with constant probability. (We will also argue, non-rigorously, that the discrete algorithm will behave like the continuous one, provided that the grid  $G$  is sufficiently fine.)

First, we claim that  $a \leq \eta$  with constant probability. By equation (145), we have

$$\Pr[a \leq \eta] \geq (0.19)\eta(1 - \frac{1}{n}). \quad (269)$$

Note that  $\eta$  is a constant, since  $\mu = \nu\beta$ . This shows the claim.

From this point on, all probabilities are conditioned on having  $a \leq \eta$ .

Without loss of generality, assume  $\vec{c} = \vec{0}$ . The algorithm succeeds when it outputs a point close to  $\vec{0}$ . Let  $\Pi_1$  be the projector onto the subspace orthogonal to  $\vec{\theta}$ , and let  $\Pi_2$  be the projector onto the direction  $\vec{\theta}$ . We will show that, with constant probability,  $|\Pi_1 \vec{b}|$  is small and  $|\Pi_2 \vec{b}|$  is not too large.

Let  $X = |\Pi_1 \vec{b}|^2$ ,  $\mu_X = E(X)$ , and let  $Y = |\Pi_2 \vec{b}|^2$ ,  $\mu_Y = E(Y)$ . By Markov's inequality,

$$\Pr[X \geq 3\mu_X] \leq \frac{1}{3}, \quad \Pr[Y \geq 3\mu_Y] \leq \frac{1}{3}.$$

Then, the union bound implies:

$$\Pr[X \leq 3\mu_X \text{ and } Y \leq 3\mu_Y] \geq 1 - \Pr[X \geq 3\mu_X] - \Pr[Y \geq 3\mu_Y] \geq \frac{1}{3}.$$

So, with probability  $\geq 1/3$ , we have  $X \leq 3\mu_X$  and  $Y \leq 3\mu_Y$ .

We now rewrite this in terms of  $|\Pi_1 \vec{b}|$  and  $|\Pi_2 \vec{b}|$ . From equations (151) and (153), we know that

$$\mu_X \leq \eta\beta^2(1908 + (Q_1/n)), \quad \mu_Y \leq \beta^2(121 + (Q_2/n)),$$

for some constants  $Q_1$  and  $Q_2$ . So, we have

$$|\Pi_1 \vec{b}| \leq \sqrt{3}\sqrt{\eta}\beta\sqrt{1908 + (Q_1/n)}, \quad |\Pi_2 \vec{b}| \leq \sqrt{3}\beta\sqrt{121 + (Q_2/n)}. \quad (270)$$

This shows that  $|\Pi_1 \vec{b}|$  (the error orthogonal to  $\vec{\theta}$ ) is small. Indeed, substituting in our choice of  $\eta$ , we see that

$$|\Pi_1 \vec{b}| \leq \frac{1}{\sqrt{2}}\mu. \quad (271)$$

However,  $|\Pi_2 \vec{b}|$  (the error parallel to  $\vec{\theta}$ ) is not so small. So the algorithm tries to guess this error and output a corrected point. It succeeds when

$$|\Pi_2 \vec{b} - u(\sqrt{3}\beta\sqrt{121 + (Q_2/n)})\vec{\theta}| \leq \frac{1}{\sqrt{2}}\mu. \quad (272)$$

Call this event  $E$ . The probability of  $E$  is the probability that a random point chosen uniformly from the interval  $[-\sqrt{3}\beta\sqrt{121 + (Q_2/n)}, \sqrt{3}\beta\sqrt{121 + (Q_2/n)}]$  lies within distance  $\frac{1}{\sqrt{2}}\mu$  of some fixed point in that interval. This probability is lower-bounded by

$$\Pr[E] \geq \frac{\frac{1}{\sqrt{2}}\mu}{2\sqrt{3}\beta\sqrt{121 + (Q_2/n)}} = \frac{1}{2\sqrt{6}\sqrt{121 + (Q_2/n)}} \frac{\mu}{\beta}, \quad (273)$$

which is a constant, since  $\mu = \nu\beta$ .

So the algorithm succeeds with constant probability.

Finally, we argue that, when the grid  $G = (\sigma\mathbb{Z})^n \cap [-L, L]^n$  is chosen properly, the discrete algorithm will behave like the continuous one. Recall from Section 6 that we can approximate a function  $f$  on  $\mathbb{R}^n$  with a function  $f_2$  on  $G$ , provided that most of the probability mass of  $f$  lies within distance  $L$  of the origin, and most of the probability mass of  $\hat{f}$  lies within distance  $\frac{1}{2\sigma}$  of the origin. This holds for our algorithm, provided that:

$$R + \beta \leq L, \quad \frac{100}{\lambda\eta} \leq \frac{1}{2\sigma}. \quad (274)$$

(The first condition follows immediately, since  $f$  is supported on a ball. The second condition follows from the decay of  $\hat{f}$ ; details omitted.)

Also, we argue that the discretization of the “direction” variable  $\vec{\theta}$  will not introduce too much error in the output of the algorithm. Our algorithm constructs a line  $\ell = \{\vec{b} + \lambda\vec{\theta} \mid \lambda \in \mathbb{R}\}$ , and if  $\vec{\theta}$  were a continuous variable, this line would pass within distance  $O(\sqrt{a}\beta)$  of the center  $\vec{c}$ . Recall from Section 6 that the discrete curvelet transform resolves  $\vec{\theta}$  within error  $\pm\sqrt{a}$  in angular distance. Since  $\vec{b}$  lies at distance  $O(\beta)$  from the center  $\vec{c}$ , the error in  $\vec{\theta}$  can increase the distance from  $\ell$  to  $\vec{c}$  by at most  $O(\sqrt{a}\beta)$ . Thus the error in the output of the algorithm increases by at most a constant factor.

We can bound the running time of our algorithm as follows. Say we choose  $L$  and  $\sigma$  so that the above inequalities are tight (up to constant factors). Let  $M$  be the number of grid points along one direction. Then  $M = 2L/\sigma \leq O(R\beta n/\mu^2)$ , and the running time is  $\leq \text{poly}(n, \log M) \leq \text{poly}(n, \log R, \log \beta, \log \frac{1}{\mu})$ .

## 7.2 Quantum algorithm for finding the center of a radial function

Let  $f$  be a radial function on  $\mathbb{R}^n$ , centered at some point  $\vec{c}$ . In particular, suppose that  $\mathbb{R}^n$  can be partitioned into concentric spherical shells of thickness  $\delta$  centered at  $\vec{c}$ , such that  $f$  is constant on each shell, and  $f$  takes on distinct values on different shells. Also, suppose that one can efficiently compute the radius of a shell, given the value of  $f$  on that shell.

Consider the following problem:

Input: a natural number  $n$ , such that  $n \geq 4$ ;  
a description of the set of grid points  $G = (\sigma\mathbb{Z})^n \cap [-L, L]^n$ ;  
real numbers  $R$ ,  $\delta$  and  $\mu$ ;  
an oracle that computes a radial function  $f$ , where  $f$  satisfies the above conditions,  
and the (unknown) center point  $\vec{c}$  lies within distance  $R$  of the origin.  
Output: a point  $\vec{z}$  in  $\mathbb{R}^n$ , which lies within distance  $\mu$  of  $\vec{c}$ .

In light of our results in Section 5, we propose the following algorithm. The basic idea is to prepare a quantum superposition over a spherical shell centered at  $\vec{c}$ , then apply the curvelet transform, and find a line that passes near  $\vec{c}$ . The algorithm does this twice, then returns the point on the first line that lies closest to the second line (note that, with high probability, the two lines are nearly orthogonal).

Set  $R' = nR$ .

For  $i \in \{1, 2\}$ , do the following:

Prepare the state  $\frac{1}{\sqrt{|G \cap B|}} \sum_{\vec{x} \in G \cap B} |\vec{x}\rangle$ , where  $B$  is a ball of radius  $R'$  around  $\vec{0}$ ,

using the methods of [2] or [12].

Compute the value of  $f$  in an auxiliary register, and measure it; call this  $y^{(i)}$ .

Using  $y^{(i)}$ , compute the radius of the spherical shell; call this  $\beta^{(i)}$ .

If  $\beta^{(i)} > R' - R$ , then return “no answer.”

Set  $\varepsilon^{(i)} = \delta/\beta^{(i)}$ , and  $\eta^{(i)} = \varepsilon^{(i)}(n-2)/e$ .

Apply the fast quantum curvelet transform, with the parameters set as follows:

$$\lambda^{(i)} = \frac{2\pi\beta^{(i)}e}{n-2}, s_{min}^{(i)} = 1, s_{max}^{(i)} = \lg \frac{1}{\eta^{(i)}} + 3.$$

Measure the scale  $a^{(i)} = 2^{-s^{(i)}}$ , location  $\vec{b}^{(i)}$  and direction  $\vec{\theta}^{(i)}$ .

If  $a^{(i)} > \eta^{(i)}$ , then return “no answer.”

End for.

If  $|\vec{\theta}^{(1)} \cdot \vec{\theta}^{(2)}| > 3/4$ , then return “no answer.”

Set  $r = \vec{\theta}^{(1)} \cdot \vec{\theta}^{(2)}$ ,  $s = \vec{\theta}^{(1)} \cdot (\vec{b}^{(1)} - \vec{b}^{(2)})$ , and  $t = \vec{\theta}^{(2)} \cdot (\vec{b}^{(1)} - \vec{b}^{(2)})$ .

Return the point  $\frac{-s+r\vec{t}}{1-r^2}\vec{\theta}^{(1)} + \vec{b}^{(1)}$ .

In order for the algorithm to succeed,  $\delta$  must be small, i.e., the radial function  $f$  computed by the oracle must be sufficiently “precise.” Let us assume that

$$\delta \leq \frac{1}{192} \cdot \frac{\mu^2}{(n-1)^2 R} \cdot \frac{1}{507 + (Q_1/n)}. \quad (275)$$

We conjecture that this algorithm then finds a solution with constant probability, independent of the dimension  $n$ . Thus, only a constant number of oracle queries are needed. This is an improvement over the classical case, where  $\Omega(n)$  queries seem to be required.

We now show how our results from Section 5 support this conjecture. Consider a “continuous” analogue of the algorithm, using the continuous curvelet transform over  $\mathbb{R}^n$ . We show that this algorithm succeeds with constant probability. (This holds provided that the spherical shell with square cross-section can be approximated by one with Gaussian cross-section, as in Section 5. This approximation is accurate when  $\delta$  is small. We will also argue, non-rigorously, that the discrete algorithm will behave like the continuous one, provided that the grid  $G$  is sufficiently fine.)

First, consider what happens for each  $i \in \{1, 2\}$ .

We quantum-sample over a ball of radius  $R'$  around  $\vec{0}$ , then measure the value of  $f$ , and get a superposition over a shell of radius  $\beta^{(i)}$  around  $\vec{c}$ . If the shell is too large, it will not lie completely within our original ball, so we only get a fragment of the shell. However, if  $\beta^{(i)} \leq R' - R$ , then we are guaranteed to get a complete shell.

We claim that we observe  $\beta^{(i)} \leq R' - R$  with constant probability. To see this, write:

$$\begin{aligned} \Pr[\beta^{(i)} \leq R' - R] &= \frac{\text{volume of ball of radius } R' - R \text{ around } \vec{c}}{\text{volume of ball of radius } R' \text{ around } \vec{0}} \\ &= \frac{(R' - R)^n}{(R')^n} = \left(1 - \frac{1}{n}\right)^n \geq 1/e^2, \end{aligned} \quad (276)$$

using the fact that  $1 - x \geq e^{-2x}$  for all  $0 \leq x \leq 1/2$ .

Next, we claim that we observe  $a^{(i)} \leq \eta^{(i)}$ , with constant probability. This follows from equation (208):

$$\Pr[a^{(i)} \leq \eta^{(i)}] > 0.045. \quad (277)$$

From this point on, we take probabilities conditioned on  $a^{(i)} \leq \eta^{(i)}$ .

Without loss of generality, assume  $\vec{c} = \vec{0}$ . Let  $\Pi_1^{(i)}$  be the projector onto the subspace orthogonal to  $\vec{\theta}^{(i)}$ , and let  $\Pi_2^{(i)}$  be the projector onto the direction  $\vec{\theta}^{(i)}$ .

We claim that  $|\Pi_1^{(i)} \vec{b}^{(i)}|$  is small, and  $|\Pi_2^{(i)} \vec{b}^{(i)}|$  is of order  $\beta$ , with constant probability. We use the same argument as in the previous section, together with equations (230) and (239). We get that, with probability  $\geq 1/3$ ,

$$|\Pi_1^{(i)} \vec{b}^{(i)}| \leq \sqrt{3} \sqrt{(n-1)\varepsilon^{(i)}\beta^{(i)}} \sqrt{507 + (Q_1/n)}, \quad |\Pi_2^{(i)} \vec{b}^{(i)}| \leq \sqrt{3}\beta^{(i)} \sqrt{23 + (Q_2/n^2)}, \quad (278)$$

for some constants  $Q_1$  and  $Q_2$ .

Using the definition of  $\varepsilon^{(i)}$ , and the fact that  $\beta^{(i)} \leq R' - R = (n-1)R$ , this implies that

$$|\Pi_1^{(i)} \vec{b}^{(i)}| \leq \sqrt{3}(n-1)\sqrt{\delta R} \sqrt{507 + (Q_1/n)}, \quad |\Pi_2^{(i)} \vec{b}^{(i)}| \leq \sqrt{3}(n-1)R \sqrt{23 + (Q_2/n^2)}. \quad (279)$$

The algorithm carries out this procedure twice, for  $i = 1$  and  $2$ . With constant probability, this produces two lines,  $\ell_1 = \{\vec{b}^{(1)} + \lambda \vec{\theta}^{(1)} \mid \lambda \in \mathbb{R}\}$  and  $\ell_2 = \{\vec{b}^{(2)} + \lambda \vec{\theta}^{(2)} \mid \lambda \in \mathbb{R}\}$ , which both pass near the point  $\vec{c}$ . The algorithm then checks that these lines are nearly orthogonal, and if they are, it returns the point on  $\ell_1$  closest to  $\ell_2$ . A straightforward calculation shows that this point is given by  $\frac{-s+rt}{1-r^2} \vec{\theta}^{(1)} + \vec{b}^{(1)}$ .

First, we claim that the lines  $\ell_1$  and  $\ell_2$  are nearly orthogonal ( $|\vec{\theta}^{(1)} \cdot \vec{\theta}^{(2)}| \leq 3/4$ ) with at least constant probability.

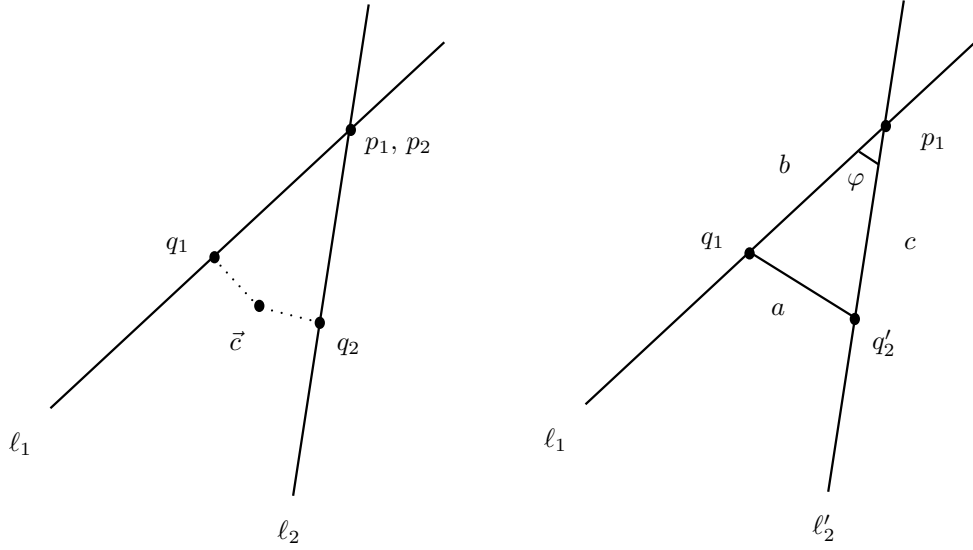


Figure 4:

We want to upper-bound the probability that  $|\vec{\theta}^{(1)} \cdot \vec{\theta}^{(2)}| > 3/4$ . Recall that these are independent random vectors, chosen uniformly from the unit sphere  $S^{n-1}$  in  $\mathbb{R}^n$ . It follows that

$$\Pr[|\vec{\theta}^{(1)} \cdot \vec{\theta}^{(2)}| > 3/4] = \Pr[|x_1| > 3/4], \quad (280)$$

where  $\vec{x} = (x_1, \dots, x_n)$  is a random vector chosen uniformly from  $S^{n-1}$ . Note that  $E(\vec{x}) = \vec{0}$ , hence  $E(x_1) = 0$ ; also,  $E(|\vec{x}|^2) = 1$ , hence  $E(x_1^2) = 1/n$ . Then by Markov's inequality,

$$\Pr[|x_1| > 3/4] = \Pr[x_1^2 > 9/16] \leq \frac{16}{9} \frac{1}{n} \leq \frac{8}{9} \quad (\text{for } n \geq 2). \quad (281)$$

(This is a rather weak bound, especially when  $n$  is large, but it is adequate for our purposes.) Thus, we observe  $|\vec{\theta}^{(1)} \cdot \vec{\theta}^{(2)}| \leq 3/4$ , with at least constant probability.

Next, we claim that when  $\ell_1$  and  $\ell_2$  are nearly orthogonal ( $|\vec{\theta}^{(1)} \cdot \vec{\theta}^{(2)}| \leq 3/4$ ), the point on  $\ell_1$  closest to  $\ell_2$  (call it  $p_1$ ) is close to  $\vec{c}$ .

Let  $q_1$  be the point on  $\ell_1$  closest to  $\vec{c}$ , and let  $p_1$  be the point on  $\ell_1$  closest to  $\ell_2$ . Similarly, let  $q_2$  be the point on  $\ell_2$  closest to  $\vec{c}$ , and let  $p_2$  be the point on  $\ell_2$  closest to  $\ell_1$ . (See Figure 4.)

We know that  $q_1$  and  $q_2$  are both close to  $\vec{c}$ :  $|q_1 - \vec{c}| \leq \Delta$ , and  $|q_2 - \vec{c}| \leq \Delta$ , where  $\Delta = \sqrt{3(n-1)}\sqrt{\delta R}\sqrt{507 + (Q_1/n)}$ . Furthermore,  $p_1$  and  $p_2$  are close together:  $|p_1 - p_2| \leq 2\Delta$ .

Now suppose that  $p_1$  is far from  $\vec{c}$ :

$$|p_1 - \vec{c}| \geq 8\Delta. \quad (282)$$

From this we will derive a contradiction.

First, note that  $p_1$  is far from  $q_1$ :

$$|p_1 - q_1| \geq 7\Delta. \quad (283)$$

Consider the line  $\ell'_2 = \ell_2 + (p_1 - p_2)$ . Define another point  $q'_2 = q_2 + (p_1 - p_2)$ . The line  $\ell'_2$  is parallel to  $\ell_2$ , it intersects  $\ell_1$  at  $p_1$ , and it passes through  $q'_2$ . Note that  $q'_2$  is close to  $\vec{c}$ :  $|q'_2 - \vec{c}| \leq 3\Delta$ .

Note that  $p_1$  is far from  $q'_2$ :

$$|p_1 - q'_2| \geq 5\Delta. \quad (284)$$

Note that  $q_1$  and  $q'_2$  are close to each other:

$$|q_1 - q'_2| \leq 4\Delta. \quad (285)$$

We will use equations (283), (284) and (285) to show that the angle between  $\ell_1$  and  $\ell'_2$  is small. (See Figure 4.) We have  $a \leq 4\Delta$ ,  $b \geq 7\Delta$  and  $c \geq 5\Delta$ .

Using the law of cosines, and the fact that  $x + \frac{1}{x} \geq 2$  for all  $x > 0$ , we get:

$$\begin{aligned} |\vec{\theta}^{(1)} \cdot \vec{\theta}^{(2)}| &= \cos \varphi = \frac{c^2 + b^2 - a^2}{2bc} \\ &= \frac{1}{2} \left( \frac{c}{b} + \frac{b}{c} - \frac{a^2}{bc} \right) \\ &\geq 1 - \frac{a^2}{2bc} \\ &\geq 1 - \frac{(4\Delta)^2}{2(7\Delta)(5\Delta)} = 1 - \frac{8}{35} > \frac{3}{4}. \end{aligned} \quad (286)$$

This contradicts our assumption that  $\ell_1$  and  $\ell_2$  are nearly orthogonal.

So we conclude that  $p_1$  is close to  $\vec{c}$ , as desired:

$$|p_1 - \vec{c}| \leq 8\Delta = 8\sqrt{3}(n-1)\sqrt{\delta R}\sqrt{507 + (Q_1/n)}. \quad (287)$$

Finally, using our assumed upper bound on  $\delta$ , we get that:

$$|p_1 - \vec{c}| \leq \mu. \quad (288)$$

So the algorithm succeeds with constant probability.

Finally, we argue that, when the grid  $G = (\sigma\mathbb{Z})^n \cap [-L, L]^n$  is chosen properly, the discrete algorithm will behave like the continuous one. Recall from Section 6 that we can approximate a function  $f$  on  $\mathbb{R}^n$  with a function  $f_2$  on  $G$ , provided that most of the probability mass of  $f$  lies within distance  $L$  of the origin, and most of the probability mass of  $\hat{f}$  lies within distance  $\frac{1}{2\sigma}$  of the origin. This holds for our algorithm, provided that:

$$R' \leq L, \quad \frac{100}{\delta} \leq \frac{1}{2\sigma}. \quad (289)$$

(The first condition follows immediately, since  $f$  is supported on a ball. The second condition follows from the decay of  $\hat{f}$ ; details omitted.)

Also, we argue that the discretization of the “direction” variable  $\vec{\theta}$  will not introduce too much error in the output of the algorithm. The key part of our algorithm involves constructing a line  $\ell = \{\vec{b} + \lambda\vec{\theta} \mid \lambda \in \mathbb{R}\}$ ; and if  $\vec{\theta}$  were a continuous variable, this line would pass within distance  $O(\sqrt{a}\beta)$  of the center  $\vec{c}$ . Recall from Section 6 that the discrete curvelet transform resolves  $\vec{\theta}$  within error  $\pm\sqrt{a}$  in angular distance. Since  $\vec{b}$  lies at distance  $O(\beta)$  from the center  $\vec{c}$ , the error in  $\vec{\theta}$  can increase the distance from  $\ell$  to  $\vec{c}$  by at most  $O(\sqrt{a}\beta)$ . Thus the error in the output of the algorithm increases by at most a constant factor.

We can bound the running time of our algorithm as follows. Say we choose  $L$  and  $\sigma$  so that the above inequalities are tight (up to constant factors). Also, suppose  $\delta$  satisfies equation (275) exactly up to constant factors. Let  $M$  be the number of grid points along one direction. Then  $M = 2L/\sigma \leq O(R^2 n^3 / \mu^2)$ , and the running time is  $\leq \text{poly}(n, \log M) \leq \text{poly}(n, \log R, \log \frac{1}{\mu})$ .

## 8 Conclusions

We introduced the curvelet transform as a tool for quantum algorithms, and demonstrated how it can be used to solve problems involving geometric objects in  $\mathbb{R}^n$ . We showed that:

(1) for functions with radial symmetry, the continuous curvelet transform concentrates probability mass near the wavefront set; (2) a quantum curvelet transform (which is a discrete approximation of the continuous curvelet transform) can be implemented efficiently; (3) this leads to quantum algorithms for finding the center of a ball in  $\mathbb{R}^n$ , given  $O(1)$  quantum-sample states, and for finding the center of a radial function in  $\mathbb{R}^n$ , using  $O(1)$  oracle queries.

One open problem is to improve our analysis of the curvelet transform. It would be nice to prove that the continuous curvelet transform concentrates probability mass near the wavefront set, for arbitrary functions on  $\mathbb{R}^n$  (this would generalize the results of this paper, [7] and [5]).

Another problem is to understand precisely how well the discrete curvelet transform approximates the continuous one.

Also, we mention that, in the case of a spherical shell, it should be possible to prove a stronger claim about  $\vec{b} \cdot \vec{\theta}$ : we showed that the variance of  $\vec{b} \cdot \vec{\theta}$  is at most  $O(\beta^2)$ , but in fact,  $\vec{b} \cdot \vec{\theta}$  should be concentrated around  $\beta$  and  $-\beta$  with high probability.

With regard to quantum algorithms, the obvious open question is: what are curvelets good for? Can they solve a hard problem that is of practical interest? Can they produce an exponential speed-up over classical algorithms?

One possible direction is to try to construct a curvelet transform over  $\mathbb{F}_q^n$ , and then apply it to the hidden polynomial problem [8, 9].

One might also ask what kinds of quantum states have “wavefront” structures, that could be analyzed using the curvelet transform. Quantum-sample states over polytopes are one candidate. (Note that one can use the techniques of [2, 12] to prepare quantum-samples over convex bodies.) The state produced by the evolution of a quantum walk is another candidate.

*Acknowledgements:* The author is grateful to John Preskill, Leonard Schulman, Andrew Childs, David Meyer, Nolan Wallach, Robert Koenig and Stephen Jordan, for helpful discussions. Supported by an NSF Mathematical Sciences Postdoctoral Fellowship.

## References

- [1] M. Abramowitz and I. A. Stegun, editors. *Handbook of Mathematical Functions*. U.S. National Bureau of Standards, 1972 (tenth printing).
- [2] D. Aharonov and A. Ta-Shma. Adiabatic quantum state generation and statistical zero knowledge. In *STOC*, pages 20–29, 2003.
- [3] D. Bacon, A. M. Childs, and W. van Dam. From optimal measurement to efficient quantum algorithms for the hidden subgroup problem over semidirect product groups. In *FOCS*, pages 469–478, 2005.
- [4] E. J. Candes, L. Demanet, D. L. Donoho, and L. Ying. Fast discrete curvelet transforms. *Multiscale Model. Simul.*, 5:861–899, 2005.
- [5] E. J. Candes and D. L. Donoho. Continuous curvelet transform: I. resolution of the wavefront set. *Appl. Comput. Harmon. Anal.*, 19:162–197, 2003.
- [6] E. J. Candes and D. L. Donoho. Continuous curvelet transform: II. discretization and frames. *Appl. Comput. Harmon. Anal.*, 19:198–222, 2003.
- [7] E.J. Candes and D. L. Donoho. New tight frames of curvelets and optimal representations of objects with piecewise-c2 singularities. *Comm. Pure Appl. Math.*, 57:219–266, 2002.

- [8] A. M. Childs, L. J. Schulman, and U. V. Vazirani. Quantum algorithms for hidden nonlinear structures. In *FOCS*, pages 395–404, 2007.
- [9] T. Decker, J. Draisma, and P. Wocjan. Efficient quantum algorithm for identifying hidden polynomials. arXiv:0706.1219v3 [quant-ph], 2007.
- [10] A. Fijany and C.P. Williams. Quantum wavelet transforms: Fast algorithms and complete circuits. arXiv:quant-ph/9809004v1, 1998.
- [11] M. H. Freedman. Poly-locality in quantum computing. arXiv:quant-ph/0001077, 2000.
- [12] L. Grover and T. Rudolph. Creating superpositions that correspond to efficiently integrable probability distributions. arXiv:quant-ph/0208112v1, 2002.
- [13] P. Hoyer. Efficient quantum transforms. arXiv:quant-ph/9702028v1, 1997.
- [14] P. Hoyer and J. Neerbek. Bounds on quantum ordered searching. arXiv:quant-ph/0009032v2, 2000.
- [15] S. P. Jordan. Fast quantum algorithm for numerical gradient estimation. *Phys. Rev. Lett.*, 95(5):050501, 2005.
- [16] A. Montanaro. Quantum algorithms for shifted subset problems. arXiv:0806.3362v2 [quant-ph], 2008.
- [17] C. Moore, A. Russell, and P. Sniady. On the impossibility of a quantum sieve algorithm for graph isomorphism. In *STOC*, pages 536–545, 2007.
- [18] O. Regev. Quantum computation and lattice problems. *SIAM J. Comput.*, 33(3):738–760, 2004.
- [19] P. W. Shor. Polynomial-time algorithms for prime factorization and discrete logarithms on a quantum computer. *SIAM J. Comput.*, 26(5):1484–1509, 1997.
- [20] H. F. Smith. A hardy space for fourier integral operators. *J. Geom. Anal.*, 8(4):629–653, 1998.
- [21] E. M. Stein and T. S. Murphy. *Harmonic Analysis: Real-variable Methods, Orthogonality, and Oscillatory Integrals*. Princeton University Press, 1993.
- [22] E.M. Stein and R. Shakarchi. *Fourier Analysis: An Introduction*. Princeton University Press, 2003.
- [23] G.N. Watson. *A Treatise on the Theory of Bessel Functions*. Cambridge, 1962 (2nd ed.).